

Generation of a Multi-Organ-Chip-Based Liver Equivalent for Toxicity Testing

vorgelegt von

Dipl.-Ing. **Eva-Maria Materne**, M.Sc.

von der Fakultät III - Prozesswissenschaften
der Technischen Universität Berlin
zur Erlangung des akademischen Grades

Doktor der Ingenieurwissenschaften

- Dr.-Ing. –

genehmigte Dissertation

Promotionsausschuss:

Vorsitzender:	Prof. Dr. Ulf Stahl
Gutachter:	Prof. Dr. Roland Lauster
Gutachter:	Prof. Dr. Jens Kurreck
Gutachter:	Prof. Dr. Horst Spielmann

Tag der wissenschaftlichen Aussprache: 28. Februar 2014

Berlin 2014
D 83

TABLE OF CONTENTS

Abbreviations.....	I
Abstract.....	II
Zusammenfassung.....	III
1 Introduction.....	1
1.1 The Liver	1
1.1.1 Liver micro-architecture.....	1
1.1.2 Zonation	3
1.1.3 Cell types and function.....	4
1.1.4 Molecular markers of hepatocyte physiology.....	8
1.2 Tissue engineering.....	9
1.2.1 Systems used for metabolism studies.....	10
1.2.1.1 Tissue slices.....	10
1.2.1.2 Primary cells.....	11
1.2.1.3 Cell lines	12
1.3 Toxicity testing state of the art	13
1.3.1 Existing microfluidic devices for liver toxicity testing	15
1.4 The Multi-Organ-Chip (MOC) technology.....	19
1.4.1 Characteristics of the MOC	19
1.5 Substances tested on MOC co-cultures.....	22
2 Aims	24
3 Materials and Methods	26
3.1 Materials.....	26
3.1.1 Cell sources	26
3.1.2 Cell culture media and supplements.....	26
3.1.3 Buffers and Reagents	27
3.1.4 Consumables	28
3.1.5 Antibodies for Immunofluorescence.....	29
3.1.6 Kits.....	29
3.1.7 Primers	30
3.1.8 Materials of the Multi-Organ-Chip.....	30
3.1.9 Devices and technical support	31
3.2 Methods	32
3.2.1 Multi-Organ-Chip fabrication	32
3.2.2 Cell culture	32
3.2.2.1 HepaRG cells	32
3.2.2.2 Hepatic stellate cells	33
3.2.2.3 Human dermal microvascular endothelial cells.....	33
3.2.2.4 Skin biopsies	33
3.2.3 Passaging of cells.....	33
3.2.4 Cell counting.....	34
3.2.5 Freezing and thawing cells	34
3.2.6 Aggregate formation	34

3.2.7 Bioreactor co-culture	35
3.2.7.1 Seeding organoids into inserts.....	35
3.2.7.2 Seeding organoids in Transwell® assisted cultures.....	35
3.2.8 Vascularisation of the channels	35
3.2.9 Bioreactor operation.....	36
3.2.10 Administration of troglitazone for toxicity testing.....	36
3.2.11 Administration of n-hexane and 2,5-hexanedione for toxicity testing	36
3.2.12 Analysis.....	36
3.2.12.1 Immunohistochemistry.....	37
3.2.12.2 Bile canalicular staining	38
3.2.12.3 qPCR.....	38
3.2.12.4 Metabolic parameters	40
3.2.13 Statistical analysis	41
4 Results.....	42
4.1 Characterisation of differentiated HepaRG cells	42
4.2 Characterisation of hSteC	43
4.3 Production of liver cell aggregates	43
4.4 Dynamic culture of organ equivalents inside the MOC - overview	46
4.5 Liver single-tissue cultures inside the MOC.....	48
4.5.1 MOC culture of liver tissue in cell culture inserts	48
4.5.2 MOC culture of liver tissue directly exposed to the fluid flow.....	49
4.6 Liver and skin tissue co-culture in the (endothelialised) MOC.....	53
4.5.2 MOC co-culture of liver and skin tissue in cell culture inserts	53
4.5.2 MOC co-culture of liver and skin tissue directly exposed to the fluid flow	56
4.5.2 MOC co-culture of liver, skin and endothelial tissue	59
4.7 Liver and neurosphere co-culture in the MOC.....	63
4.8 Multi-tissue sensitivity to troglitazone at fluid flow	65
4.5.2 MOC co-culture of liver and skin tissue at troglitazone exposure	65
4.5.2 MOC co-culture of liver, skin and endothelial tissue at troglitazone exposure	67
4.9 Multi-tissue sensitivity to n-hexane and 2,5-hexanedione at fluid flow	71
5 Discussion	75
6 Conclusion	94
7 Perspectives	95
7.1 Improvements of the liver equivalent	95
7.2 Endothelialisation	96
7.3 Systemic improvements	96
8 References	98
9 Acknowledgment.....	106
10 Publications	108
11 Appendix	109

Abbreviations

3T3 NRU-PT	3T3 Neutral Red Uptake Phototoxicity Test
BSEP	Bile salt export pump
cDNA	Complementary DNA
CK 8/18	Cytokeratin 8/18
CPS-1	Carbamoyl phosphate synthetase 1
Cyp	Cytochrome P450
DILI	Drug-induced liver injury
DMEM	Dulbecco's Modified Eagle Medium
DMSO	Dimethyl sulfoxide
dNTP	Deoxyribonucleotide triphosphate
ECVAM	European Centre for the Validation of Alternative Methods
EDTA	Ethylene diaminetetraacetic acid
FCS	Fetal calf serum
Fig	figure
GSTA	Glutathione S-transferase alpha
HDMEC	Human dermal micro-vascular endothelial cells
hSteC	Hepatic stellate cell
LDH	Lactate dehydrogenase
LSEC	Liver sinusoidal endothelial cell
MDR-1	Multidrug resistance protein 1
MOC	Multi-organ-chip
mRNA	Messenger RNA
MRP-2	Multidrug resistance protein 2
OECD	Organisation for Economic Co-operation and Development
PBS	Phosphate-buffered saline
PDMS	Polydimethylsiloxane
pPCR	Quantitative PCR
RT	Room temperature
TBP	TATA-binding protein
TUNEL	Terminal deoxynucleotidyl transferase dUTP nick end labeling
TZD	Thiazolidinedione
UGT	UDP-glucuronosyltransferases
ZO-1	Zona occludens 1

Abstract

The unique importance of the liver for organismal homeostasis and blood detoxification has led to an evolutionary optimisation of the human liver architecture at the scale of its smallest functional unit – the liver lobule. Unsurprisingly, such a super-optimised tissue is especially vulnerable to inconsistencies, such as toxic effects. The ever-growing amount of new substances released to the market and the limited predictability of current *in vitro* test systems for drug-induced liver injury (DILI) has led to an ample need for new substance testing solutions. Especially, the application of miniaturised, dynamically perfused chip-based systems is gaining much attention recently due to their ability of imitating *in vivo*-like nutrient supply, shear stress and defined microenvironments of the cells.

In this thesis, a novel 3D co-culture system comprising the hepatic HepaRG cell line and non-parenchymal hepatic stellate cells (hSteC) is presented and its suitability as *in vitro* liver test system is evaluated. These 3D tissue equivalents were, furthermore, cultivated inside a multi-organ-chip (MOC) to assess the effects of fluid flow on the cells. Single tissue cultures, as well as two to three organ co-cultures including skin biopsies, endothelial cells and neurospheres were performed analysing the versatility of the MOC and the possibility for multi-organ culture in a combined media circuit, observing organ-organ crosstalk.

It could be shown, that liver aggregates spontaneously produced liver-typical extracellular matrix components like fibronectin and collagen type I indicating the formation of an *in vivo*-like environment. Cells polarised de-novo, forming bile-canalicular like structures as shown by ZO-1 and MRP-2 expression. Prolonged culture in the MOC led to a more pronounced expression of these markers, as well as of functional markers like cytochrome P450 enzymes indicating the generation of a functional and metabolically competent organ equivalent. Furthermore, first indicators for functional liver zonation on cytochrome P450 3A4 level were obtained in Transwell® assisted cultures. Analysing the release of albumin to the culture medium over a culture period of up to 14 days revealed a significantly increased production rate in liver equivalents cultured under dynamic conditions in the MOC compared to standard static controls.

Co-cultivating liver aggregates with skin biopsies revealed that a metabolic steady state in terms of glucose consumption and lactate production could be achieved after 5 to 8 days of co-culture in a combined medium circuit. The long-term stability of these cultures was proven by 28-day cultivation. These co-cultures were shown to be glucose limited, which led to a reduction in albumin production by the liver equivalents. Still, viability of the cells was maintained and strongly increased compared to static cultures. The stable consumption of glucose and production of

lactate indicated the establishment of an artificial but balanced co-existence between the tissues, proving the feasibility of two (or even more) tissue co-cultures in a combined medium over prolonged periods of time. Similarly, the co-cultivation with endothelial cells and neurospheres led to a glucose-limited, but still viable and metabolically competent system.

Exposing MOC co-cultures to pharmaceutical substances at regimens relevant to respective guidelines successfully revealed a dose-dependent response of cultures. The chronic application of troglitazone to the co-cultures over 7 to 14 days proved a sensitivity of liver equivalents to this hepatotoxic anti-diabeticum. Dose dependent *in vivo*-like up-regulation of metabolic enzyme cytochrome P450 3A4 and induction of toxicity could be shown. Furthermore, the *in vivo* elimination half-life of troglitazone could successfully be reproduced in a liver-skin-endothelial cell co-culture MOC system.

Chronical application of 2,5-hexanedione to a liver-neurosphere co-culture also led to dose-dependent toxicity. Furthermore, a slightly higher sensitivity of the co-culture compared to single-tissue MOC cultures was observed. First hints of n-hexane toxicity in liver-neurosphere co-cultures could be obtained.

Taken together, this MOC co-culture system not only presents a useful mean for maintaining hepatocyte viability and metabolic activity over prolonged periods of time, but also a tool to study organ-organ interactions under control and toxic environments useful for drug testing.

Zusammenfassung

Die Leber hat als zentrales Organ des gesamten Stoffwechsels eine einzigartige Bedeutung in der Aufrechterhaltung der metabolischen Homöostase, der Gallenproduktion und damit einhergehend dem Abbau und der Ausscheidung von Medikamenten und Giftstoffen. Diese Fülle an Stoffwechselfunktionen und die daraus resultierende, evolutionär hoch spezialisierte strukturelle Segregation der metabolischen Aktivitäten der Leber stellt eine große Herausforderung bei der frühzeitigen Erkennung von medikamenteninduzierten Leberschädigungen dar. Die Generierung miniaturisierter Leberäquivalente zur Substanztestung bedarf daher besonderer Aufmerksamkeit in Hinblick auf die Komplexität des Organs.

Im Verlauf dieser Arbeit wurden Leber-Aggregate aus Hepatozyten und nicht-parenchymalen Ito-Zellen generiert und charakterisiert. Diese Leber-Äquivalente wurden in dem von uns

entwickelten Multi-Organ-Chip (MOC) sowohl als Einzelorgankultur als auch als Co-Kulturen mit Hautbiopsien, Endothelzellen und Neurosphären kultiviert.

Es konnte gezeigt werden, dass die Zellen der Aggregate lebertypische extrazelluläre Matrixbestandteile wie Fibronektin und Kollagen Typ I produzieren. Zudem polarisierten Hepatozyten *de-novo* und bildeten Gallenkapillaren. Die Verlängerung der Kulturzeit in MOCs über 14 Tage führte zu einer weiteren Verbesserung der Polarisation sowie der Expression funktioneller Marker wie der Cytochrom-P450-Enzyme. Die Analyse der Albuminkonzentration im Medium ergab eine deutlich erhöhte Produktionsrate in Leber-Äquivalenten die unter dynamischen Bedingungen im MOC kultiviert wurden im Vergleich zu Kontrollen unter statischen Bedingungen.

Co-Kulturen von Leber Aggregaten mit Hautbiopsien erreichten ein metabolisch stabiles Niveau nach 5 bis 8 Tagen ein. Es konnte gezeigt werden, dass diese Co-Kulturen glukoselimitiert waren, was zu einer Verringerung der Albuminproduktionsrate führte. Ebenso führte die Co-Kultivierung mit Endothelzellen und Neurosphären zu einer Glukoselimitierung. Dennoch konnten die Zellen in einem vitalen, metabolisch kompetenten Zustand über eine Kulturzeit von 28 Tagen erhalten werden.

Die Applikation von hepatotoxischen Substanzen wie Troglitazon zu Leber-Haut-Kulturen führte zu einer *in vivo*-ähnlichen, dosisabhängigen Hochregulation des metabolischen Enzyms Cytochrom-P450 3A4 und zur Induktion von Toxizität. Ebenso konnte die *in vivo* Halbwertszeit von Troglitazon erfolgreich in Leber-Haut-Endothelzell MOC Co-Kulturen reproduziert werden.

Auch die Toxizität von 2,5-Hexandion in Leber-Neurospären Co-Kultur war dosisabhängig und darüber hinaus wurde eine etwas höhere Sensitivität in Co-Kulturen im Vergleich zu Einzelorgan-kulturen im MOC beobachtet. Erste Hinweise auf eine Toxizität von n-Hexan in diesen Co-Kultursystemen wurden deutlich.

Zusammengenommen stellt das präsentierte MOC Co-Kultursystem nicht nur ein geeignetes Mittel für die Aufrechterhaltung der Vitalität und metabolischen Aktivität von Hepatozyten über längere Zeiträume dar, sondern auch ein Model um Kommunikationen zwischen Organen zu untersuchen. Es konnten sowohl homöostatische als auch toxische Umgebungen für die Zellen in den MOC simuliert und analysiert werden, was für die Nutzung des Systems für Wirkstofftests von besonderer Bedeutung ist.

1 Introduction

1.1 The Liver

The liver is the largest gland of the human body weighing about 1.5 kg. The organ is located in the upper right corner of the abdomen having a close association with the small intestine. The mean blood supply to the liver is 1.5 l/min accounting for $\frac{1}{3}$ of total cardiac output.¹ 25 to 30% of this flow comes from the hepatic artery, which transports blood rich in oxygen, whereas the major part drains the liver from the portal vein, which brings blood rich in nutrients.² Therefore, processing the nutrient-enriched venous blood that leaves the digestive tract is one major task of this organ.

The number and variety of processes, in which the liver is involved remains unique. The liver performs over 500 metabolic functions, resulting in the synthesis of products that are released into the blood stream (e.g. glucose derived from glycogenesis, plasma proteins, clotting factors and urea), or that are excreted to the intestinal tract (bile). Also, several products are stored in the liver parenchyma (e.g. glycogen, fat and fat soluble vitamins). Hence, in its role as central organ for metabolism and biotransformation processes the liver provides high-energy substances for the energy balance of the whole organism.¹ Furthermore, the privileged location between the gastrointestinal tract and circulatory system allows the liver to affect the bioavailability of extra-vascular applied drugs (first-pass effect). It is the central organ for detoxification of endogenous and exogenous substances through metabolism and excretion into the bile. Xenobiotics are converted into water-soluble and thus easy to excrete metabolites. The realisation of these diverse tasks requires an evolutionarily optimised complex and heterogeneous micro-architecture.

1.1.1 Liver micro-architecture

The micro-architecture of the liver is built up of 1 to 1.5 million hepatic lobules, which have a cylindrical shape approximately 1.1 mm in diameter and 1.7 mm in height.³ This minimal functional unit is capable of performing all the tasks essential for liver function. Hence, modelling this unit is the primary goal of all liver tissue engineering. The hepatic lobule resembles a hexagon with portal tracts at the corners and a central vein in the middle (Fig. 1). This lobule consists of radially arranged plates of up to 25 liver cells placed in a row between the portal triads and the central vein. Between the liver cell plates Disse's space and the sinusoids are located.³ The sinusoids

are lined with specialised liver sinusoidal endothelial cells. These sinusoidal vessels have an inner diameter of 6-10 μm and a length of 300-500 μm .^{4,5,6,7} The vessel volume makes up to 7-11% of the total liver lobule volume (+5% space of Disse).^{6,8} Disse's Space is a 0.2 to 1.4 μm wide, zone which spans between the hepatocyte plates and the liver sinusoidal endothelial cells.^{4,8} Hence, all molecules exchanged between plasma and hepatocytes must traverse this space. The bidirectional flux of macro molecules is facilitated by the lack of a basement membrane.^{9,10} Thick, cross banded collagen type I fibres can be found throughout Disse's space, whereas only minor quantities of collagen type III, IV and V are present. The most abundant extracellular matrix component is fibronectin. It appears as an almost continuous lining along the full length of the hepatic sinusoids. To simulate the physiological environment of liver cells *in vitro*, a co-culture with these extracellular matrix components is beneficial.

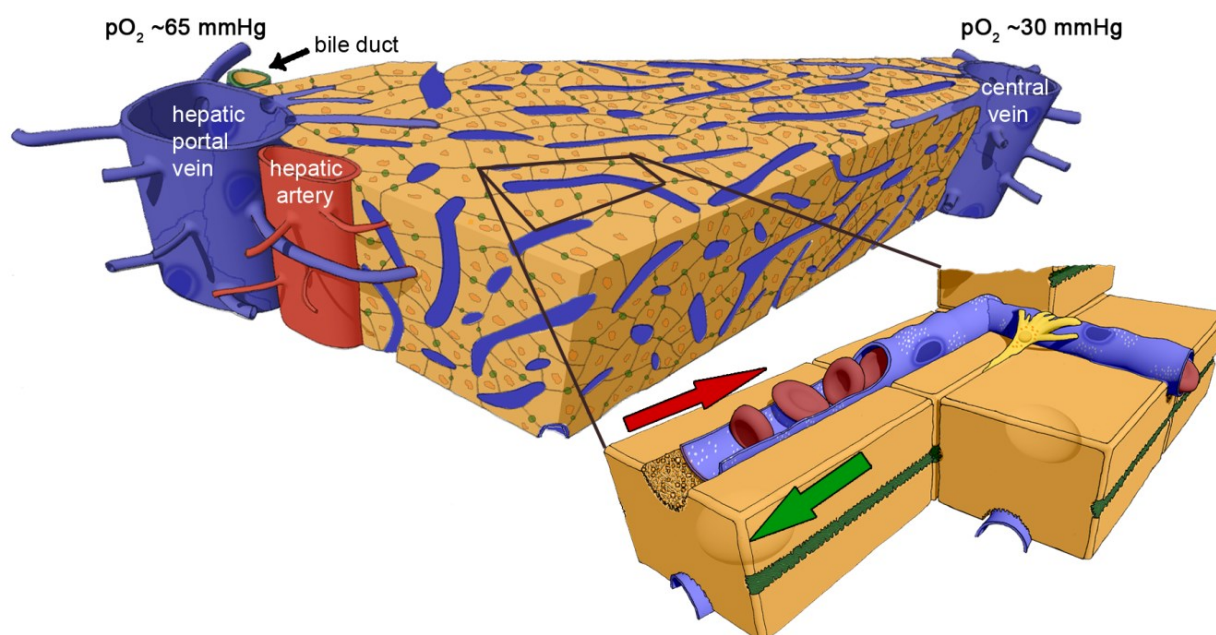


Fig. 1 Liver architecture at lobule level. A dynamic blood flow from the outer surface to the centre of the lobule (red arrow) ensures a stable oxygen gradient, whilst a reverse bile flow takes place in segregated bile canaliculi (green arrow and channels). The space of Disse, generated by tight interactions between liver cells (brownish) and endothelial sinusoids (blue), accounts for efficient substance uptake. Ito cells (yellow) are responsible for matrix formation and remodelling in the space of Disse.

The total human liver blood flow accounts for approximately 30% of the cardiac output. Blood coming from the terminal branches of the portal veins and the hepatic arterioles flows through the sinusoids towards the central vein with a velocity of 144 $\mu\text{m}/\text{sec}$ delivering 2000 nmol/mL oxygen to the surrounding hepatocytes.⁴ Hence, blood contact time to hepatocytes ranges only from 2 to 4 seconds. During this short period, all substance uptake, metabolism and excretion into the blood

have to be performed. The blood pressure in the hepatic artery is considered to be the same as the aortic pressure, being highly pulsatile between 120 and 80 mmHg with a frequency equal to heart rate, whereas the pressure in the portal vein has no pulsation and a pressure of 10-12 mmHg.² Vessel compliance causes a gradual decrease in pulsation as the artery branches inside the liver. At the sinusoidal level, the pulsation amplitude decreases to near zero and pressure of the blood coming from the artery drops to approximately 2-5 mmHg.² In total, in the sinusoids, both portal venous and hepatic arterial pressure sum up to 3-5 mmHg. Hence, a laminar flow without pulsations is the best approximation to the *in vivo* situation. When modelling the flow rates for *in vitro* test systems, one has to consider, that the hepatocytes are shielded from the direct flow by the sinusoidal endothelial cells. Powers et al. reported that shear stress on the hepatocytes surface should never exceed 2 dyne/cm².¹¹

1.1.2 Zonation

As the blood flows from the portal triads along the sinusoids towards the central vein it is gradually depleted from oxygen (ΔpO_2 30-35 mmHg), which is taken up by the cells of the liver. This results in an oxygen gradient, as well as gradients in hormones and other substances and leads to the formation of spatially defined, highly specialised functional zones of the liver lobule.¹² This enables hepatocytes of their respective zone to fully concentrate their cellular and molecular capacities onto the single function to which they are dedicated. Differences between cells of differing zones include the presence of key enzymes, receptors and subcellular structures such as mitochondria and smooth endoplasmic reticulum in the cells.¹ This reflects on the cell's function (Table 1). For example at periportal regions, where oxygen tension is higher, oxidative energy metabolism, gluconeogenesis, amino acid catabolism, ureagenesis from amino acids and bile acid formation occurs. Additionally, certain plasma proteins such as albumin and fibrinogen are synthesised mainly in the periportal area. At the perivenous zone however glycolysis, lipogenesis, glutamine synthesis from ammonia and biotransformation are predominantly performed.¹³

Table 1 Zonation of function in liver parenchymal cells

Periportal zone	Perivenous zone
<i>Oxidative energy metabolism</i>	
<i>Glucose release</i>	<i>Glucose uptake</i>
Gluconeogenesis	Glycolysis
Glycogen synthesis from pyruvate	Glycogen synthesis from glucose
Glycogen degradation to glucose	Glycogen degradation to pyruvate
<i>Urea formation</i>	<i>Glutamine formation</i>
Ureagenesis from amino acid nitrogen and NH ₃	Glutamine from NH ₃
<i>Protective metabolism</i>	<i>Xenobiotic metabolism</i>
Glutathione peroxidation and conjugation	Monooxygenation
	Glucuronidation
<i>Plasma protein formation</i>	
Albumin	α-Fetoprotein
Fibrinogen	Angiotensinogen
<i>Bile acid formation</i>	
Bile acid synthesis from cholesterol	

As a result of this zonation, most toxicologic and pathologic events in the liver show a considerable degree of zonal preferences. Monooxygenation by the cytochrome P450 system followed by conjugation with either glucuronic or sulphonic acid is predominantly situated at the perivenous zone, as well as cytochrome P450- independent metabolism of xenobiotics.¹⁴ For example, the conversion of ethanol via acetaldehyde to acetate by alcohol dehydrogenase and acetaldehyde dehydrogenase is situated perivenously.¹⁴

1.1.3 Cell types and function

A single liver lobule contains approximately 10^5 cells in total with a yield and volume distribution as shown in Table 2. The parenchymal cells of the liver (**hepatocytes**) account for 80% of the parenchymal volume and 60% to 70% of total cell count.⁸ These cells are 19 to 25 μm in size and have a clearly contoured cell membrane which is divided into three compartments, defined by morphological and functional cellular polarisation.⁶ About 37% of the external membrane of the hepatocytes is sinusoidal surface, also termed basolateral membrane (Fig. 2). The absorptive and secretory function of which is increased six-fold by numerous microvilli with a length of 0.5 μm .^{3,8} These microvilli lie in Disse's space, some even protrude through the fenestrae into the

sinusoids and thereby have direct contact with the blood.^{1,3} The apical surface makes up 15% of the cells surface area. Here, 2 to 3 neighbouring hepatocytes are in contact to each other and form bile canaliculi by an invagination of their plasma membrane.⁸ These canaliculi are 1-2 μm in diameter.² Also here, microvilli extend into the bile canaliculi, expanding the surface area of the apical plasma membrane that is available for secretion of bile.¹ The remaining 50% of the external hepatocyte membrane constitute the smooth intercellular fissure, which is connected with Disse's space. This fissure is sealed from the canaliculi by tight junctions, allowing only an exchange of water and cations to take place.³ Hence, as these cells possess not only a single apical and basal surface, but have multiple apical (bile canalicular) surfaces and two basolateral surfaces, re-establishing cell polarity *in vitro* is more challenging than with other cells.

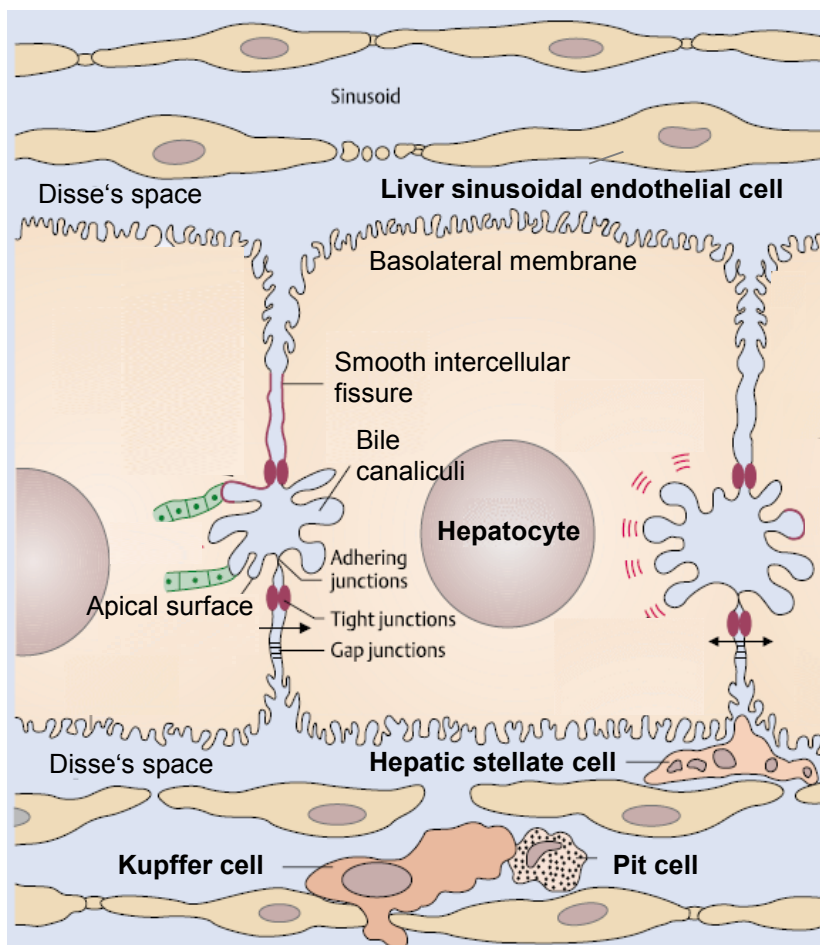


Fig. 2 Liver architecture at cellular level. Polarised hepatocytes form bile canaliculi with adjacent cells, whereas their basolateral membrane is in contact with Disse's space. Hepatic stellate cells and sinusoidal endothelial cells are in direct contact with the hepatocytes, whereas Kupffer cells and Pit cells reside in the sinusoids.

The energy production in primary hepatocytes is highly dependent on oxidative phosphorylation. Each cell contains over 1500 mitochondria which consume oxygen at a rate of 0.3 to 0.9 $\text{nmol/sec}/10^6$ cells.^{5,8,15,16} The oxygen tension inside the sinusoids is typically lower than in the

capillaries of other organs, due to the portal blood supply.¹⁷ At the periportal area oxygen tensions of 60-70mmHg can be found, whereas at the perivenous area oxygen tension falls to 25-35 mmHg.⁴ *In vivo* a continuous supply of over 2000 nmol/mL of oxygen to hepatocytes is provided, while *in vitro* due to oxygen's low solubility in culture media cells are supplied with less than 200 nmol/mL.¹⁸ Therefore, as oxygen is rapidly depleted *in vitro* due to its low solubility in culture medium and due to the high metabolic activity of the cells, physiologically relevant microenvironments with scales and oxygen supply rates based on known or predicted cellular requirements are needed.

Table 2 Yield and volume distribution of cells within the liver lobule ^a

	Cell number [% of total]	Cell volume [% of total]
Hepatocytes	60-65	78
Sinusoidal endothelial cells	10-20	2.8
Kupffer cells	8-12	2.1
Ito (stellate) cells	3-8	1.4
Pit cells	<2	

^a The extracellular space accounts for 16% of total liver volume (5% space of Disse, 11% sinusoidal lumina).⁴

Non-parenchymal cells of the liver also play an important role in substance toxicity. In general there are four different cell populations recognised: (1) fenestrated endothelial cells (2) phagocytic Kupffer cells (3) extraluminal stellate cells, also referred to as fat-storing cells of Ito, lipocytes or perisinusoidal cells and (4) PIT cells, which are immunoreactive natural killer cells that are attached to the luminal surface of the sinusoid and are part of a population of liver-associated lymphocytes.³

(1) **Liver sinusoidal endothelial cells** (LSEC) are highly specialised microvascular cells.

The open pores in their membranes are termed fenestrae. These fenestrae have a diameter of 100 to 200 nm, occur at a frequency of 9-13 per μm^2 and occupy 6-8% of the endothelial surface.¹⁹ Furthermore, LSECs show a high endocytotic capacity. This function is reflected by the presence of numerous endocytotic vesicles and by the effective uptake of a wide variety of substances from the blood by receptor-mediated endocytosis.¹⁹ It was shown that these cells clear soluble macromolecules and colloids of size $< 0.23 \mu\text{m}$.²⁰ Some substances are processed by the endothelial cells themselves (endocytosis), whereas others are transported across the endothelium to the surrounding tissues (transcytosis).¹⁹

In *in vitro* co-culture, sinusoidal endothelial cells were reported to support long-term hepatocyte function, stabilising urea and albumin secretion for up to a month in culture.^{4,17} However, LSEC proliferate only very slowly and important features, such as scavenger function and fenestration, are severely decreased or disappear completely after a cultivation period of more than 1-2 days, which hampers *in vitro* co-cultivations.²⁰

- (2) **Kupffer cells** form almost 80% of the resident macrophage population in the liver. They play an important role in defence reactions by presenting antigens and by releasing numerous signalling molecules, including hydrolytic enzymes, nitric oxide and superoxide, which can lead to hepatic damage. Inflammatory cytokines such as interleukin-1, interleukin-6 and tumour necrosis factor- α may be released after activation.^{21,22} Additionally, Kupffer cells were shown to have a high endocytotic and also cytotoxic activity.¹⁴ They not only ingest and degrade old erythrocytes, but also bacteria and various endotoxins.⁴ Immune-mediated liver injury develops secondary to a defect in the immune tolerance induction mechanisms. The liver has the unique ability to induce tolerance to large amounts of foreign antigens, transported through the portal system. Kupffer cells mediate this process by inducing apoptosis of activated T cells, immune deviation, and active suppression. Disruption of this process of immune tolerance may lead to toxic immune and autoimmune responses.²³

Under *in vitro* culture conditions, isolated Kupffer cells were shown to be vital for at least 4 days and have an endocytotic ability.²⁴ Co-cultures of hepatocytes and Kupffer cells have been shown to mimic *in vivo*-like damage due to drug toxicity.

- (3) **Hepatic stellate cells** (hSteC) are vitamin A-storing specialised pericytes that extend processes throughout the space of Disse. They are the main matrix-producing cell type in the liver and play an important role in regeneration, differentiation and inflammation.^{4,14,25} They have been shown to produce many different growth factors like hepatocyte growth factor, insulin-like growth factor and transforming growth factor- β 1.²⁶ In regeneration, hSteC were proposed to play an important role in angiogenesis and vascular remodelling. After partial hepatectomy hSteCs participate in revascularisation by excreting a laminin trail between newly replicating avascular islands of hepatocytes that endothelial cells follow to form sinusoids.²⁷ During liver fibrosis, these cells become activated, acquiring a myofibroblast-like phenotype and starting to produce more extracellular matrix.

Also in *in vitro* culture, when plated on rigid substrates, hSteC rapidly become activated.^{4,22} Hence, when using hSteC one has to keep in mind that these cells behave under standard culture conditions as they would in an injured liver.²⁵ Still, when co-cultivating hSteC with hepatocytes it was shown, that these cultures maintain hepatocyte specific functions like albumin and cytochrome P450 expression for more than 2 months.^{26,28,29}

1.1.4 Molecular markers of hepatocyte physiology

Albumin is constantly synthesised by the liver at a rate of 150 to 250 mg/kg/day (making 10 to 18 g of albumin daily in a 70-kg man). It makes up more than half of the total protein present in serum, accounting for 70% of the colloid osmotic pressure. Albumin serves in the transport of bilirubin, hormones, metals, vitamins and drugs.³⁰

Cytochrome P450 (CYP) enzymes are present in different cell types and tissues and also in different sub-cellular compartments. From 57 putatively functional cytochrome P450 genes in the human the function of about 25% is still unknown. Fifteen human cytochromes P450 are known to metabolise xenobiotics, all of them being from the Cyp1, Cyp2 and Cyp3 families. Cytochrome P450 7A1 is responsible for bile acid synthesis.³¹

UDP-glucuronosyltransferases (**UGT**) are central phase II enzymes of drug metabolism. 10 out of 19 UGTs are substantially expressed in adult human liver. UGT-1A1 is the only enzyme responsible for elimination of the heme metabolite bilirubin. Furthermore, the enzyme is involved in the metabolism of many drugs including the chemotherapeutic irinotecan and paracetamol. Glutathione S-transferase alpha (**GSTA**) also belongs to phase II metabolising enzymes. It belongs to the most abundantly expressed glutathione S-transferases in liver.³²

Carbamoyl phosphate synthetase 1 (**CPS-1**) catalyses the first and rate-limiting step of the urea cycle, the major pathway for nitrogen disposal in humans. It is the most abundant protein in hepatic mitochondria, accounting for ~ 20% of the matrix protein mass.³³

Tight junction-associated protein zona occludens 1 (**ZO-1**) is classified as member of the membrane associated guanylate kinase family. It is a cytoplasmic adaptor protein, linking the membrane proteins to the actin cytoskeleton. ZO-1 is critical to junction assembly and permeability, thus playing a crucial role in cell polarisation and bile secretion.³⁴

Bile salt export pump (**BSEP**, also known as ABCB11), multidrug resistance protein 1 (**MDR-1**, also known as ABCB1) and multidrug resistance protein 2 (**MRP-2**, also known as ABCC2) belong to the family of canalicular transport proteins. BSEP is critical for ATP-dependent transport of bile

salts across the hepatocyte canalicular membrane and for bile salt-dependent bile secretion. MDR-1 transports exogenous and endogenous metabolites or toxins, hormones, hydrophobic peptides and bile salts. MRP-2 contributes to bile formation by transporting glutathione, a major driving force for bile salt-independent bile flow. All these markers are indicators for hepatocyte polarisation due to their location in the canalicular membrane.¹

The production of **lactate** is an established marker for cellular stress, caused by hypoxia, tissue repair (proliferation), oxidative stress or mitochondrial disturbances.³⁵ Still, as already described by Otto Warburg, cancerous cells consume high rates of glucose even at normal oxygen tension. This high glycolytic activity at normal oxygen tension, known as the Warburg Effect (also referred to as aerobic glycolysis), is linked to an altered proliferative state of the cells. This led to the finding, that most continuous cell lines consume large amounts of glucose under normal *in vitro* culture conditions, of which up to 50 to 90% is converted to lactate.^{36,37} Especially, in cultures where the glucose concentration is not intentionally controlled at a low level, the molar ratio of lactate production to glucose consumption ranges from 1 to 2 depending on the cells used. This ratio increases not only with stress induced by e.g. hypoxia, but also with the residual glucose concentration in the culture medium. Under physiological conditions, the glucose concentration in the blood normally does not exceed 1 to 1.3 g/L. The altered glucose concentrations in cell culture media might therefore lead to an altered glycolysis acting as defence mechanism against the high extracellular and intracellular glucose concentrations. For HepaRG cells cultured as monolayer under standard confluent *in vitro* culture conditions (2 g/L glucose), a steady state lactate production rate of about 2 mM/24h was reported.³⁵ Further altered lactate production rates might be interpreted as cellular stress.

1.2 Tissue engineering

The field of tissue engineering has traditionally exploited living cells in a variety of ways to restore, maintain, or enhance tissues and organs.³⁸ Especially, in the field of liver tissue engineering, the generation of liver assist devices or even transplants has been of high interest for many decades, aiming to bridge the gap between the numerous liver transplants required in medicine and the severe shortage of donor organs existing.³⁸ The current potential impact of this field, however, is even broader. In the future, engineered tissues could not only reduce the need for organ replacement, but could greatly accelerate the development of new drugs by supplying research units with adequate healthy or diseased tissue models.³⁹ The global market for tissue engineering and regeneration products reached \$55.9 billion in 2010 and is expected to further grow to \$89.7 billion by 2016. The contribution of the European region was 43.3% of the market in 2010, a value

of \$24.2 billion. This market is expected to reach \$36.1 billion by 2016.⁴⁰ The future importance and potential of this field of research has also more and more been recognised by government and regulatory authorities, providing project funding like the Go-Bio initiative which enabled this work.

This vastly expanding field of research is dependent on several essential requirements. The production of engineered tissues requires an adequate source of healthy expandable cells, the optimisation of culture environments, and the creation of bioreactors, which mimic the environment of the body. In the following, cell sources and culture conditions for hepatic tissue engineering will be discussed.

1.2.1 Systems used for metabolism studies

Engineered hepatic tissue is supposed to evaluate the metabolism, clearance and toxicity of a substance under *in vivo*-like conditions. Therefore, several model systems have been used. Precision-cut liver slices, freshly isolated primary hepatocytes, plated or cryopreserved hepatocytes and immortalised cell lines are under evaluation.^{17,41} The preservation of hepatocyte phase I and II metabolising enzyme functions are of high importance in these systems. Phase I metabolism (oxidation) is performed mainly by cytochrome P450 oxidases and phase II metabolism (conjugation) is performed by a variety of transferases.

1.2.1.1 Tissue slices

The most complex metabolising system, tissue slices are a well-accepted *in vitro* system for pharmacological and toxicological studies. Culture conditions such as oxygen tension, media and supplements have been optimised to increase cell viability and reduce degenerative changes in the tissue.⁴² Still, necrosis occurs after 48-72 hours and metabolic enzyme levels are reduced after 6-72 hours.^{43,44} Hence, only short- and middle-term hepatic metabolism, hepatotoxicity and enzyme induction studies have been performed with this tool.⁴¹ Especially, if the whole metabolic profile of a compound is of interest, this system is used. The *in vivo* situation concerning phase I and II drug metabolism is reflected very well in liver slices and the correlation between *in vivo* and *in vitro* xenobiotic metabolism often lead to a good predictability.⁴⁴ Additionally, toxic effects mediated or modified by non-parenchymal cells can be studied, as the physiological liver micro-architecture is maintained and all cell types found *in vivo* are contained.^{41,44} The possibility to

cryopreserve these structures with retained function after thawing renders them a convenient and easy-to-handle system.⁴¹ Detailed information on the use of precision-cut liver slices can be found in various reviews, partly also including comparisons of drug metabolism between slices and isolated hepatocytes, as well as between the *in vivo* situation and *in vitro* systems.^{45,46,47,48} However, due to their limited availability and reduced viability over long-term periods, this system is only applicable under limited conditions.

1.2.1.2 Primary cells

Primary cells are considered the gold-standard for *in vitro* drug metabolism and enzyme induction studies.⁴⁴ These cells can be cultivated in suspension or plated on culture substrata. **Hepatocytes in suspension** show a stable expression of metabolising enzymes for up to 4 hours. This is sufficiently long to determine the metabolic stability of a test compound and to allow the identification of the main metabolites. However, this incubation period is too short to allow the generation of some minor, particularly phase II metabolites.⁴¹ Freshly isolated **hepatocytes plated on culture plates** retain a high activity of both phase I and II enzymes and allow for mid-term incubation of 24 to 72 hours (even though cytochrome P450 expression declines over the first 24 to 48 hours).^{44,49} This enables the accumulation of large amounts of metabolites, also of phase II.⁴¹ Furthermore, these cells can be used for enzyme induction and inhibition studies and allow for medium-throughput screening of compounds.⁴⁴ However, plating the cells on a rigid substratum leads to changes in cell morphology, structure, polarity, gene expression and metabolic function. Overall a de-differentiation of the cells can be observed within a culture period of 24 to 72 hours.^{50,51} Whereas cells, when cultivated in a sandwich configuration between two layers of extracellular matrix, were shown to maintain their production and secretion of physiologic levels of albumin, transferrin, fibrinogen, bile salt and urea for 6 to 8 weeks.⁵ **Cryopreserved cells** were reported to have a decreased metabolic capacity.⁴¹ Even when using well-defined freeze/thaw conditions nearly half of the cryopreserved suspended hepatocytes lose their ability to attach to plastic after thawing. However, when the cells are first encapsulated or entrapped, e.g., in alginate gels, viability is well maintained after cryopreservation and CYP activities are comparable to those measured in fresh hepatocyte monolayer cultures.⁵² Still these cryopreservation techniques are not standardised yet and hence, these cells are mostly used only for the assessment of hepatic drug uptake.⁵³ Changing the cell culture format to 3D cultures, adding flow to the cultures or co-cultivating the hepatocytes with other cells generally improves maintaining the cellular functions.^{5,17,41,44} However, restricted access to human liver tissue and the very limited ability of adult differentiated hepatocytes to proliferate in culture, hinders widespread use of these cells.⁴⁹

1.2.1.3 Cell lines

Liver-derived cell lines have been widely used as an *in vitro* model for the study of hepatocellular functions, as well as in toxicity studies.⁴⁹ These cells grow continuously and have an almost unlimited lifespan, therefore they are easily available. Culture conditions are simpler than those of primary hepatocytes. But concerning the metabolism of compounds, most of the cell lines express biotransformation activities only to a limited extend.⁴⁹

Hepatocyte cell lines can be obtained by oncogenic immortalisation or from tumours.⁵² But as immortalised cell lines tend to be genetically unstable, only a few expressing liver-specific functions have been described. The **Fa2N-4** cell line for example, which originated from human hepatocytes transfected with the SV40 large T antigen gene, expresses various drug-metabolising enzymes, including some major cytochrome P450 iso-enzymes and transporters. But the expression of constitutive androstane receptor (CAR) and several hepatic uptake transporters is significantly lower (>50-fold) in Fa2N-4 cells compared to primary hepatocytes. Hence, the induction of cytochrome P450 2B6 and 3A4, two of the most important cytochrome P450 isoforms in drug metabolism, varies strongly from the expected *in vivo* values.⁵⁴

The **HepG2** cell line is among the most widely used human hepatoma cell lines. Like other hepatomas it retains in part a differentiated adult phenotype.⁴⁹ But it was shown, that since its establishment in the 1970s the cell line has lost many liver-specific functions, especially of phase I enzymes involved in xenobiotic metabolism.^{52,55} As this expression profile of phase I and II metabolising genes varies between passages, it can be difficult to compare data across laboratories.⁴⁴ Still, up-regulation of specific genes by test substances could be shown. Hence, HepG2 cells may be useful to study the regulation of drug-metabolising enzymes, but not for biotransformation studies. Subclones expressing higher drug-metabolising activities have been established from some hepatoma cell lines, like HepG2/C3A, BC2 from HBG and Huh-7.5 from Huh7. Still, all of these cells are unstable at high confluence, a stage essential for reaching a high differentiation level.⁵²

The recently established human hepatoma cell line **HepaRG** was derived from a female suffering from liver carcinoma. It has a stable karyotype and a high proliferative capacity.⁴⁴ When seeded at low density, the cells rapidly recover markers of hepatic bipotent progenitors and actively divide until they reach confluence. Then, cells differentiate into hepatocyte-like and biliary-epithelial like cells. Differentiated HepaRG cells express the major cytochrome P450 iso-enzymes, various phase II enzymes, transporters and the key nuclear factors, CAR, pregnane X receptor (PXR),

and peroxisome proliferator-activated receptors (PPARs).^{44,52} Maximum xenobiotic metabolism capacity is attained at terminal differentiation of the cells which is reached after a 2-week exposure to 2% DMSO, which is a cytochrome P450 enzyme inducer.⁵² The proportion of hepatocyte-like cells compared to biliary epithelial-like cells after differentiation was reported to be approximately 55%.⁵⁶ Cells were shown to have not only a high expression of major cytochrome P450 iso-enzymes after differentiation, but expression was also inducible by specific substances. This is of high importance, especially in toxicity testing. Still, the expression of liver-specific functions was shown to vary compared to *in vivo* hepatocytes and as they represent a phenotype from a single donor, their predictive value for the human population is reduced.⁴⁴

1.3 Toxicity testing state of the art

According to the United Nations, more than 624 pharmaceutical products have been banned, withdrawn, severely restricted, or not approved by governments since the late-1950s.⁵⁷ Drug-induced liver injury (DILI) is one of the most prominent reasons. This underlines the exposure of the human liver to toxic agents against the background of its gate-keeping drug metabolism and detoxification duty in man. Choosing adequate systems for testing these substances therefore is of prime importance.

Currently, two testing strategies are pursued routinely. Firstly, animal models are used to study the systemic effects of administered compounds. These models fail in forecasting potential risks due to their phylogenetic distance to humans. Species-specific differences in metabolism lead to a failure rate of 46% of new chemical entities in subsequent clinical studies in humans due to toxicity.⁵⁸ Already in 1959 William Russell and Rex Burch published “The principles of Humane Experimental Technique” introducing their concept of the three R’s. By replacing, reducing and refining animal experiments they aimed to optimise the at that time prevalent substance testing procedures.⁵⁹ Back then, *in vitro* tissue culture models were not as advanced as of today and tissue engineering therefore was not a main focus of their work. Today, new approaches and breakthroughs have enabled us to more and more replace animal tests with human tissue models.

Therefore, the second routinely used strategy for substance testing is the application of industrially established high throughput hepatocyte test assays in 2D or 3D tissue. Still, these assays are limited to the assessment of perturbations only at the molecular, organelle and cellular levels of hepatocytes. These static cell culture assays using isolated liver enzymes, primary cells or human cell lines may show similar metabolic profiles as human *in vivo* cells, still un-physiologic culture conditions can alter gene expression of cells and lead to loss of differentiation and un-

predictive readouts. Furthermore, systemic analysis of a compounds effects is not possible using these culture models. Hence, a much better match of *in vitro* liver models to human *in vivo* biology is urgently required to predict the mode-of-action at liver organ level, and to eventually trace the entire adverse outcome pathway of an unknown toxic agent from the molecular initiating event up to the individual human organism.

A transformation of the health protection system was proposed also by e.g. the National Research Council in the USA. Their report “Toxicity Testing in the 21st Century: A Vision and a Strategy” (2007) called for fundamental changes to the way in which environmental agent toxicity is assessed. Especially, the use of computational toxicology in combination with *in vitro* human cell culture was envisaged to screen large numbers of chemicals for their toxic potential. This has been backed by all the relevant governmental institutes.^{60,61,62} In the EU, driven by animal protection movement spirit and regulatory pressure, an impressive number of scientific initiatives in this regard have been funded over the last decade. Furthermore, the European Commission had made about 238 million Euros available between 2007 and 2011 for such research. These studies were also aimed at the integration of existing *in vivo* data with *in vitro* and *in silico* approaches.⁶³ Already in 1991, the European Centre for the Validation of Alternative Methods (ECVAM) was established within the European Commission Joint Research. The main objective of ECVAM is to promote the scientific and regulatory acceptance of alternative methods which are of importance to the biosciences and which reduce, refine and replace the use of laboratory animals.⁶⁴

During the last three decades, many test guidelines have been provided by the Organisation for Economic Co-operation and Development (OECD) having relevance to the three R's. The first *in vitro* test assay to be recognised by the OECD as an alternative to animal tests was the 3T3 Neutral Red Uptake Phototoxicity Test (3T3 NRU-PT). It consists of the immortalised mouse fibroblast cell line, Balb/c 3T3 and is based on a comparison of the cytotoxicity of a chemical when tested in the presence and in the absence of exposure to a non-cytotoxic dose of simulated solar light. This assay, validated by ECVAM in 1997 and 1998 showed high sensitivity and specificity.^{65,66} Based on extensive validation testing, the 3T3 NRU-PT was adopted in 2000 by the EU and later in 2004 by the OECD as Test Guideline 432. Since then, the 3T3 NRU-PT has been used quite extensively within the pharmaceutical industry. This system, as well as *in vitro* skin sensitisation and penetration tests have gained wide acceptance and were able to replace animal experiments on a wide range.

1.3.1 Existing microfluidic devices for liver toxicity testing

So far, no human *in vitro* test guideline for the evaluation of liver toxicity on organ level exists. This is partly due to the high complexity of this organ and partly to the lack of well-characterised model systems.

Adapting *in vitro* culture conditions to the highly specialised needs of hepatocytes is of particular interest, as *ex-vivo* cultured cells tend to lose their metabolic activities as described above. Under *in vitro* conditions a variety of important culture parameters, like nutrient and oxygen supply, removal of accumulating products and mechanical force acting on the cells often cannot be controlled thoroughly and, hence, leads to a loss of function in cells.^{67,68} Thus, steadier and especially more quantifiable *in vitro* conditions are required for keeping cells viable over prolonged periods of time. Circulatory systems, where medium components are regularly removed and substituted for fresh ones, are mostly better characterised and controllable than static cultures. It was reported previously that in static culture cell secretions and culture medium nutrients generate diffusion gradients around the cells, limiting their development. The application of defined medium flow rates allow the nutrients and cell secretions to mix with the medium through perfusion.⁶⁹ This allows the generation of defined cellular microenvironments, ensuring a stable cellular phenotype and metabolising enzyme expression throughout the whole assay duration.¹⁷

Recent general reviews of “organ-on-a-chip” and “body-on-a-chip” devices describe the technological improvements in this emerging field over the last decade.^{70,71,72,73} In the following major publications for liver micro-bioreactors are discussed.

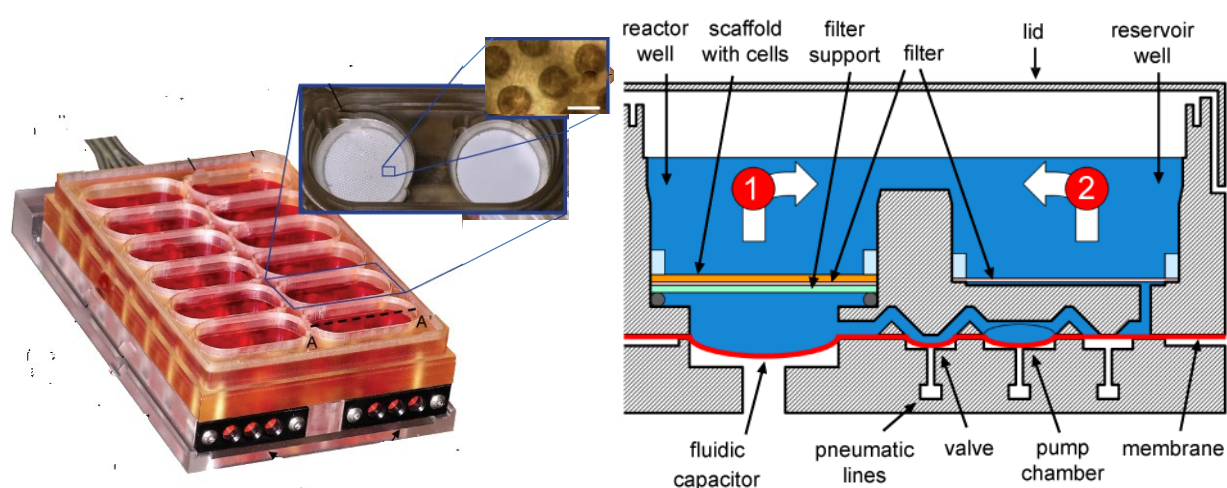


Fig 3 Systems emulating higher level liver lobule architecture. Perspective view photograph of a parallel multiplate bioreactor hosting 12 liver equivalents and the schematic cross-section of a single liver equivalent culture compartment operated by a peristaltic micropump. A sinusoidal architecture was rebuilt by co-culturing hepatocytes and endothelial cells within microchannels (240 μm long) of a scaffold. (Reprinted from ref. 74, with permission)

A high level of architectural resemblance to the *in vivo* situation was obtained by Domansky and colleagues in their microfluidic co-culture system. They built an array of multiple bioreactors into a multiwell plate comprising 12 autonomous microfluidic systems, each being perfused by an integrated pneumatic micro-pump circulating a total volume of 3 ml. Each tissue culture scaffold contained 769 multichannels (0.24 mm deep, 0.34 mm diameter) and was seeded with rat hepatocytes and endothelial cells at a 1:1 ratio. A continuous adjustable oxygen gradient could be established over long operating times. The scaffold supported near physiological tissue densities and the functional zonation of hepatocytes could be stipulated. The large channels of the scaffold support self-assembly of the two cell types in dynamic conditions.⁷⁴ Even though being highly optimised, this system has liquid to tissue ratios much higher than *in vivo* and it does not allow for the integration of additional organs hampering systemic analyses.

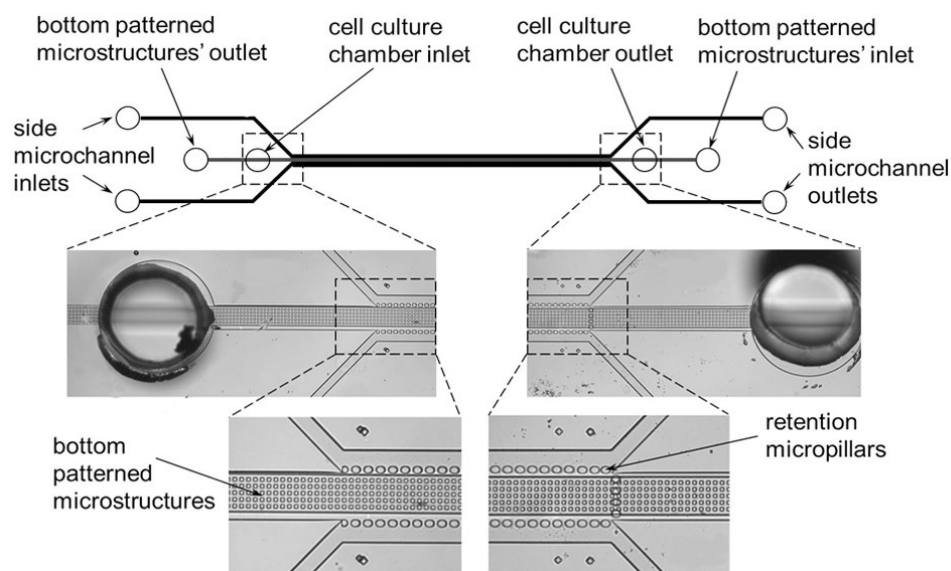


Fig. 4 System arranging hepatocytes in cord-like structures. Schematic layout of a system arranging hepatocytes in cord-like structures with additional microstructures at the channel bottom allowing traverse fluid flow. (Reproduced from ref. 77, with permission)

Another interesting approach pursued by many research groups is the arrangement of hepatocytes in cord-like structures with the potential to ensure physiological hepatocyte polarisation, release of bile into canaliculi and artificial functional zonation.^{75,76,77} A very interesting system is that of Zhang and colleagues. They developed a microfluidic channel-based system (1 cm long, 200 μm wide, 100 μm high) with an integrated array of micropillars.⁷⁵ Cells were perfusion-seeded into these structures, achieving a high 3D cell-cell interaction. The cells preserved their 3D cyto-architecture and cell-specific functions for the whole cultivation period of up to one week. The use of intercellular polymeric linkers, such as polyethyleneimine-hydrazide,

which stabilised the multicellular aggregates, facilitated the establishment of a more natural extracellular matrix environment.⁷⁶ This intercellular linker gradually disappeared from the cell surface within two days, allowing the cells to secrete their own matrix. This may promote more *in vivo*-like cellular phenotypes when compared to microfluidic systems incorporating no or exogenous matrices. An increased albumin production and higher phase I and II enzymatic activities, which improved the sensitivity of the hepatocytes to acetaminophen-mediated hepatotoxicity, was shown. Still, it is not obvious if specific zonation characteristics can be stably achieved within this system.⁷⁸ Another formation of 3D cord-like tissue structures was presented by Goral and colleagues.⁷⁷ Unlike other perfusion-based micro-devices, the bottom of the cell culture chamber was patterned with microstructures, which provided an additional control of hepatocyte polarity forming extended bile canalicular structures (Fig. 4). Cell culture media could not only be perfused through the cell compartment from the side-channels, but also via these patterned microstructures on the bottom, minimising cell spreading and cell–surface interactions. After two weeks of perfusion culture, the cells remained viable and had formed cord-like structures. An extended bile canalicular network and the formation of gap junctions between the 3D structured cells could be shown.⁷⁷ A clear segregation of bile within the cords could be achieved. The patterned microstructures at the bottom were the first step toward technical approaches allowing the separation of bile. These systems allowed for the culture of hepatocytes under well defined *in vivo* like conditions, however no co-culture with additional organs is feasible.

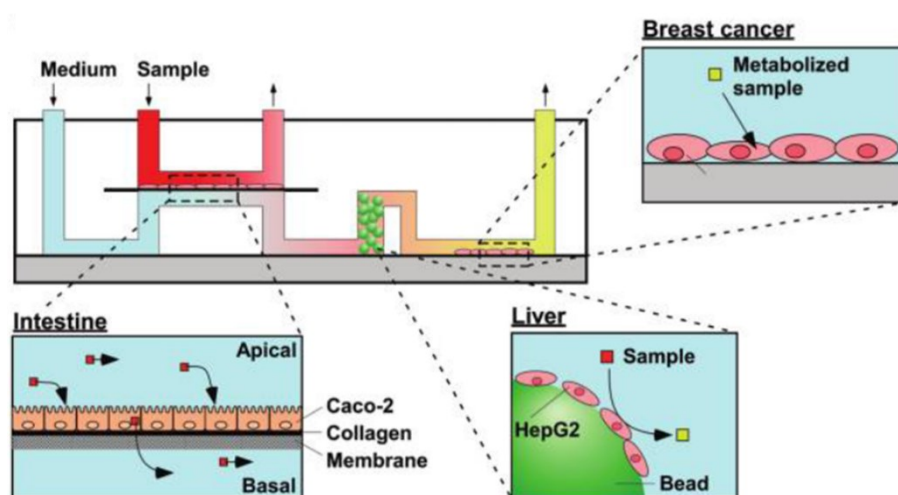


Fig. 5 Organ co-culture in a combined media circuit. Schematics of a multi-tissue device exposing hepatocytes on microspheres in a packet cylinder to substances delivered through an intestine barrier. (Reproduced from ref. 79, with permission)

Co-culture systems combining more than one organ equivalent and hence, allowing for systemic like organ-organ crosstalk were presented by Imura and colleagues as well as Shuler and colleagues. A co-culture system of carcinoma cell line HepG2 with Caco-2 (intestinal epithelial tumour) and MCF-7 cells (human breast carcinoma cell line) aiming to emulate the hepatic metabolism combined with intestinal absorption was used for the assessment of human breast carcinoma cell responsiveness to four commonly used drugs.^{79,80} The system provided an unidirectional flow in a chip format supporting the constant perfusion of HepG2 cells cultured on microspheres. Human MCF-7 cells were consecutively arranged in a single micro-channel, while drugs were provided through a fluid-tight monolayer of human Caco-2 cells into the culture medium flow of the channel in front of the liver compartment. The Caco-2 cell layer mimicked the absorptive properties of the human intestine. Still, the hepatocyte arrangement on spheres is artificial and no polarisation or functional zonation could be demonstrated.

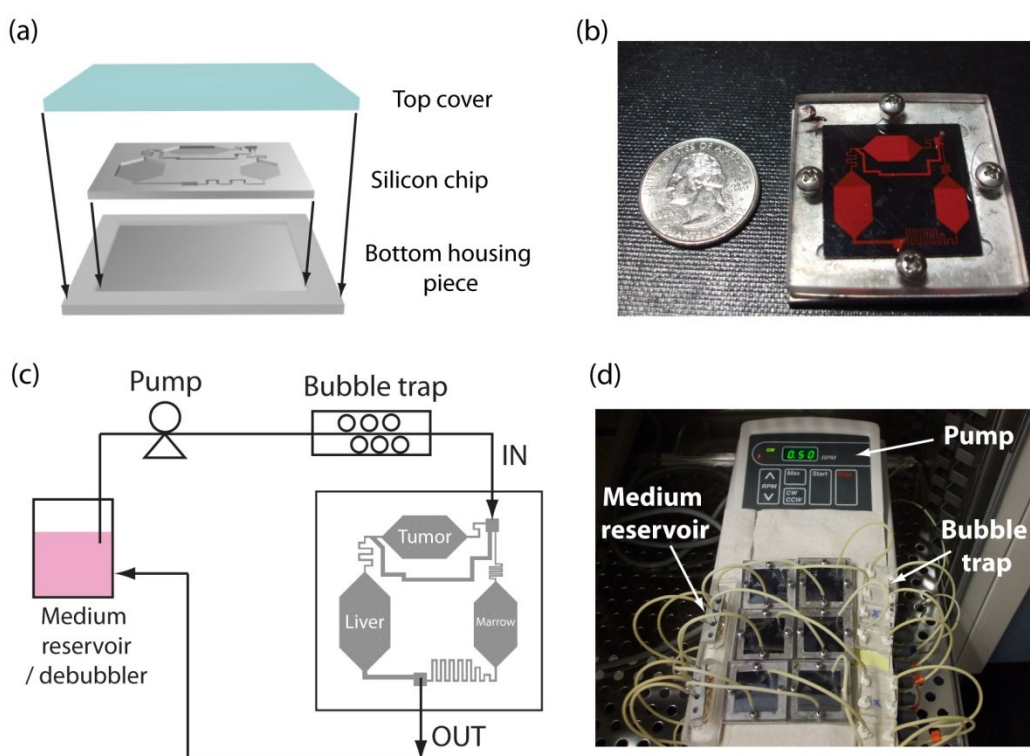


Fig. 6 Organ co-culture in a combined media circuit. A) and c) Schematic layout and b) and d) perspective view photograph of multi-organ system combining a liver equivalent, tumour and marrow equivalent. (Reproduced from ref. 82, with permission)

A system developed for pharmacokinetic and pharmacodynamic modelling by Shuler's group supported 3D hydrogel cultures of several human cell lines.^{81,82} It combined cultures of human hepatoma cells HepG2/C3A with colon cancer cells and myeloblasts in separate cell culture

chambers. The system provided *in vivo*-like tissue mass ratios inside the culture compartments, a culture medium inflow split that was equivalent to the respective blood flow split in humans, and relevant residence times in the tissue compartments. Furthermore, the microfluidic chip design was reported to support physiological shear stress and liquid-to-cell ratios comparable to those of the respective organs, and it could be operated over periods of up to four days. In order to ensure proper residence times and volumetric velocities, the flow rate in that system had been adjusted to a velocity of 168 $\mu\text{m/s}$ in the liver compartment, which is close to the *in vivo* situation, however cell density and liver compartment architecture were not. Apart from the unphysiologic architecture, this is one of the few systems which combined several culture compartments into a combined circulation supporting molecular crosstalk. To the best of my knowledge, it represents the first dynamic micro-scale system supporting a physiologically based pharmacokinetic, quantitative structure–activity relationship (QSAR) and quantitative *in vitro* to *in vivo* extrapolation modelling. Shuler and co-workers also published an in-depth description of the potential that microfluidic technologies can have for systematic drug toxicity studies.⁸³

1.4 The Multi-Organ-Chip (MOC) technology

So far, human micro-bioreactor systems for the evaluation of liver functionality under constant perfusion are rare and the few advanced systems, enabling 3D cultivation often do not allow for the integration of secondary organs into a combined media circuit. Therefore, we developed a multi-organ-chip (MOC) platform, aiming to integrate various organ equivalents into a standardised culture environment and applying physiological flow conditions.

1.4.1 Characteristics of the MOC

The multi-organ-chip (MOC) designed during the course of this study allowed for the dynamic culture of multiple organ equivalents under various culture conditions over prolonged periods of time. The MOCs were constructed the size of a microscopic glass slide to facilitate the integration into standardized culture and analysis routines. Furthermore, this glass bottom allowed for online live-cell-imaging and tissue analysis by being microscopically accessible.

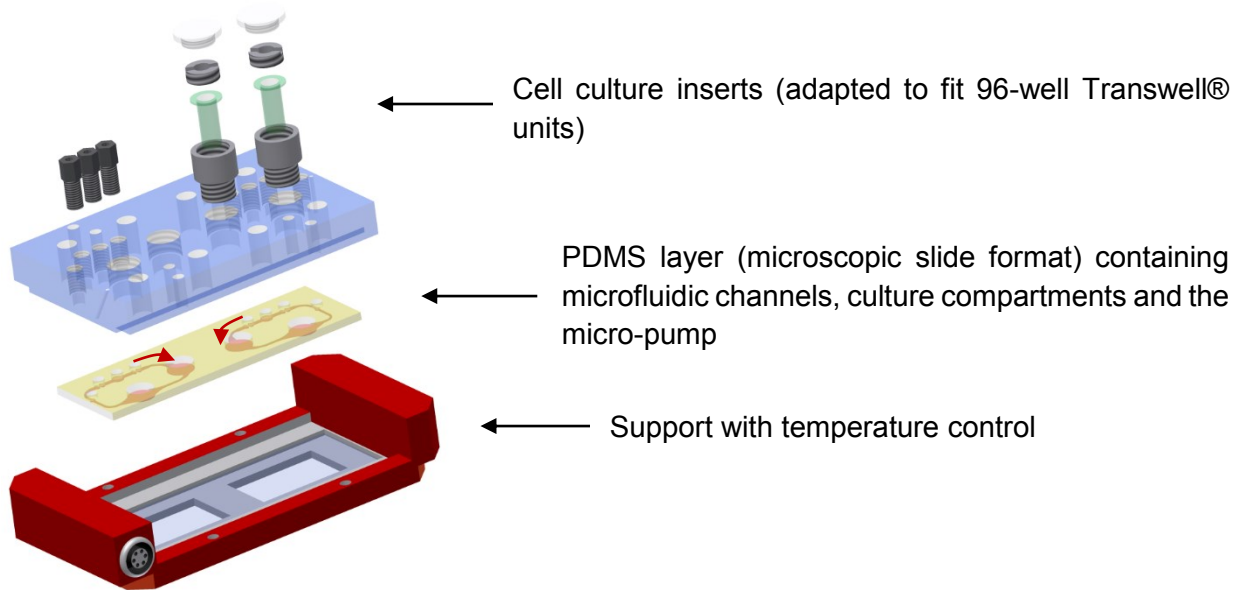


Fig. 7 The microfluidic MOC device at a glance. Explosion view of the device, showing cell culture inserts and lids (black) holding Transwell® units (green), a polycarbonate channel plate (blue), the PDMS-glass chip accommodating two microvascular circuits (yellow; footprint: 76 mm x 25 mm; height: 2 mm) and a heatable MOC-holder (red). Arrows indicate the chosen pumping direction.

MOCs were fabricated applying replica moulding of chemically inert and biocompatible polydimethylsiloxane (PDMS), resulting in a single 2 mm high PDMS layer containing the respective arrangement of channels, micro-pumps and openings for culture compartments (Fig. 7). A rapid prototyping procedure for the flexible fabrication of various designs of MOCs was established. The two tissue MOC layout used during the course of this study consisted of two separate co-culture circuits with each two cell culture compartments per circuit (Fig. 8). Here, microfluidic channels had a width of 500 μm and a height of 100 μm . The two cell culture compartments (inserts) had a diameter of 5 mm each. The small size of the MOC allowed for a maximum of 800 μl medium per circuit. It was reported previously that very low medium-to-cell volume ratios enabled cells to emulate their *in vivo* cellular micro-niches.⁸⁴

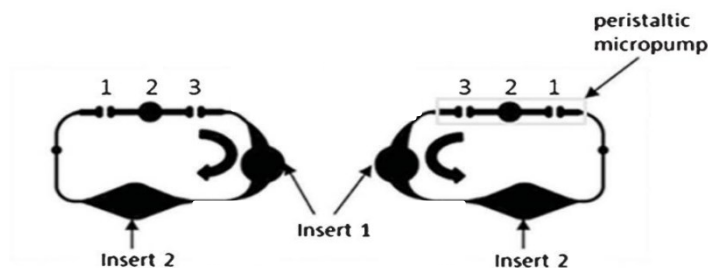


Fig. 8 Top view of the two tissue MOC layout. The two separate microfluidic circuits are illustrated (channel height: 100 μm ; width: 500 μm) each accommodating two insert areas (insert diameter: 5 mm). The peristaltic micropump consisting of three consecutive chambers drive the fluid flow in the direction of the arrows.

The PDMS layer was permanently bonded by low pressure plasma to a standard microscope glass slide with a footprint of 25 mm, thereby forming the respective fluid-tight microfluidic MOC device with standard channel heights of 100 μm .

The integrated peristaltic on-chip micro-pump was modified from Wu and co-workers and consisted of 3 PDMS membranes of 500 μm thickness in a row.⁸⁵ They were consecutively actuated by applying pressure and under-pressure. Using this micro-pump instead of conventional external pumping systems minimised the fluid-to-tissue ratio within the whole system. The pump control units fabricated by Fraunhofer IWS (Dresden, Germany) and Bioclinicum (Moscow, Russia) provided a selectable number of media flow velocities and shear stresses in the microfluidic circuit. The pumps were capable of faultlessly circulating media at sterile conditions over weeks at flow rates ranging from 7 ml/min (lowest frequency) to 70 ml/min (highest frequency). The mean velocity increased almost linearly with the pumping frequency. The frequency of pulsatile operation could be increased up to 2.4 Hz, which corresponded to a high but still physiological heart activity of 144 beats per minute in humans.⁸⁶ Furthermore, by regulating the amount of pressure applied to the pump-membranes, the peak velocities and hence, the shear forces experienced by the cells could be adjusted. Pressures of 0.1 to 0.6 bar, corresponding to maximal shear stress values of 25 dyn/cm², were applicable by the control units.

Each of the perfused tissue culture compartments was designed to the scale of a single well of a standard 96-well plate to fit industrially applied standard formats of *in vitro* culture. This allowed the direct exposure of cultures to fluid flow at the bottom of the cell culture compartments as well as the cultures to be shielded from the underlying fluid flow by standard Transwell® inserts. The latter mode, in addition, facilitated the culture of skin at the air–liquid interface.

A schematic drawing of a cut through a final MOC device is illustrated in Fig. 9. The direct exposure of tissue to fluid flow (left side) and the alternative co-culture setting in Transwells® separating tissues from the fluid flow by a 10- μm porous membrane (right side) are depicted. Arrows indicate the direction of fluid flow in a liver-skin co-culture setup. Culture compartments were designed to hold a maximum of 300 μl medium without Transwell® units and 150 μl medium containing Transwell® units.



Fig. 9 Schematic sections through the tissue culture compartments. Both submersed tissue cultures in the fluid flow (left image) and cultures in Transwell® (right image) are supported. Arrows indicate the direction of fluid flow in the MOC.

The design aimed to provide two important physiological features: mechanical coupling of tissues and their molecular crosstalk with each other. The standard tissue culture format easily enabled the combination of validated static tissue cultures of different origins within a common fluid flow.

Due to the small dimensional features of the microfluidic bioreactor, the fluid flow inside these reactors was laminar and turbulence was not likely to occur. Hence, the mass transfer relied mainly on diffusion, as is the case in the human liver.⁸⁷ As mentioned above, the laminar flow pattern also allowed for the controlled application of shear stress to the cells. Flow rates inducing high shear stress ($> 5 \text{ dyn/cm}^2$) were reported to have a negative effect on the cellular functions, whereas lower shear stress (of 0.33 dyn/cm^2) allowed for the preservation of stable cultures, measured as albumin and urea synthesis rates.⁸⁸ As the MOC also had a very high surface area to volume ratio, the oxygen supply to the cultures was very effective, especially as the oxygen permeable material PDMS was used for the reactor. This was of high importance as a poor oxygenation of liver cell cultures was reported to lead to a reduction in cell functionality and survival.⁸⁸

1.5 Substances tested on MOC co-cultures

During the course of this study, three substances were tested for their toxic potential. Troglitazone was analysed on liver-skin co-cultures, whereas *n*-hexane and 2,5-hexanedione were administered to liver-neurosphere co-cultures.

Troglitazone belongs to the thiazolidinedione (TZD) class of compounds representing a family of drugs used for the treatment of noninsulin-dependent type 2 diabetes mellitus. The first commercialised TZD drug, troglitazone (trade name: Rezulin), was withdrawn from the U.S. market after numerous reported cases of severe idiosyncratic liver damage and failures leading to liver transplantation or death.⁸⁹ The mechanisms of troglitazone-induced hepatotoxicity are not fully understood and seem to be multifactorial, one of the potential factors being the formation of reactive metabolites after enzyme-mediated bioactivation. The major pathway for troglitazone metabolism is P450 3A4-mediated oxidation.⁹⁰

***n*-hexane** has been widely used in a number of commercial and industrial applications, although it has been withdrawn from use in many contexts as it is an established neurotoxin. Hexane neuropathy is linked with direct action of the metabolite, **2,5-hexanedione** on neural tissues.⁹¹ 2,5-hexanedione reacts with neurofilament lysine ϵ -amines, yielding 2,5-dimethylpyrrole adducts, which are critical to the mechanism of toxicity. Alkylpyrroles are susceptible to autoxidative

dimerisation with subsequent cross-linking of neurofilaments. Aside from direct effects on cytoskeletal elements, mechanisms indirectly involving adduct formation may result in acute cytotoxicity. These may include oxidative stress, inhibition of key regulatory proteins, decrease of cellular reducing agents such as glutathione and disruption of the cellular energy supply.⁹²

2 Aims

There is an urgent need for improving current state of the art substance testing using *in vitro* cell culture techniques. Model systems emulating *in vivo* liver functions as closely as possible therefore need to be generated out of appropriate cells, in a 3D environment and cultivated under *in vivo* like conditions.

In this study the generation of a dynamically perfused multi-organ-chip (MOC) based test system, being biocompatible, microscopable and able to support the cultivation of various single- and multi-tissue cultures over prolonged periods of time was envisaged. Co-culturing tissues engineered from cell lines, primary cells and tissue biopsies of various organs in a common combined media circuit would allow for the analysis of organ interactions at steady state as well as at substance exposure.

Here, the generation of functional liver equivalents out of HepaRG-hSteC co-cultures is presented. We hypothesised that co-cultures in a 3D environment of tightly fused cells aid in the differentiation of HepaRG cells towards mature hepatocytes, re-establishing cell polarity and expressing functional liver markers. hSteC were supposed to aid in the generation of liver-typical extracellular matrix, as well as in the maintenance of hepatocytes in differentiated state. With such a system it was expected that the cellular interactions and metabolic functions of the liver were mimicked.

In the following, cultures of these liver equivalents in the multi-organ-chips produced in our laboratory were envisaged. The continuous perfusion with media was expected to improve cell viability over prolonged periods of time, as well as enhance hepatocyte differentiation due to the increased nutrient supply.

Co-cultures of liver equivalents with other organs like skin and neuronal tissue were targeted to show as a proof of principle, that *in vitro* multi-tissue cultures in a combined media circuit were feasible. Tissue-tissue interactions were intended to be analysed. Combining these organ co-cultures in multi-organ-chips comprising endothelialised channels was supposed to further enhance the system leading to more physiologically relevant environments and behaviours.

Finally, exposing co-cultures to substances leading to toxicity and analysing dose-dependent responses were scheduled. Experiments with substances being directly toxic to the liver as well as substances becoming toxic after being metabolised were envisaged.

The MOC system would advance our understanding of the advantages of dynamic culture over standard static *in vitro* systems, the feasibility of multi-organ co-cultures and their crosstalk as well as the effect of substances administered to the cultures in a systemic approach.

3 Materials and Methods

3.1 Materials

3.1.1 Cell sources

Undifferentiated HepaRG cells were obtained from Biopredic International (Rennes, France) acknowledging the terms of the provider's material transfer agreement. Human hepatic stellate cells (hSteC) were purchased from ScienCell Research Laboratories (Carlsbad, CA, USA).

Skin biopsies and endothelial cells were isolated from prepuce samples obtained from a pediatric surgery after routine circumcisions. Samples with an average size of 2.5 cm² were stored and transported in 10 ml phosphate-buffered saline (PBS) at 4°C and prepared for further culture within 4 hours following surgery.

Neurospheres were obtained from our collaboration partner Catarina Brito of the Animal Cell Technology Unit (iBET, Portugal).

3.1.2 Cell culture media and supplements

Table 3 Media

Media	Components	Conc.	Manufacturer
DMEM (Dulbecco's modified Eagle's medium)	DMEM incl. Glutamine, high glucose		Invitrogen
	FCS	10%	PAA
	Penicillin	100 units/ml	ThGeyer
	Streptomycin	100 µg/ml	ThGeyer

Table 3 continued

HDMEC-Medium	Endothelial Cell Growth Medium MV2		All Promocell
	FCS	5%	
	hEGF	5 ng/ml	
	R3 IGF	20 ng/ml	
	Hydrocortisone	0.2 µg/ml	
	Ascorbic acid	1 µg/ml	
	VEGF	0.5 ng/ml	
	hbFGF	10 ng/ml	
	Penicillin	100 units/ml	
	Streptomycin	100 µg/ml	
HepaRG-Medium	William's Medium E		PAA
	FCS	10%	PAA
	Human insulin	5 µg/ml	PAA
	L-glutamine	2 mM	PAA
	Hydrocortisone hemisuccinate	5 x 10 ⁻⁵ M	PAA
	Penicillin	100 units/ml	ThGeyer
	Streptomycin	100 µg/ml	ThGeyer
hSteC-Medium	SteCM basal medium		All ScienCell
	Stellate cell growth supplement		Research
	FCS	2%	Laboratories
	Penicillin	100 units/ml	
	Streptomycin	100 µg/ml	

3.1.3 Buffers and Reagents

Table 4 Buffers and Reagents

Product	Manufacturer
Cell Culture	
PBS (Phosphate buffered Saline) pH 7.4	PAA
Trypsin/EDTA	PAA
Trypan blue	Sigma
DMSO	Carl Roth

Table 4 continued

Staining		
Ethanol		Roth
Acetone, 99.7 %		Roth
ClearMount™ solution		Life Technologies
Goat serum		Sigma
Carboxyfluorescein diacetate		
Chip production		
PDMS Casting Sylgard® 184		Dow Corning
Elastosil® RT 601 (A+B)		Wacker
Wacker® primer G790		Wacker

3.1.4 Consumables**Table 5 Consumables**

Product	Type	Manufacturer
Cell culture dish	CellstarR 6, 12, 24 Well	Greiner Bio-One
Cryomold	Tissue-Tek	Sakura
HTS Transwell® Permeable Supports	96-Well, Polyester-Membrane, Pore size: 0.4; 1.0	Corning
HTS Transwell® Receiver plate	96-Well	Corning
Microtitre-plates	96-well	Greiner Bio-One
O.C.T.™ Compound		Tissue Tek®
Object slide	SuperFrost R Plus	Thermo Scientific
PAP-Pen		Pen Science Services
Perfecta3D® Hanging Drop Plate	384-Well	3D Biomatrix
Petri dish	60 mm	Greiner Bio-One
Punch	4 and 5 mm diameter	Stusche
Tissue culture flask	T 25, T 75,	Greiner Bio-One, Corning
Ultra-low attachment plate	24-well	Corning

3.1.5 Antibodies for Immunofluorescence

Table 6 Antibodies for immunofluorescence

Product	Manufacturer
Collagen I, mouse anti-human	Sigma
Fibronectin, mouse anti-human	Millipore
Laminin, rabbit anti-human	Millipore
Cytochrome P450 3A4, mouse anti-human	Santa Cruz
Cytochrome P450 7A1, rabbit anti-human	Santa Cruz
ZO-1, rabbit anti-human	Santa Cruz
MRP-2, rabbit anti-human	Santa Cruz
Cytokeratin 8/18, mouse anti-human	Santa Cruz
Vimentin C-20 R, IgG, rabbit anti-human, 200 µg/ml	Santa Cruz
Ki67, IgG, rabbit anti human, 400 µg/ml	Abcam
Conjugates secondary antibodies	
Alexa Fluor® 594, goat anti-mouse	Invitrogen
Alexa Fluor® 594, goat anti-rabbit	Invitrogen
Alexa Fluor® 488, goat anti-rabbit	Cell Signaling
Alexa Fluor® 488, goat anti-mouse	Invitrogen

After immunofluorescence staining, samples were counterstained with Hoechst 33342 (Life Technologies).

3.1.6 Kits

Table 7 Kits

Product	Manufacturer
ApopTag® Fluorescein In Situ Apoptosis Detection Kit	Merck Millipore
Albumin ELISA Quantitation Set	Bethyl Laboratories
Glucose LiquiColor® (Oxidase) kit	Stanbio
LDH Liqui-UV kit	Stanbio
LAC 142 Kit	Diaglobal
NucleoSpin® RNA isolation kit	Macherey-Nagel
SensiFAST™ Sybr No-ROX kit	Bioline
TaqMan® Reverse Transcription cDNA kit	Applied Biosystems

3.1.7 Primers

Table 8 qPCR primers

Name	Direction	Sequence
Albumin	Forward	5'-TGCAAGGCTGACGATAAGGAG
	Reverse	5'-TTTAGACAGGGTGTGGCTTTACAC
CPS-1	Forward	5'-CCCAGCCTCTCTTCCATCAG
	Reverse	5'-GCGAGATTTCTGCACAGCTTC
Cytochrome P450 1A2	Forward	5'-ATCCCCCACAGCACACAAG
	Reverse	5'-CCATGCCAAACAGCATCATC
Cytochrome P450 2B6	Forward	5'-ACCAGACGCCTTCAATCCTG
	Reverse	5'-GGGTATTTTGCCACACCAC
Cytochrome P450 2E1	Forward	5'-CATCAAGGATAGGCAAGAGATGC
	Reverse	5'-TCCAGAGTTGGCACTACGACTG
Cytochrome P450 3A4	Forward	5'-GGAAGTGGACCCAGAACTGC
	Reverse	5'-TTACGGTGCCATCCCTTGAC
UGT-1A1	Forward	5'-ATGCAAAGCGCATGGAGAC
	Reverse	5'-GGTCCTTGTGAAGGCTGGAG
GSTA-2	Forward	5'-CTGAGGAACAAGATGCCAAGC
	Reverse	5'-AGCAGAGGGAAGCTGGAAATAAG
MDR-1	Forward	5'-TGGATGTTTCCGGTTTGGAG
	Reverse	5'-TGTGGGCTGCTGATATTTTGG
MRP-2	Forward	5'-ACCTCATCCAGTCCACCATCC
	Reverse	5'-GGCCATGCTGTAGAAAAGACCTC
BSEP	Forward	5'-GCAGACACTGGCGTTTGTG
	Reverse	5'-ATGTTTGAGCGGAGGAAGTGG
TBP	Forward	5'-CCTTGTGCTCACCCACCAA
	Reverse	5'-TCGTCTTCCTGAATCCCTTTAGAATAG

3.1.8 Materials of the Multi-Organ-Chip

Table 9 Materials of the Multi-Organ-Chip

Equipment	Type	Manufacturer
Casting station		GeSiM
Channel master	A040-705	GeSiM
Channel plate	M3	SMC
	M5	GeSiM
Hexagon Socket Head Male Connector	M3	SMC
I-Fitting, PEEK	A040-706	Bülte
Insert spacer	A040-708	Wagner Kunststofftechnik

Table 9 continued

Injection port spacer	M5	RCT
Lid	A040-709	Bülte
Membrane spacer, POM	A040-710	GeSiM
MOC-Support	MOC-I J-28 UNF6 M10 (PEEK)	GeSiM
Needle, unbevelled		BBraun
Object glass slide	76x26mm	Thermo Scientific
Peristaltic pumps		Capitalis Technology and BioClinicum
Pump connectors		SMC
Pump spacer		Feinmechanik Willi Müller
Surgical scalpel, disposable	A040-702	Menzel
Syringe	1ml	BD
Syringe adapter	POM	Idex
Transwell®-holder, PEEK	A040-716	Bülte

3.1.9 Devices and technical support

Table 10 Devices and technical support

Device	Type	Manufacturer
CO ₂ -Incubator		Sanyo
Digital camera	E-3	Olympus
Fluorescence microscope	BZ9000	Keyence
Light microscope	Axiovert 40C	Zeiss
Microplate-reader	FLUOstar Omega	BMG Labtech
Microtome	CM 1950	Leica
Neubauer counting chamber	Improved	A. Hartenstein
Plasma-chamber	Femto	Diener
Vacuum desiccator		Nalgene

3.2 Methods

3.2.1 Multi-Organ-Chip fabrication

Multi-Organ-Chips were fabricated applying standard soft lithography and replica moulding of PDMS. The fabrication procedure was subdivided into two parts:

I. Casting of chips

The casting of the micro-systems was as follows: A polycarbonate cover-plate was treated with a silicon rubber additive (WACKER® PRIMER G 790; Wacker Chemie, Munich, Germany) at 80°C for 20 min. Teflon screws were inserted to create four PDMS-free compartments for culture and six 500 µm thick PDMS membranes to connect the micro-pumps. The prepared cover-plate was plugged to the master mould (channel height 100 µm, width 500 µm) and PDMS (10:1 v/v ratio of PDMS to curing agent) was injected into this casting station. The set-up was incubated at 80°C for 60 min.

II. Bonding and filling of chips

The resulting 2-mm high PDMS layer containing the respective arrangement of channels, micro-pumps and openings for culture compartments was permanently bonded by low pressure plasma oxidation (Femto; Diener, Ebhausen, Germany) to a glass microscope slide with a footprint of 75 x 25 mm (Menzel, Braunschweig, Germany), thus forming the fluid-tight microfluidic MOC device with standard channel heights of 100 µm. Respective adapters were screwed into the polycarbonate cover-plate and chips were subsequently filled with respective medium using 1 ml syringes.

3.2.2 Cell culture

All cell culture work has been performed sterile under a laminar flow workbench. Cell cultures were incubated at 37°C, 5% CO₂ and 95% air humidity.

3.2.2.1 HepaRG cells

HepaRG cells were obtained from Biopredic International (Rennes, France) and maintained as described by Gripon *et al.*⁹³ Undifferentiated cells were maintained in 75 cm² tissue culture flasks at a seeding density of 2 x 10⁴ cells/cm² for two weeks, according to the manufacturer's instructions. Medium was renewed every 2 or 3 days. Induction of differentiation was initiated by

maintaining the cells in growth medium (HepaRG-medium) for 2 weeks in order to reach cellular confluence. Differentiation medium containing 2% dimethylsulfoxide was then added for a cultivation period of another 2 weeks. When differentiation was completed, the cells were used for further experiments.

3.2.2.2 Hepatic stellate cells

Human hepatic stellate cells (hSteC) were seeded at 5×10^3 cells/cm² in poly-L-lysine-coated 75 cm² tissue culture flasks in hSteC-medium for maintenance, according to the manufacturer's instructions. Medium was exchanged every 2 or 3 days. Cells were harvested for further use at 90% confluence.

3.2.2.3. Human dermal microvascular endothelial cells

Human dermal micro-vascular endothelial cells (HDMECs) were isolated from human foreskin by my colleagues Katharina Schimek and Ilka Wagner and grown in MDMEC-medium.⁸⁶ HDMECs were expanded until 70-90% confluence at a 3 day feeding regimen. Cells between the 3rd and 8th passage were used for all studies to ensure that the cells retained their primary endothelial characteristics.

3.2.2.4. Skin biopsies

Human juvenile prepuce was obtained from a paediatric surgery after routine circumcisions, with written consent and ethics approval as per the guidelines of the Ethics board of the Charité - Universitätsmedizin Berlin. Routinely, samples were sterilised in 80% ethanol for 30 sec and punched to biopsies with 4 or 5 mm diameter by my colleague Ilka Wagner, depending on the culture set-up chosen. One biopsy was loaded into a single MOC culture compartment for cultivation. Samples from one donor were used for each MOC-based test series and the respective control in static culture.

3.2.3 Passaging of cells

First, medium was removed from the cell layer and cells were washed twice with PBS+. To detach the cells from the culture ware, pre-warmed Trypsin/EDTA was added to the cells, followed by an

incubation period of 3 to 5 min. The reaction was stopped by the addition of double volume of respective cell specific medium containing FCS. The cell suspension was centrifuged at 150 g and room temperature (RT) for 5 min. Medium was removed and cells were re-suspended in fresh medium.

3.2.4 Cell counting

Counting the cells, 10 μ l cell suspension were mixed with 10 μ l trypan blue. This dye can penetrate cell membranes of dead cells staining them blue. 10 μ l of the mix were added below the cover glass of a Neubauer counting chamber. Living and dead cells were counted in four large squares below the microscope.

3.2.5 Freezing and thawing cells

For long term storage of cells, the respective cells were detached from the plastic ware as described in 3.2.3. The cell pellet was then re-suspended in FCS containing 10% DMSO to make up a final concentration of 1 to 1.5×10^6 cells/ml. The suspension was slowly cooled down to -80°C . After freezing was completed, cells were transferred to liquid nitrogen for long-term storage. Thawing the cells was carried out at 37°C in a water bath. Shortly before the whole suspension was melted, it was transferred to 10 ml of pre-warmed culture medium. Afterwards, cells were centrifuged at 150 g for 5 min, re-suspended in fresh culture medium and seeded to respective cell culture ware.

3.2.6 Aggregate formation

Liver micro-tissue aggregates were formed in Perfecta3D® 384-Well Hanging Drop Plates, according to the manufacturer's instructions. Briefly, 20 μ l cell suspension containing 4.8×10^4 hepatocytes and 0.2×10^4 hSteC were pipetted to each access hole. After two days of hanging drop culture, aggregates were transferred to ultra-low attachment 24-well plates with a maximum of 20 aggregates per well.

3.2.7 Bioreactor co-culture

3.2.7.1 Seeding organoids into inserts

Following culture in ultra-low attachment wells for a maximum of 3 to 4 days, 20 aggregates were loaded into a single tissue culture compartment of each MOC circuit. Similarly, skin biopsies of 4 mm diameter were loaded directly into the respective culture compartment for co-culture. Additional MOCs were loaded solely with skin biopsies for comparison. Subsequently, 300 µl of medium was added to each culture compartment, which was then hermetically closed by a lid.

3.2.7.2 Seeding organoids in Transwell® assisted cultures

Liver micro-tissues and epidermal-side up skin biopsies of 5 mm diameter were cultured each in a separated single insert of a 96-well Transwell® unit. Therefore, two wells per circuit from a 96-well Transwells® plate (0.4 µm pore size) were cut below the bracket with an incandescent knife and removed. Organoids were transferred into the excised Transwells® which were positioned into the Transwell®-holders and screwed into the MOC. Transwells® was hung inside the chip with the membrane fitting directly over the circuit. Tissue culture compartments were filled with a total volume of 150 µl medium each to inoculate the MOC.

3.2.8 Vascularisation of the channels

Experiments performed in endothelialised MOCs were prepared as follows: Prior to seeding human dermal microvascular endothelial cells into the MOC, each circuit was flushed with HDMEC medium and incubated statically for 3 days. Then cells were harvested, concentrated by centrifugation and viable cell count determined. Cell populations with a viability > 90% were used for seeding the chip. The cell suspension was adjusted to a concentration of 2×10^7 cells/ml, 200 µl of this suspension was injected through one of the two compartments of each circuit. Therefore, the cells were transferred to a 1 ml syringe, which was thereafter connected to a female Luer x¹/₄-28 male adapter. This fitting was then screwed to a special thread MOC adapter. After even cell infusion into both circuits the device was incubated at 5% CO₂ and 37°C under static condition for 3 h to allow the cells to attach to the channel walls. To reach a full coverage of cells also on the upper side of the channels, the seeding procedure was thereafter repeated once, incubating the chip upside-down for 3 h after seeding. Afterwards, 300 µl fresh medium was added to each compartment and flushed through the PDMS channels using the on-chip micro-pump. Cell culture

medium was replaced every 1 to 2 days and cell growth monitored by light microscopy.⁸⁶

3.2.9 Bioreactor operation

Pumping conditions were set to 0.6 bar and 1.5 to 2 Hz. During the first 5-7 days, a 40% to 50% media exchange rate was applied at 12 h intervals. From day 6-8 onwards, the exchange rate was reduced to 24 h intervals. Daily samples were collected for respective analyses. Experiments were performed in quadruplicate or more.

3.2.10 Administration of troglitazone for toxicity testing

Troglitazone was dissolved in DMSO and stored frozen at a concentration of 20 mM until used, and then diluted in culture medium to a level of 0.25% DMSO. Medium containing 0.25% DMSO was used for control cultures. Liver micro-tissue and skin biopsy co-cultures in MOCs were prepared and cultured as described above. The organ equivalents in the MOCs were cultured for one to five days prior to exposure and were, subsequently, exposed to varying concentrations (0 μ M, 5 μ M and 50 μ M) troglitazone, respectively. Application of troglitazone was repeated at 24 h intervals simultaneously with the medium change.

3.2.11 Administration of n-hexane and 2,5-hexanedione for toxicity testing

n-hexane was added directly to the respective culture compartments of the MOC, 2,5-hexanedione was dissolved in the culture medium to make a final concentration of 16 mM and 32 mM. Medium containing no substance was used for control cultures. Application of n-hexane and 2,5-hexanedione was repeated at 24 h intervals simultaneously with the medium change.

3.2.12 Analysis

Following the completion of an experiment, liver equivalents were frozen in Tissue Tek® OCT compound and stored at -80 until further analysis.

3.2.12.1 Immunohistochemistry

Preparation of cryostat micro-sections

Frozen samples were transferred to the cryostat and allowed to adapt to cryochamber temperature of -20°C and object head temperature of -18°C for up to 15 min. Specimens were fixed to deeply grooved specimen discs using Tissue Tek®. First redundant Tissue Tek® was removed from the edges of the samples, then specimens were trimmed at step sizes of 50 µm until the centre of the specimen was reached. These 50 µm sections were collected in pre-cooled 1.5 ml Eppendorf Tubes®. Central sections of 8 µm thickness were transferred to SuperFrost R Plus object slides. 4 to 6 slides were prepared per sample. The rest of the specimen was cut at 50 µm and collected as described above. Object slides containing samples were allowed to dry at room temperature for 1 h to 3 h and subsequently stored at -20°C for immunofluorescence staining. The collected 50 µm sections were re-suspended in 400 µl RA1 buffer containing β-mercaptoethanol and stored at -80°C for RNA isolation.

Immunofluorescence staining

For immunofluorescence staining, representative central cryosections of tissues were fixed in acetone at -20°C for 10 minutes. Staining was performed in a total volume of 50 µl as follows:

- I. 3x wash with PBS for 5 min
- II. Block with serum for 20 min at RT
- III. Incubate with primary antibodies overnight at 4°C
- IV. 3x wash with PBS for 5 min
- V. Incubate with secondary antibody for 45 min at RT
- VI. Counterstain nuclei with Hoechst 3342

To obtain a double staining with two primary antibodies on one sample, after reaching step V steps I to V were repeated with the second antibody pair, before counterstaining with Hoechst.

Live dead staining

Furthermore, apoptosis and proliferation were analysed by immunohistological end-point staining at the end of each MOC experiment using TUNEL (TdT-mediated dUTP-digoxigenin nick end labelling) / Ki67 markers. Briefly, eight-micron cryostat sections per sample were stained for

apoptosis using the TUNEL technique (ApopTag® Peroxidase In Situ Apoptosis Detection Kit, Merck Millipore, Darmstadt, Germany) according to the manufacturer's instructions. The apoptosis staining was combined with a nuclear stain using Hoechst 33342 and, in case of staining for proliferation, the antibody Ki67 was used.

3.2.12.2 Bile canalicular staining

Monolayers of HepaRG cells were subjected to bile canalicular staining using carboxyfluorescein diacetate. Differentiated HepaRG cells metabolise carboxyfluorescein diacetate and excreted it to the bile, staining canaliculi with a green fluorescence. Therefore, differentiated cells were washed three times with PBS and treated with carboxyfluorescein diacetate (1 mg/ml in DMSO) at a final concentration of 2 µg/ml for 5 to 10 minutes at 37°C. Cultures were subsequently rinsed several times with PBS and incubated for further 30 min in HepaRG-medium before being viewed and photographed.

3.2.12.3 qPCR

Gene expression analysis was carried out on mRNA level by semi-quantitative real time PCR.

RNA isolation and cDNA preparation

Isolation of mRNA was performed using the NucleoSpin® RNA II kit (Macherey-Nagel, Germany) following the manufacturer's instructions.

Monolayer cultures were washed with PBS and directly re-suspended in 350 µl RA1 buffer containing 1:1000 beta-mercaptoethanol. Liver equivalents were collected after the MOC cultures were stopped, frozen in Tissue Tek® at -80°C and cut in the cryostat to 50 µm sections (see above). The sections were collected and resuspended in 400 µl RA1 buffer containing 1:1000 beta-mercaptoethanol. For the elution step, 10 µl RNase-free H₂O was used. Isolated RNA was stored at -80°C.

cDNA was synthesised by reverse transcription of 400 ng total RNA by the Taq-Man® Reverse Transcription Reagents cDNA kit (Applied Biosystems, USA) as follows:

400 ng RNA
2 µl TaqMan 10x buffer
0.5 µl oligo dTs
0.5 µl Random Hexamer
4.4 µl MgCl₂ (25 mM)
0.3 µl Reverse Transcriptase
0.4 µl RNase Inhibitor
4 µl dNTPs (25 mM each)
in 20 µl H₂O (DMSO free)

Transcription was performed in a thermo cycler (PqLab, Germany) with an annealing step for 10 min at 25°C, an elongation step for 40 min at 48°C and an inactivation step for 5 min at 95°C to inactivate the reverse transcriptase. cDNA samples were stored at -20°C until further use.

Real-time qPCR

Real-time qPCR experiments were conducted by using the SensiFAST™ Sybr No-ROX One-Step Kit (Bioline, Luckenwalde, Germany) with 1 µl cDNA and 1 µl primer mix in a volume of 20 µl. 96-well PCR plates (Biozym Scientific, Germany) were read with Stratagene MX 3005P™ Multiplex Quantitative PCR System (Agilent Technologies, USA).

To achieve complete dissociation of the RNA-DNA double strand samples were heated to 95°C for four minutes. Next cDNA was melted at 95°C for 12 seconds followed by a primer annealing step at 64°C for 11 seconds and an elongation step at 72°C for 12 seconds. These steps were repeated for 40 cycles. A dissociation curve was recorded by dissociating the strands for three minutes at 95°C, cooling them to 64°C and stepwise heating up to 95°C again. The fluorescence intensity of SybrGreen was measured with every 0.5°C increment. This dissociation curve verified the amplification of specific products without a contamination by unspecific side products of primer dimers.

The expression of genes was recorded as a specific Crossing point (Cp) value which was normalised to the expression of a housekeeping gene *TATA box binding protein (TBP)*. This gene was chosen based on literature research for HepaRG housekeeping genes.⁹⁴ Housekeeping gene ratios were plotted in logarithmic charts, which allowed the comparison of expression strength of several genes. Expression ratios were calculated according to the following formula:

$$E^{\text{cp}_{\text{HK}}} / E^{\text{cp}_{\text{gene}}}$$

with E = amplification efficiency, HK = housekeeping gene and $gene$ = gene of interest.

3.2.12.4 Metabolic parameters

LDH

Tissue viability was monitored daily by the measurement of lactate dehydrogenase (LDH) released into the supernatants. In brief, samples were immediately measured for LDH concentration and then stored at -80°C for further analysis of glucose, lactate and albumin. All absorbance-related measurements were performed in 96-well microtitre-plates in a microplate-reader. The LDH concentration of the medium was measured using the LDH Liqui-UV kit (Stanbio Laboratory, Boerne, USA), according to the manufacturer's instructions with minor modifications based on our own standard curves: An amount of 100 µl of reagent was used and 1 µl of the sample was added for each measurement.

Albumin

The Human Albumin ELISA Quantitation Set (Bethyl Laboratories, Montgomery, USA) was used to measure the albumin concentration, according to the manufacturer's instructions.

Glucose

Glucose consumption, lactate production and albumin synthesis was monitored daily to assess the metabolic activity of the tissues in the MOC. The Glucose LiquiColor® Oxidase kit (Stanbio Laboratory, Boerne, USA) was used with minor modifications: 100 µl of reagent was used and 1 µl of sample was added

Lactate

Lactate concentration of the medium was measured using the LAC 142 kit (Diaglobal, Berlin, Germany), according to the manufacturer's instructions with minor modifications based on our own standard curves: 99 µl of the reagent was mixed with 1 µl of sample and absorbance was measured at 520 nm, using medium as a reference.

3.2.13 Statistical analysis

An unpaired student t-test was applied to the data sets, using GraphPad Prism® software version 5.0 (GraphPad Software Inc., USA). P-values smaller than or equal to 0.05 were considered significant. * indicates $p \leq 0.05$, ** $p \leq 0.01$ and *** $p \leq 0.001$.

4 Results

Functional liver equivalents generated out of HepaRG cells and human hepatic stellate cells (hSteC) were characterised and subsequently cultivated in the multi-organ-chip (MOC) for up to 28 days. Cultures were performed as liver single-tissue mono-cultures, as well as co-cultures, combining the liver equivalents with skin biopsies, endothelial cells or neuronal tissue. Additionally, toxicity testing using troglitazone, n-hexane and 2,5-hexanedione were performed.

First, the generation of functional liver equivalents required the characterisation of the cell types used, the optimisation of 3D culture conditions and finally the characterisation of equivalents produced.

4.1 Characterisation of differentiated HepaRG cells

During differentiation of HepaRG cells as described in 3.2.2, cells changed their morphology from disperse growing elongated cells towards a confluent monolayer of polygonal-shaped cells with a network of bright spots in between the cells. To confirm the polarisation and formation of functional bile canaliculi, fully differentiated monolayers were treated with carboxyfluorescein diacetate, which was subsequently metabolised and excreted to the bile. After a post-incubation period of up to 30 min, bile canaliculi could be detected in cells differentiated towards the hepatic lineage by green fluorescence (Fig. 10). No fluorescence was observed in the area of cells differentiated towards biliary-epithelial-like cells (cholangiocytes). The formation of a functional bile canaliculi-like network confirmed the terminal differentiation of cells towards the hepatic lineage.

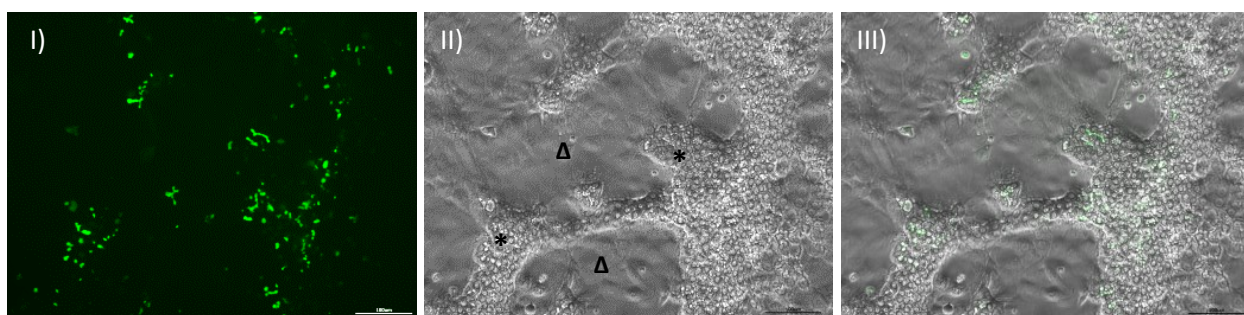


Fig. 10 Fluorescence and light microscopy of differentiated HepaRG monolayer treated with carboxyfluorescein diacetate. I) Green fluorescent image of carboxyfluorescein diacetate secreted into bile canaliculi (green). II) Brightfield image of HepaRG cells differentiated towards the hepatic lineage (*) or towards cholangiocytes (Δ) III) Overlay of the two channels. Scale bar: 100 μ m

4.2 Characterisation of hSteC

hSteC, representing liver non-parenchymal cells, were cultivated in 8-well chamber slides until reaching confluence and stained as described in 3.2.12. The cells stained positive for extracellular matrix components collagen type I (collagen I), fibronectin and laminin as shown in Fig 11. Furthermore, cells were positive for vimentin (data not shown). Having confirmed the cells ability to produce liver-typical extracellular matrix, these cells were admixed to HepaRG cells to form cellular aggregates.

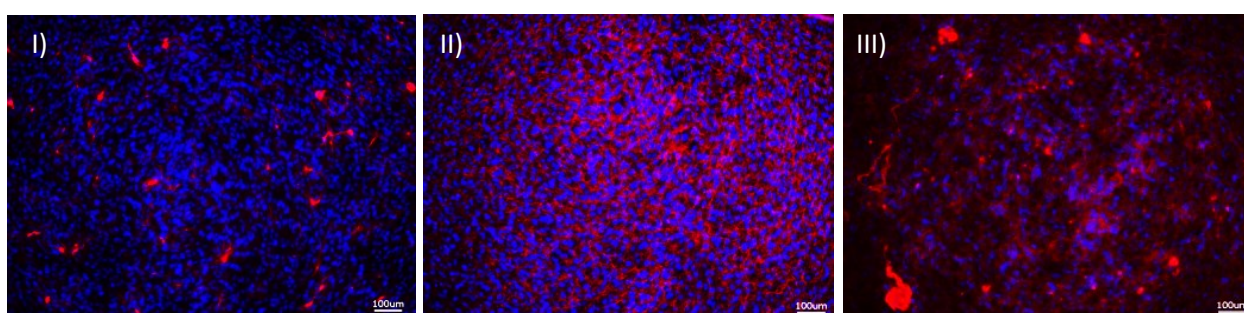


Fig. 11 Fluorescence microscopy of immunostained hSteC monolayer for I) collagen type I (red) II) fibronectin (red) and III) laminin (red). Nuclear stain (blue). Scale bar 100 μ m.

4.3 Production of liver cell aggregates

Liver cell aggregates were produced out of HepaRG cells and hSteC at a ratio of 24 to 1 with a total of 5×10^4 cells per aggregate. A preliminary work performed by the bachelor student Ute Süßbier under my supervision revealed that this ratio was optimal for aggregation and generation of functional liver tissue. These aggregates formed during 2 days of hanging drop culture had a disk-shaped morphology with a medium diameter of 300-400 μ m and a height of 200-300 μ m, as determined microscopically. A reliable production of 300 spheres per 384-Well Hanging Drop Plate was achieved. After two days, aggregates were transferred to ultra-low-attachment 6-well plates (20 aggregates per well) until further use after up to 4 days.

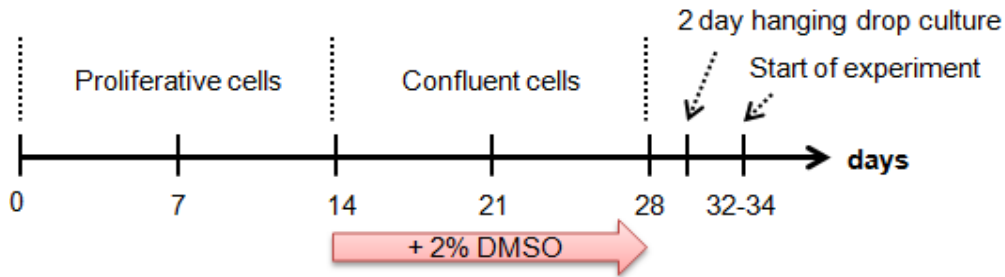


Fig. 12 Schematic representation of the aggregation process. Cells were cultured for two weeks until reaching confluence. Then, DMSO was added to induce differentiation. After differentiation was completed, cells were aggregated in hanging drop plates. Aggregates were used no longer than 3 to 4 days after production.

If cultured under static conditions for more than 2 days, aggregates moved together and fused to form a single huge cell aggregate (Fig. 13). To avoid this, ultra-low-attachment plates containing aggregates were placed on a rocker inside the incubator.

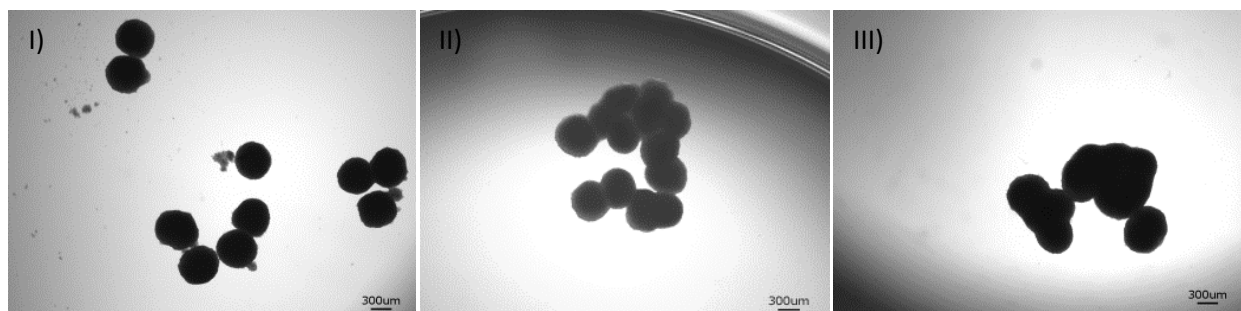


Fig. 13 Light microscopy of human liver aggregates cultivated in ultra-low-attachment plates. I) Aggregates on day 0 were well dispersed, II) started to fuse on day 5 and III) formed densely packed fused aggregates on day 7 of static culture. Scale bar 300 µm.

Immunohistochemical staining of the newly formed aggregates for vimentin and cytokeratin 8/18 revealed that the hSteCs were distributed equally throughout the whole aggregate (Fig. 14). Furthermore, staining for tight junction protein ZO-1 and apical transporter MRP-2 was weak but positive in 2 days old aggregates, indicating that cells had not yet polarised anew completely and reformed bile canaliculi-like structures only to a certain extent. TUNEL / Ki67 staining revealed that proliferative cells were distributed homogeneously throughout the aggregate, whereas no apoptotic cells could be observed. Also, fibronectin staining was homogeneously distributed throughout the whole sphere.

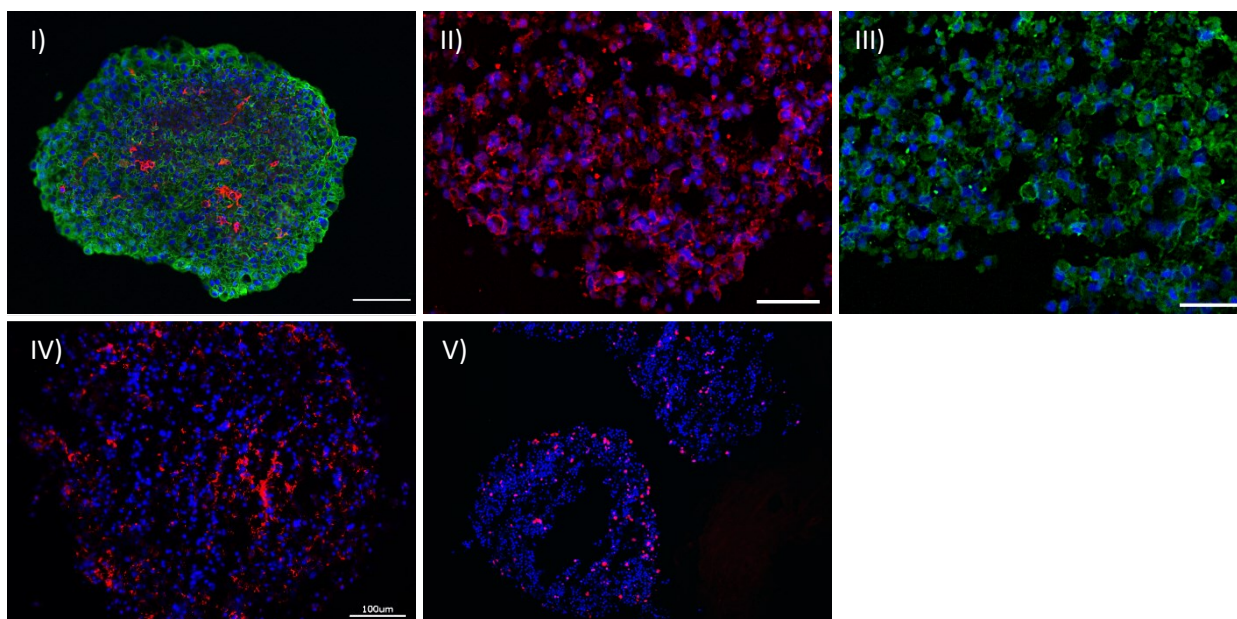


Fig. 14 Immunostaining of 2 day old liver aggregates for **I)** vimentin (red) and cytokeratin 8/18 (green) shows an equal distribution of hSteC throughout the HepaRG cell aggregate. **II)** Tight junction marker ZO-1 (red) and **III)** canalicular transporter MRP-2 (green) were weak but positive, indicating that cells had not yet polarised anew completely reforming bile canaliculi-like structures. **IV)** Fibronectin (red) staining was homogenously distributed throughout the aggregate. **V)** TUNEL / Ki67 staining showing proliferative cells (red) distributed throughout the aggregate and absence of apoptotic cells (green). Nuclear stain (blue). Scale bar 100 µm.

Furthermore, aggregates cultured for up to 4 days under static conditions were analysed by qRT-PCR as described in 3.2.12. Aggregates that had been treated for 3 days with 20 µM rifampicin (a known cytochrome P450 3A4 inducer) were included into the analysis, as well as undifferentiated and differentiated HepaRG monolayer cells. The transcription level for albumin varied strongly within the differentiated HepaRG monolayers (Fig. 18). Differentiation of the cells in the presence of DMSO had been performed for one to three weeks, with the cells being differentiated longest having the highest albumin expression. Similarly, the expression levels for BSEP (canalicular transport protein), CPS-1 (urea cycle) and GSTA-2 (phase II metabolising enzyme) increased with differentiation time, proving approximation towards the major hepatic phenotype. Newly formed aggregates, as well as aggregates treated for 3 days with rifampicin showed a similar expression level as differentiated cells for most markers. Interestingly, cytochrome P450 expression was lower in newly formed aggregates than in differentiated HepaRG cells, which might be due to the omission of DMSO during the aggregation process. DMSO is a known cytochrome P450 inducer. Still, treating aggregates with rifampicin, expression levels increased significantly to levels even higher than in terminally differentiated monolayers, proving inducibility of cytochrome P450 3A4 in newly formed aggregates.

Having proven metabolic capacity and viability of aggregates, henceforth also termed liver equivalents, dynamic cultures in the MOC were envisaged.

4.4 Dynamic culture of organ equivalents inside the MOC - overview

Culturing the liver equivalents inside the MOC, 20 aggregates corresponding to 10^6 cells were seeded in one tissue culture compartment of each MOC circuit.

First, liver aggregates were cultured in the MOC as single tissue cultures, later additional organs like skin, vasculature and neuronal aggregates were co-cultured with the liver equivalents. The respective culture conditions like pumping velocity, culture medium and feeding rate were adapted to the respective organ cultures and are stated at the beginning of each chapter. Furthermore, organ equivalents were cultured either inside Transwell® (TW®) cell culture inserts or directly exposed to the fluid flow inside the cell culture compartment of a MOC (see Fig. 4 introduction).

Analysis included online measurements of LDH, glucose, lactate and albumin from media supernatants and end-point analysis of organ equivalents by qRT-PCR and immunohistochemistry. Experiments were always performed in triplicate or quadruplicate. In total 9 different experimental conditions are discussed in the following (Table 11).

Table 11 overview of MOC culture conditions

Nr.	Organs	Substance tested	Culture setup	Pump setup	Feeding regimen	Time [days]
1	Liver	None	TW®	2 Hz 0.6 bar	24 h (50%)	14
2	Liver	None	Exposed to flow	2 Hz 0.6 bar	24 h (50%)	14
3	Liver & Skin	None	TW®	2 Hz 0.6 bar	12 h for 7 days, than 24 h (40%)	28
4	Liver & Skin	None	Exposed to flow	2 Hz 0.6 bar	12 h for 7 days, than 24 h (40%)	14
5	Liver & Skin & Vasculature	None	liver exposed to flow, skin in TW®	2 Hz 0.6 bar	12 h for 5 days, than 24 h (50%)	15
6	Liver & Neurons	None	Exposed to flow	1.5 Hz 0.6 bar	12 h for 5 days, than 24 h (45%)	14
7	Liver & Skin	Troglitazone, starting day 1	Exposed to flow	2 Hz 0.6 bar	12 h for 5 days, than 24 h (40%)	7
8	Liver & Skin & Vasculature	Troglitazone, starting day 5	liver exposed to flow, skin in TW®	2 Hz 0.6 bar	12 h for 5 days, than 24 h (50%)	15
9	Liver & Neurons	n-hexane or 2,5-hexanedione, starting day 5	Exposed to flow	1.5 Hz 0.6 bar	12 h for 5 days, than 24 h (40%)	14

TW®: cell culture insert (Transwell®)

Experiments were performed in HepaRG medium, with the exception of those including vasculature, which were performed in 80% HepaRG and 20% HDMEC medium.

4.5 Liver single-tissue cultures inside the MOC

Table 12 culture conditions of liver single tissue cultures inside the MOC

Nr.	Organs	Substance tested	Culture setup	Pump setup	Medium	Feeding regimen	Time [days]
1	Liver	None	Culture insert (TW®)	2 Hz 0.6 bar	HepaRG	24 h (50%)	14
2	Liver	None	Exposed to flow	2 Hz 0.6 bar	HepaRG	24 h (50%)	14

4.5.1 MOC culture of liver tissue in cell culture inserts

The experimental setups of liver single tissue cultures inside the MOC are described in Table 12. First, liver equivalents were cultured in Transwell® cell culture inserts. Therefore, aggregates were placed in 96-well Transwell® units of a pore size of 0.4 µm that were hung inside the chip with the membrane fitting directly over the perfusion circuit. A daily media exchange rate of 50% total culture volume was performed.

Aggregates adhered to the bottom membrane of the Transwell® separating the culture insert from the underlying MOC channel and spread out slightly. End-point immunohistochemical staining revealed that after a culture period of 14 days HepaRG cells in the aggregates had produced the liver-typical extracellular matrix protein fibronectin, whereas a co-staining of vimentin and collagen I showed that hSteC, still distributed throughout the whole aggregates, had also actively secreted matrix (Fig. 15 a). Staining for phase I metabolic enzymes cytochrome P450 3A4 and 7A1 was intense, whereat cytochrome P450 3A4 was slightly higher expressed at the side of the aggregate facing the MOC channel, hinting at zonal differences within the aggregate. ZO-1 and MRP-2 staining were strongly positive and showed a network-like arrangement, suggesting the establishment of bile duct-like structures (Fig. 15 b).

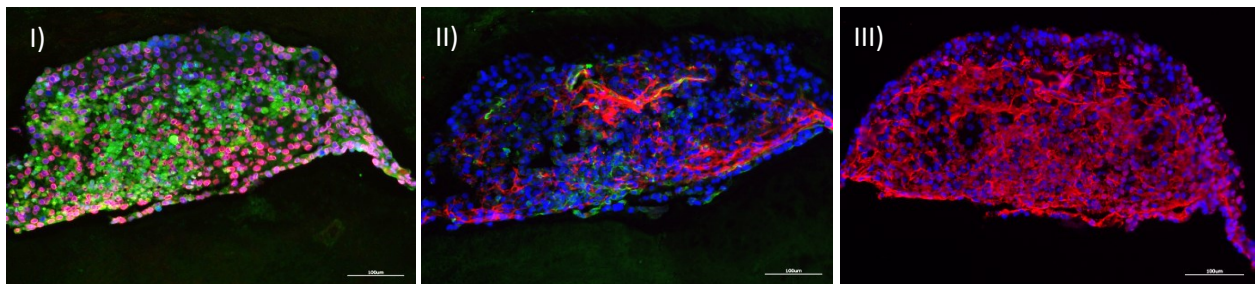


Fig. 15 a Immunostaining of aggregates cultured in MOC Transwell® for 14 days. I) cytochrome P450 3A4 (red) and 7A1 (green) expression show a gradual increase in the direction of fluid flow. **II)** Collagen I (red) and vimentin (green) expression overlap, suggesting collagen I production by hSteC. **III)** Fibronectin (red) distributed homogeneously over the whole aggregate. Nuclear stain (blue). Scale bar 100µm.

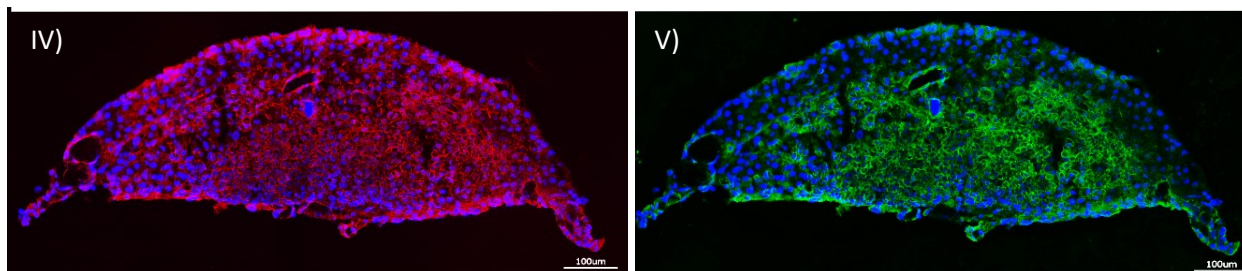


Fig. 15 b Immunostaining of aggregates cultured in MOC Transwell® for 14 days. IV) Formation of tight junctions exemplified by ZO-1 (red) staining and **V)** expression of canalicular transporter MRP-2 (green). Nuclear stain (blue). Scale bar 100µm.

Hence, cultivating newly formed liver equivalents in the MOC for 14 days showed the establishment of liver extracellular matrix and the expression of phase I metabolising enzymes as well as bile of canaliculi-like structures. As cultures were shielded from the underlying current by Transwell® inserts, the effects of direct exposure to the fluid flow were assessed next.

4.5.2 MOC culture of liver tissue directly exposed to the fluid flow

Cultivating liver aggregates in the MOC in a directly exposed manner, led to the adherence of the aggregates to the bottom glass surface of the MOC. Cells grew out of the aggregate strongly, but still keeping a 3D structure over the whole cultivation period of 14 days.

End-point immunohistochemical staining for cytokeratin 8/18 and vimentin again revealed a homogenous distribution of hSteC through the entire aggregate, although hSteC were slightly more abundant at the outside of the liver equivalents having grown out along the glass surface (Fig. 16). Especially, hSteC were very prone to attach to the plasma treated glass surface of the MOC, to grow out and, thereby, to destroy the shape of the aggregates. Staining for cytochrome P450 3A4 showed a slightly higher expression of this protein in the cells on the surface of the aggregate and those that had grown out of the sphere, being in direct contact with the fluid flow. This was comparable to the previous experiment, where the cells growing along the membrane facing the current showed strongest cytochrome P450 3A4 expression. Accordingly, more proliferative cells were detected among the grown out cells as well as in the outer sheath of the aggregate by TUNEL / Ki67 staining. Only very few apoptotic cells could be detected and then only in the core of aggregates, having no direct access to the culture medium (Fig. 16).

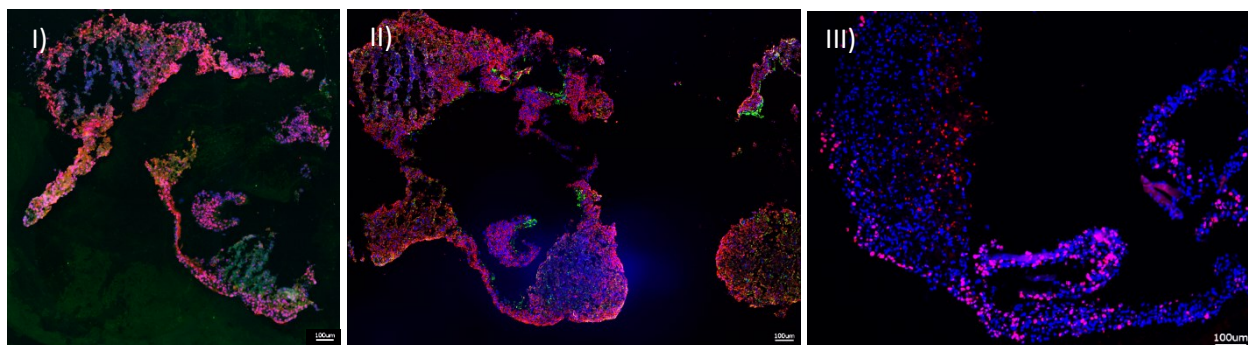


Fig. 16 Immunostaining of aggregates cultured in the MOC at direct exposure to fluid flow for 14 days. I) Cytochrome P450 3A4 (red) and 7A1 (green) expressed slightly higher at the outside of the aggregate. II) Vimentin (red) and cytokeratin 8/18 (green) shows a slightly higher abundance of hSteC at the outside of HepaRG cell aggregate. III) TUNEL / Ki67 staining showing proliferative cells (red) distributed throughout the aggregate and absence of apoptotic cells (green). Proliferating cells were more abundant among the cells that had grown out of the aggregate. Nuclear stain (blue). Scale bar 100 µm.

The metabolic activity of the liver equivalents analysed from the media supernatants indicated a stable glucose consumption of about 530 µg per day per 10^6 cells that slightly decreased during the first 5 days of culture, reaching a steady state thereafter. As only part of the media was exchanged every day, the total glucose level present in the media after media exchanged dropped to 1.53 g/L at steady state. Hence, about 35% of the amount of glucose present in the media was used up by liver equivalents every day, indicating sufficient feeding rates. Analyses of lactate production rate revealed an average of about 230 µg per day per 10^6 cells (≈ 2.5 mM) (Fig. 17), which was comparable to standard HepaRG monolayer culture as described above (introduction). The stable glucose consumption and lactate production from day 5 onwards indicated the establishment of a stable steady state and that liver equivalents had adjusted to the culture conditions of the MOC.

Albumin production by the aggregates constantly increased in the MOC cultures from 5 µg per day per 10^6 cells reaching peak values of 20 µg per day per 10^6 cells (Fig. 17). For comparison, some aggregates were cultured under static conditions in a 24-well plate, receiving the same feeding rate as MOC cultures. These static aggregates had slightly higher albumin production rates at the beginning of the experiment, not needing to adapt to dynamical culture conditions, but production rates then constantly decreased until reaching a final value of 1 µg per day per 10^6 cells. From day 10 of culture, significantly increased albumin production rates were obtained in MOC cultures compared to statically cultured aggregates.

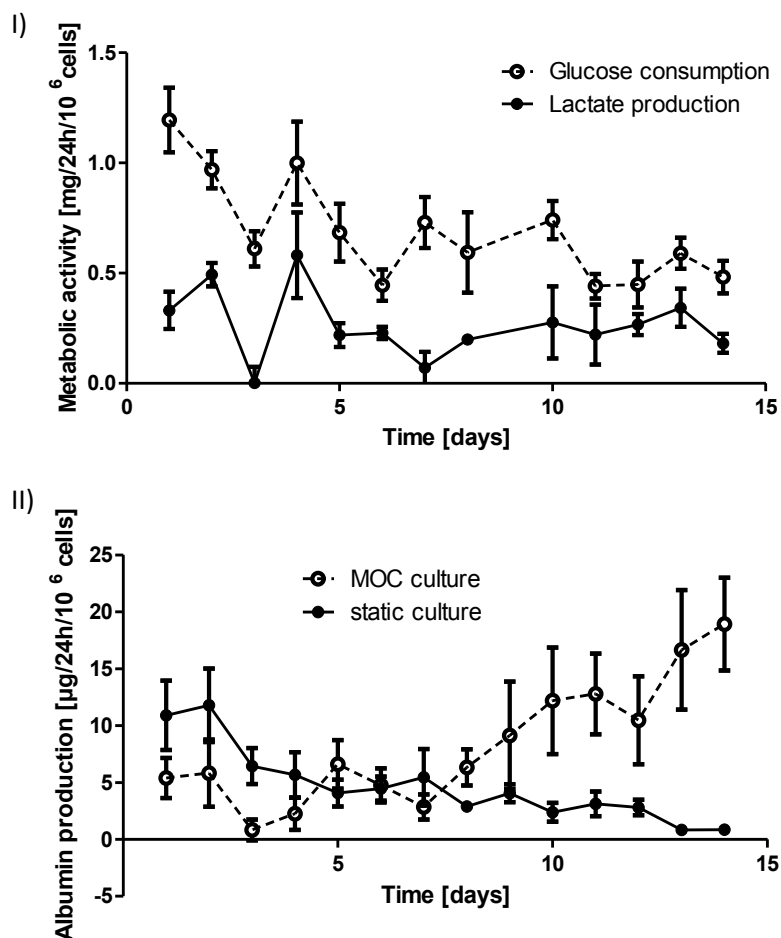


Fig. 17 14-day metabolic activity of liver equivalents at direct exposure to fluid flow. I) Glucose consumption and lactate production of MOC cultures. **II)** Albumin production profile of MOC and static 24-well plate cultured aggregates. Data are means \pm SEM ($n = 4$).

The increased albumin production capacity over time could also be observed on mRNA level. qRT-PCR analysis of the aggregates showed a significant increase in albumin mRNA level as well as in phase II metabolising enzyme UGT-1A1 mRNA level of aggregates cultured for 14 days in the MOC compared to aggregates cultured for 2 to 5 days under static conditions. For phase I and II metabolising enzymes cytochrome P450 1A2, 2B6 and 3A4 and GSTA no significant differences could be detected on mRNA level (Fig. 18). Similarly, ABC transporters BSEP, MDR-1 and MRP-2 were expressed but showed no difference between aggregates cultured for 14 days in the MOC and day 0 aggregates.

The exposure of the liver equivalents directly to the fluid flow of the MOC, hence, led to an increased proliferation of the cells along the bottom glass surface. This had no effect on the expression of phase I metabolising enzyme cytochrome P450 3A4 as detected by immunohistochemistry and qPCR. Aggregates were metabolically active, reaching a steady state after day 5 of MOC culture and producing albumin at rates significantly higher than corresponding static cultures.

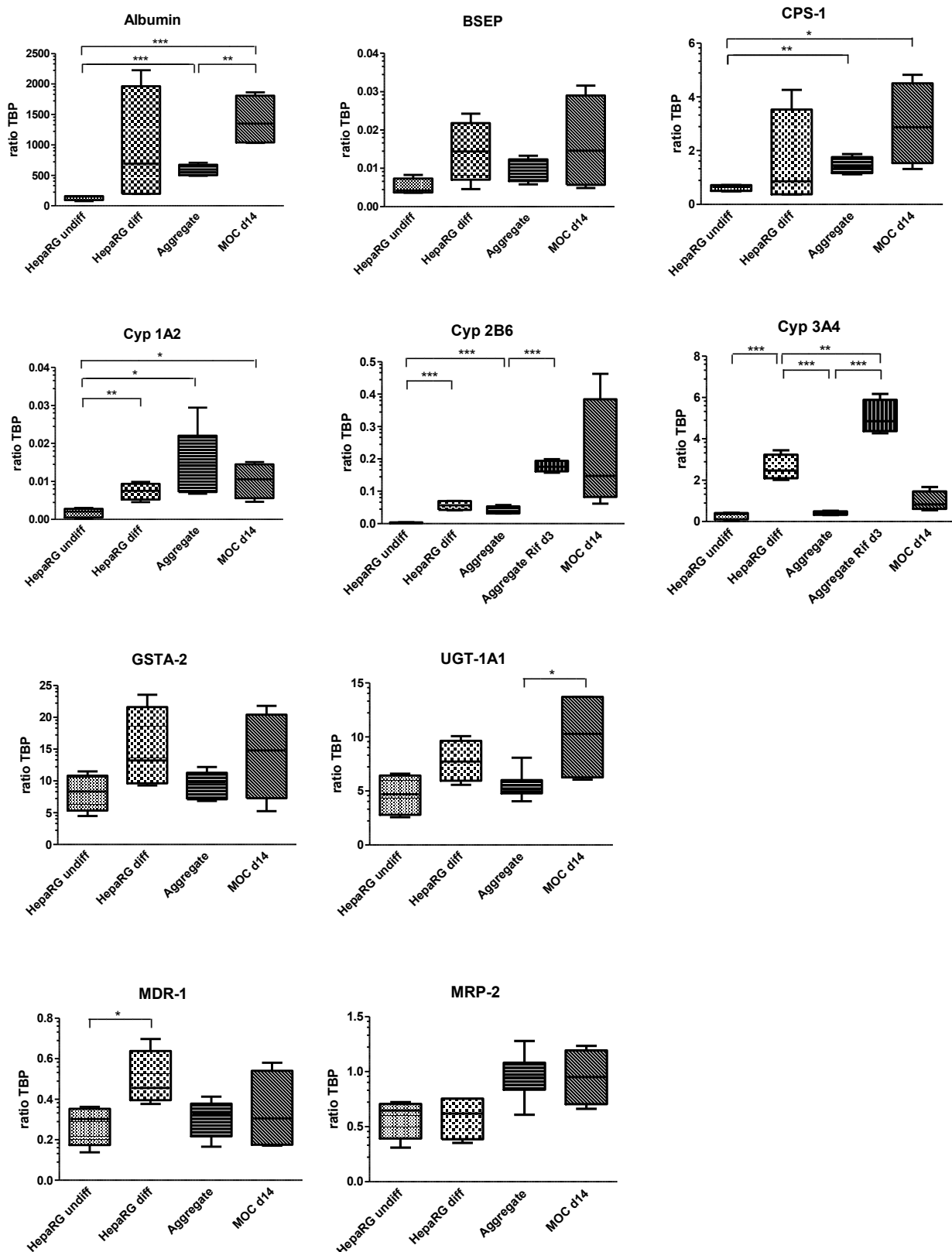


Fig. 18 Real-time qPCR of HepaRG monolayers and aggregates. Transcription levels of selected marker genes were analysed in undifferentiated (**HepaRG undiff**) and differentiated (**HepaRG diff**) HepaRG monolayers, as well as in newly formed aggregates (**Aggregate**), aggregates treated for 3 days with rifampicin (**Aggregate Rif d3**) and 14 day MOC cultures being directly exposed to fluid flow (**MOC d14**) presented as box plot. Data are normalised to TBP ($n = 4$). P-values smaller than or equal to 0.05 were considered significant. * indicates $p \leq 0.05$, ** $p \leq 0.01$ and *** $p \leq 0.001$.

4.6 Liver and skin tissue co-culture in the (endothelialised) MOC

Table 13 culture conditions of liver, skin and endothelial tissue co-cultures inside the MOC

Nr.	Organs	Substance tested	Culture setup	Pump setup	Medium	Feeding regimen	Time [days]
3	Liver & Skin	None	Culture insert (TW®)	2 Hz 0.6 bar	HepaRG	12 h for 7 days, than 24 h (40%)	28
4	Liver & Skin	None	Exposed to flow	2 Hz 0.6 bar	HepaRG	12 h for 7 days, than 24 h (40%)	14
5	Liver & Skin & Vasculature	None	liver exposed to flow, skin in culture insert (TW®)	2 Hz 0.6 bar	HepaRG 80% & HDMEC 20%	12 h for 5 days, than 24 h (50%)	15

Co-culturing liver equivalents with human skin biopsies was again performed in Transwell® units as well as directly exposed to fluid flow. Therefore, human juvenile prepuce samples with an average size of 2.5 cm² were stored in 10 ml phosphate buffered saline (PBS) at 4°C following surgery. Processing skin biopsies for further culture was performed in our laboratory within 4 hours. After removal of excess adipose tissue, punch-biopsies of 4 mm and 5 mm diameter were prepared for directly exposed and Transwell® cultures respectively. This was performed by my colleague Ilka Wagner, who managed the following experiments together with me. Profound analysis of respective human skin samples by immunohistochemistry can be found in her doctoral thesis „Multi-organ-chip based skin models for research and substance testing “.

4.5.2 MOC co-culture of liver and skin tissue in cell culture inserts

In experiment 3 of MOC culture, liver aggregates as well as skin punch-biopsies of 5 mm diameter were placed each in a separated single insert of a 96-well Transwell® unit, which were then combined in a common media circuit. The height of the tissue and the amount of medium added enabled the tissue to be either air / liquid interface as for the skin or submerged culture as for liver equivalents. Co-cultures were performed over 28 days with a 12 h medium exchange rate during the first 7 days of culture and a daily media exchange thereafter. The culture over 28 days was

envisaged in order to evaluate the possibility of long-term co-cultures over periods required for sub-systemic repeated dose toxicity testing.

Liver equivalents adhered to the Transwell® membrane and flattened, forming elongated 100 to 150 µm thick discs of cells on top of the membrane. This was comparable to liver single-tissue experiments performed before only that due to the increased time of culture, aggregates flattened stronger.

The Analysis of media supernatants again revealed a robust steady state metabolic activity from day 4 onwards throughout the entire culture period (Fig. 19). The increased glucose consumption rate during the first 7 days of culture was due to the increased feeding rate of every 12 h. From day 8 onwards the feeding rate was reduced to every 24 h and, subsequently, glucose consumption rates dropped, which might hint at a glucose limitation during this later phase. The glucose consumption averaged at approximately 520 µg per day per MOC circuit and lactate production at 180 µg per day per MOC circuit at steady state, which was comparable to liver single-tissue cultures. Notably, the co-culture contained about 5 times the amount of cells as the previous single-tissue culture.

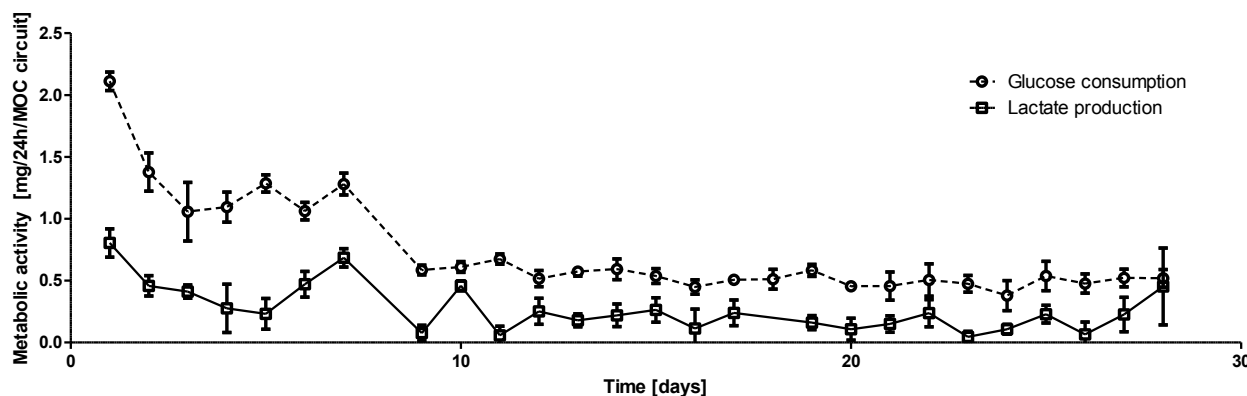


Fig. 19 28-day metabolic activity of liver-skin co-culture in Transwells®. Glucose consumption and lactate production of MOC cultures. Data are means \pm SEM (n = 4).

Albumin secreted to the media differed strongly from previous experiments, being high in the beginning of co-culture (30 µg per day per circuit on day 2 of culture) and then decreasing continuously until no more albumin was released to the supernatant on day 20 (Fig. 20). Skin biopsies and liver equivalents that had been statically co-cultured over 28 days in multi-well plates for comparison showed a similar profile starting at lower concentrations of 19 µg per day per MOC circuit.

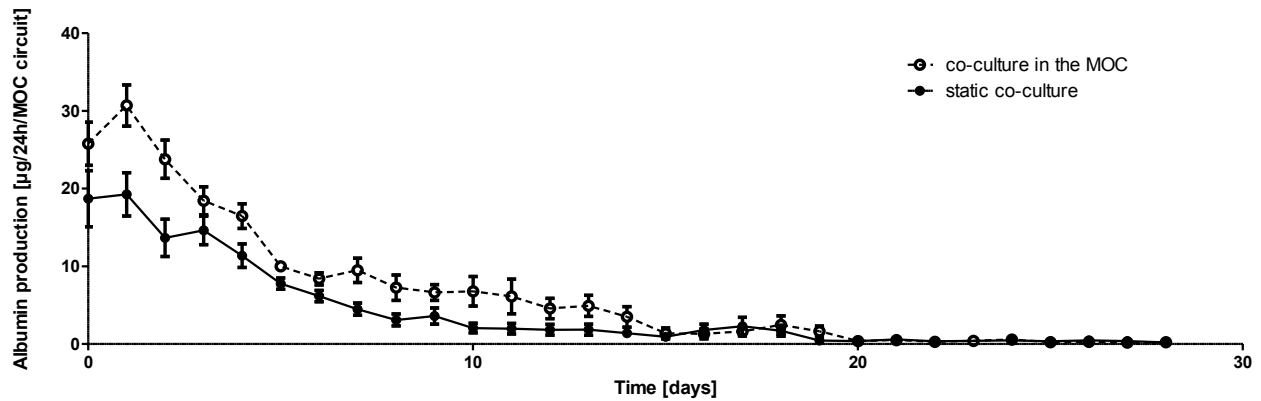


Fig. 20 28-day albumin release of liver-skin co-culture in Transwells® and static multi-well plates. Albumin release profile of MOC and static co-culture. Data are means \pm SEM (n = 4).

TUNEL / Ki67 staining of the tissues revealed that apoptosis was relatively low in both liver and skin tissues, whereas statically co-cultured tissues showed a strong increase in apoptotic cells (Fig. 21). Furthermore, liver equivalents were stained for the expression of cytochrome P450 3A4 and cytochrome P450 7A1 as well as for the production of collagen I (Fig. 22). Cytochrome P450 3A4 and 7A1 showed equal intensity in dynamically and statically cultured cells, still expression was more defined in MOC cultures. Collagen I expression was much more intensive in MOC cultures compared to static cultures, especially at the border of the aggregate.

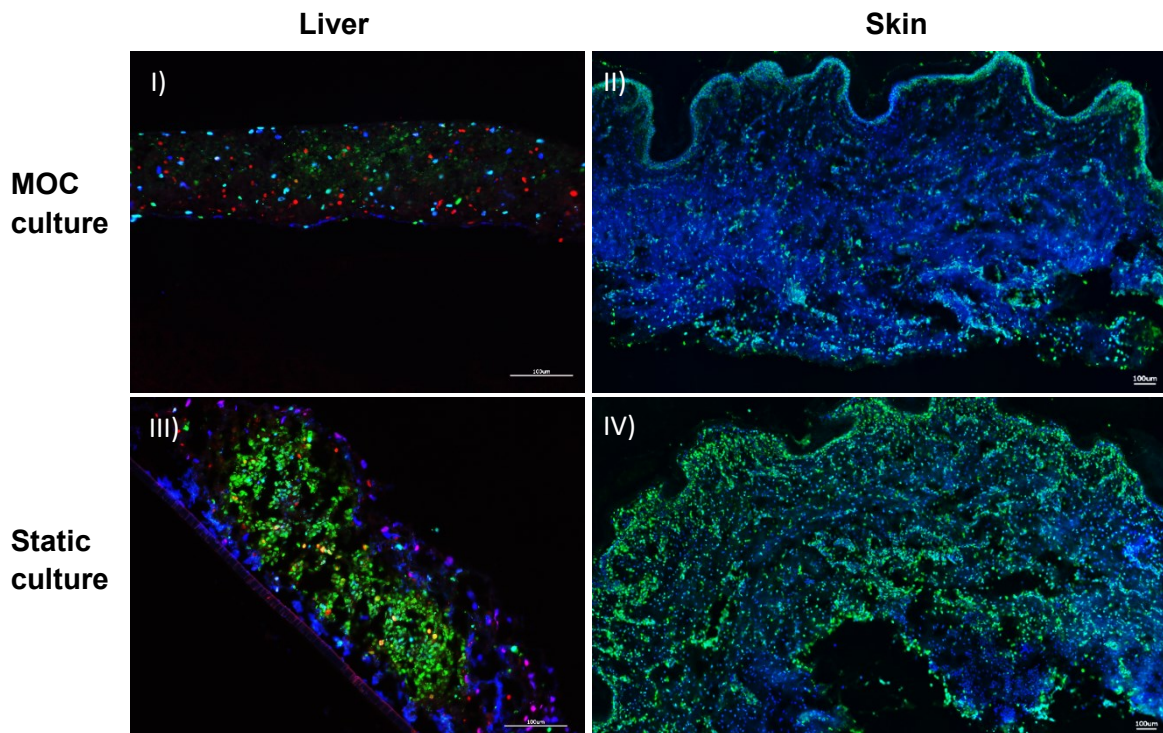


Fig. 21 TUNEL / Ki67 staining of 28 day MOC Transwell® cultures. I) and III) showing liver equivalents and II) and IV) skin biopsies. I) and II) dynamic cultures in the MOC showed less apoptotic cells (green) and slightly more proliferating cells (red) than III) and IV) statically cultured organ equivalents. Nuclear stain (blue). Scale bar 100 µm.

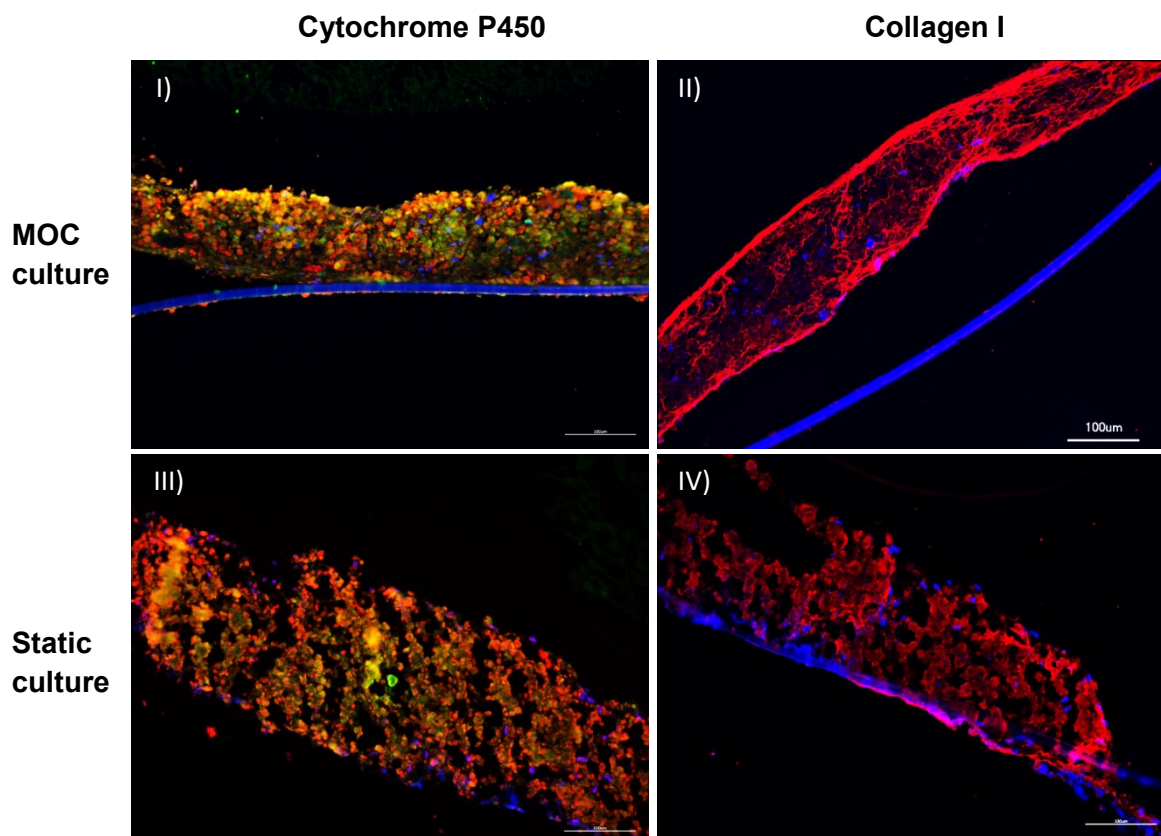


Fig. 22 Immunostaining of 28 day MOC Transwell® cultures. Liver equivalents co-cultured with skin biopsies in MOC for 28 days were stained for **I)** and **III)** cytochrome P450 3A4 (red) and 7A1 (green) and **II)** and **IV)** collagen I (red). Dynamic cultures in the MOC showed higher expression of **II)** collagen I and **I)** more defined cytochrome P450 expression than **III)** and **IV)** statically cultured organ equivalents. Nuclear stain (blue). Scale bar 100 µm.

Summarising, a 28-day co-culture of liver and skin tissue in Transwells® resulted in metabolically stable and viable cells. Viability was significantly increased compared to statically co-cultured liver and skin tissues. First hints at a glucose limitation in the two-organ co-culture were obtained. The albumin production of MOC co-cultures were similar to static cultivations, showing completely different curves than previous single-tissue cultures.

4.5.2 MOC co-culture of liver and skin tissue directly exposed to the fluid flow

Evaluating the effects of fluid flow on the two-organ culture, human liver and skin tissue co-cultures were also performed over a period of 14 days as cultures being directly exposed to the fluid flow in the MOC (experiment 4). Skin biopsies of 4 mm diameter as well as liver equivalents were placed directly inside the cell culture areas of the MOC. In parallel, control experiments in the MOC containing liver only and skin tissue only were performed.

Liver aggregates again adhered to the bottom glass slide and grew out slightly. Skin biopsies were completely submerged in media. In co-cultures, a constant LDH activity of about 20 U/L from cultivation day 6 onwards was measured in the media supernatants (Fig. 23). This was not altered when the daily feeding rate was reduced from every 12 hours to every 24 hours starting on day 7 of culture.

The metabolic activity of the co-cultures showed to be high but constantly decreasing until day 7 and a steady state with low fluctuations both for lactate production (averaging at about 350 μg per day per circuit) and glucose consumption (of about 470 μg per day per circuit) was observed thereafter (Fig. 23). Notably, lactate release was about 50% higher than the corresponding values of the 28-day studies, whereas glucose consumption values were comparable.

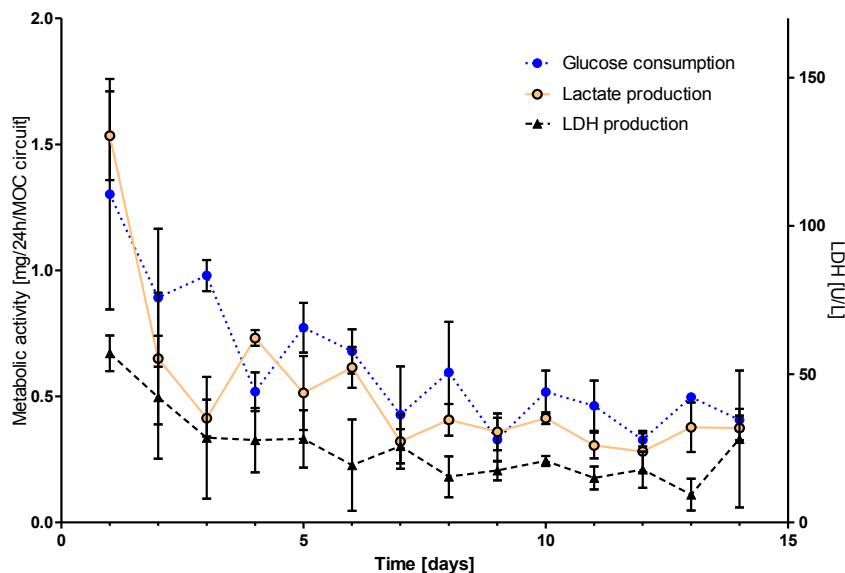


Fig. 23 14-day metabolic activity of liver-skin co-culture at direct exposure to fluid flow. I) Glucose consumption, lactate production and LDH activity of MOC co-cultures. Data are means \pm SEM (n = 4).

The amount of albumin released from the co-culture to the medium, again, was high at the first day of culture (35 μg per day per circuit) and, similarly so, in separate skin single-tissue MOC cultures that were performed in parallel (Fig. 24). The concentration in the supernatants then declined steeply until day 4 of culture, when it stabilised in the co-cultures as well as in skin single-tissue cultures at around 0. The amounts of albumin produced by separate liver single-tissues that were run in parallel, were stable over the whole culture period at about 5 μg per day per circuit. Hence, the increased albumin concentrations measured during the first days of co-culture resulted from the skin. Liver single-tissue cultures constantly produced albumin during the whole cultivation period, which was not observed in the co-culture.

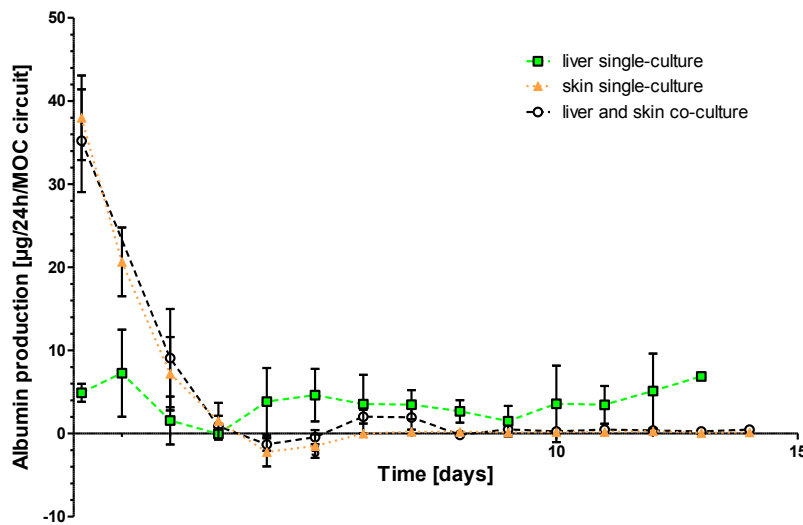


Fig. 24 14-day albumin release of liver-skin co-culture at direct exposure to fluid flow. Albumin release profile of liver and skin single-cultures and liver-skin co-cultures in the MOC. Data are means \pm SEM (n = 4).

TUNEL / Ki67 staining revealed that proliferative cells could be found throughout the whole aggregate being slightly more abundant at the outside, whereas apoptotic cells were only detected within the core of liver equivalents (Fig. 25).

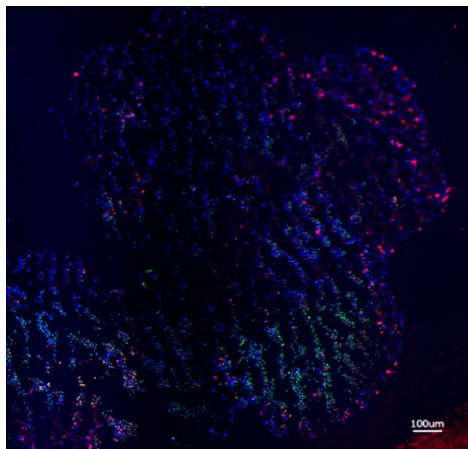


Fig. 25 TUNEL / Ki67 staining of aggregates co-cultured in MOC at direct exposure to fluid flow. TUNEL / Ki67 staining showing proliferative cells (red) distributed throughout the aggregate. Apoptotic cells (green) were found only in the core of aggregates. Nuclear stain (blue). Scale bar 100 μ m.

Taken together, co-culturing liver and skin tissues at direct exposure to the fluid flow led to a 50% increase in lactate production compared to Transwell® assisted co-cultures. Still, liver equivalents showed only few apoptotic cells in the core of the aggregates and many proliferating cells were detected. The increased albumin concentration in co-cultures during the first 4 days resulted from the skin tissue, whereas the albumin produced by the liver (as suggested from single-tissue liver experiments) was not detected in the co-culture from day 4 onwards.

Continuing, co-cultures of liver and skin tissues were performed in endothelialised MOCs, combining previous culture techniques by cultivating the skin tissue in Transwell® inserts and liver equivalents as directly exposed to the fluid flow cultures.

4.5.2 MOC co-culture of liver, skin and endothelial tissue

Having evaluated liver and skin tissue co-cultures under different conditions, a further step towards the *in vivo* situation was performed by introducing an endothelialisation of the MOC channels in experiment 5. Therefore, primary human HDMECs were isolated from human foreskin samples of 2 patients by my colleagues Ilka Wagner and Sven Brinker. Cells were expanded and seeded at a density of 2×10^7 cells / ml into the channels of the MOC. The procedure for the endothelialisation of MOCs was established in our laboratory by Katharina Schimek and can be found in her work.⁸⁶ MOCs whose channels were fully covered with endothelial cells after 7 to 12 days of culture, were loaded with liver equivalents as free swimming aggregates as well as human skin biopsies in Transwell® culture inserts. Skin samples were obtained from 4 patients and processed into 5 mm punch biopsies before loading them into Transwell® 96-well units. Cultures were performed in 20% HDMEC medium and 80% HepaRG medium to support endothelial cells. Therefore, the results of this experiment could not be compared with previous cultures being performed in HepaRG medium only and, hence, single-tissue cultures of liver, skin and endothelial cells as well as all different combinations of co-cultures (each $n = 4$) were performed in parallel under the same conditions. Media exchange was performed once a day during endothelialisation, every 12 hours for the first 5 days of organ co-culture and every 24 hours thereafter.

Liver aggregates again adhered to the bottom glass slide, grew out slightly and started to fuse where they met each other. Skin biopsies were cultured in Transwell® units and hence exposed to air-liquid interface. Endothelial cells covering the whole channel surface stayed confluent over the whole cultivation period.

The metabolic activity of the cultures including skin biopsies had a slightly increased glucose consumption during the first 3 days of culture, compared to cultures without skin. The three-tissue co-cultures showed a glucose consumption profile similar to skin single-tissue cultures over the whole cultivation period. For all cultures, again, a high but constantly decreasing metabolic activity until day 6 was observed and a steady state with low fluctuations thereafter (Fig. 26). At steady state, skin single-tissue cultures had a mean glucose consumption level of 470 µg per day and MOC circuit, single-tissue liver equivalents consumed 530 µg per day and circuit and the respective co-culture 630 µg per day and circuit. Notably, the added glucose consumption rates of both single-tissue cultures together were higher than the actual values obtained in the co-culture, again hinting at a glucose limitation in the multi-organ culture. The amount of lactate released to the medium differed strongly between the cultures during the first 5 days, but reached a similar steady state thereafter. Especially, cultures comprising skin biopsies had an increased

lactate release to the medium (500 μg per day per circuit for skin single-tissue cultures and 720 μg per day per circuit for three-tissue cultures, compared 270 μg per day per circuit for liver and endothelial cell single cultures). This was in good correlation with the glucose consumption data. Looking at the ratio of glucose consumption and lactate production of the three-tissue-cultures in mmol/L, a nearly double amount of lactate released to the medium compared to glucose consumed was observed during the first 4 days, settling to a near 1:1 ratio at steady state (Fig. 27).

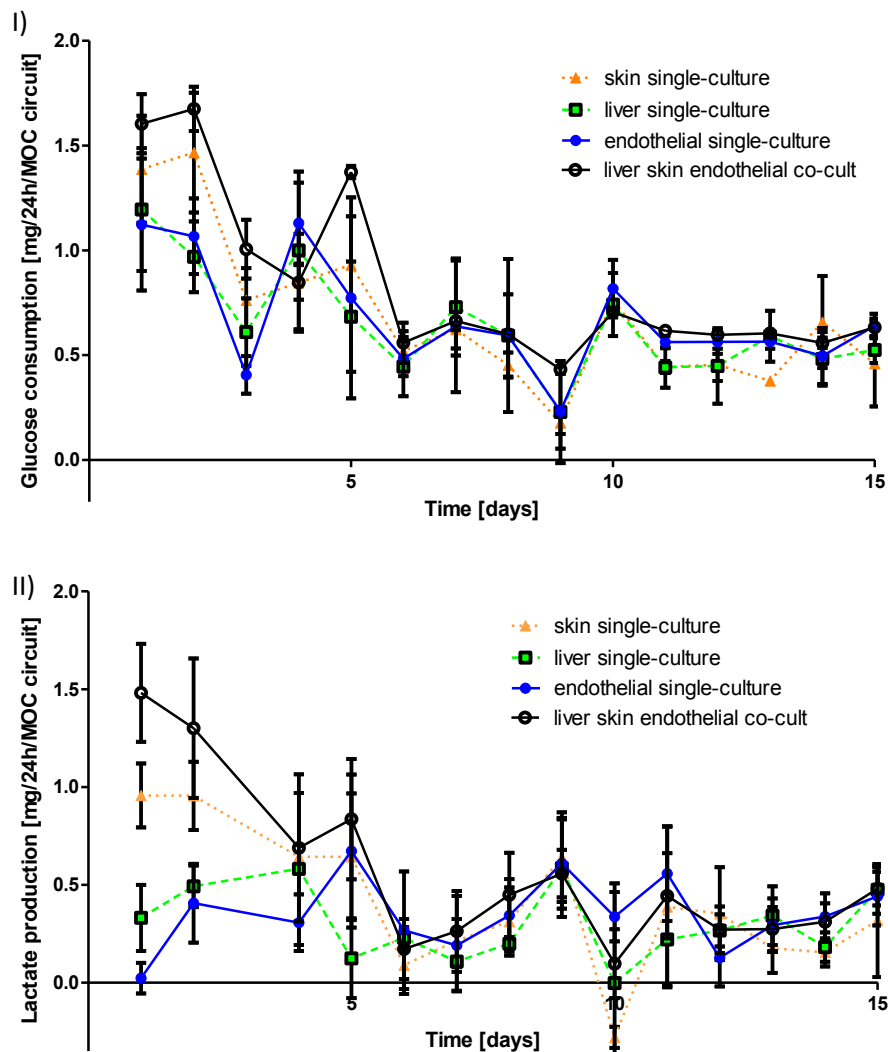


Fig. 26 15-day metabolic activity of single-cultures and liver-skin-endothelial cell co-culture. I) Glucose consumption in single tissue cultures and co-cultures was similar, whereas II) lactate production varied between culture setups during the first 3 days of culture. Data are means \pm SEM ($n = 4$).

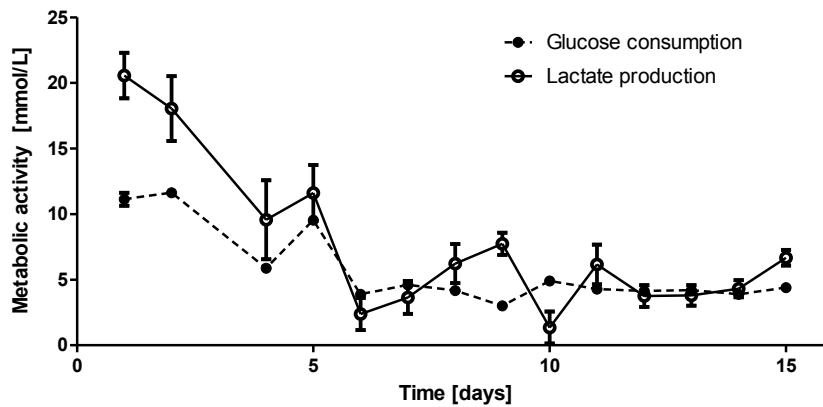


Fig. 27 15-day metabolic activity of liver-skin-endothelial cell co-culture. Glucose consumption and lactate production calculated as mmol/L showed a ratio of 2:1 during the first 4 days of culture, settling to a near 1:1 ratio afterwards. Data are means \pm SEM (n = 4).

The amount of albumin produced by liver single-tissue cultures increased continuously over the cultivation period reaching peak values of 18 μ g per MOC circuit (Fig. 28). An albumin release from the co-culture to the medium was high during the first 4 days of culture, reaching peak values of 10 μ g per MOC on day 4 and decreasing thereafter, just as in separate skin single-tissue cultures. No albumin release was detected for endothelial cell single cultures.

Furthermore, qRT-PCR revealed that the levels of albumin expression in liver equivalents decreased significantly with the number of organs co-cultured. The transcriptional level for albumin was especially low in the three-tissue co-culture (Fig. 28). Hence, decreased amounts of albumin found in the three-tissue co-culture were due to decrease production rates.

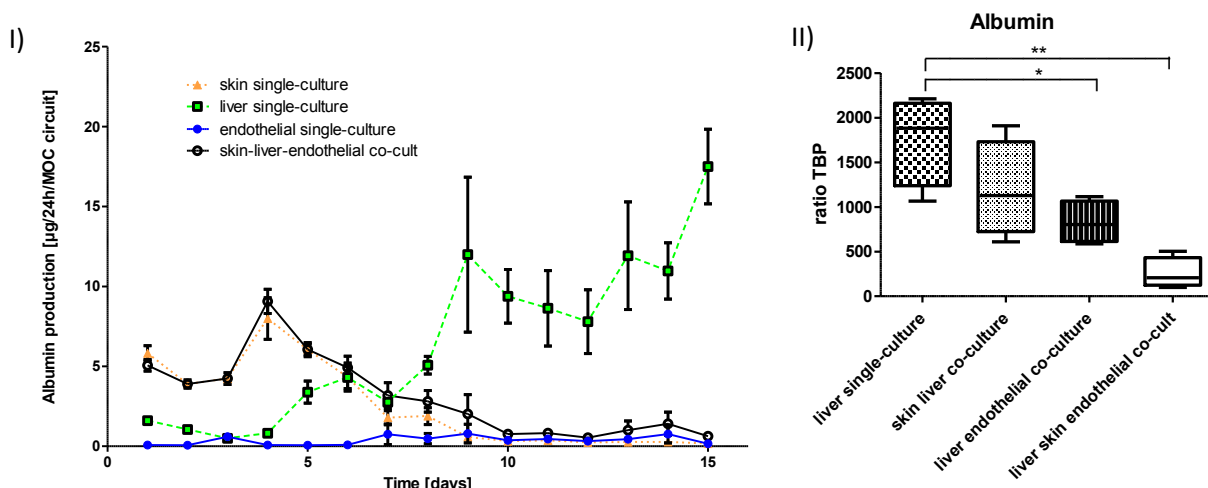


Fig. 28 15-day albumin production of liver-skin-endothelial cell co-culture. I) Albumin production in single and co-cultures. Albumin was released from skin during the first 5-10 days, whereas production increased only in liver single-tissue cultures. II) Transcription levels for albumin were analysed on day 15 in single-tissue culture as well as in different co-cultures. mRNA levels for albumin decreased with the number of organ co-cultured with the liver. Data are means \pm SEM (n = 4). P-values smaller than or equal to 0.05 were considered significant. * indicates $p \leq 0.05$ and ** $p \leq 0.01$.

Immunohistochemical staining for TUNEL / Ki67 in liver equivalents of three-tissue cultures as well as single-tissue cultures showed a homogenous distribution of proliferating cells throughout the aggregates, whereas no apoptotic cells could be observed (Fig. 29).

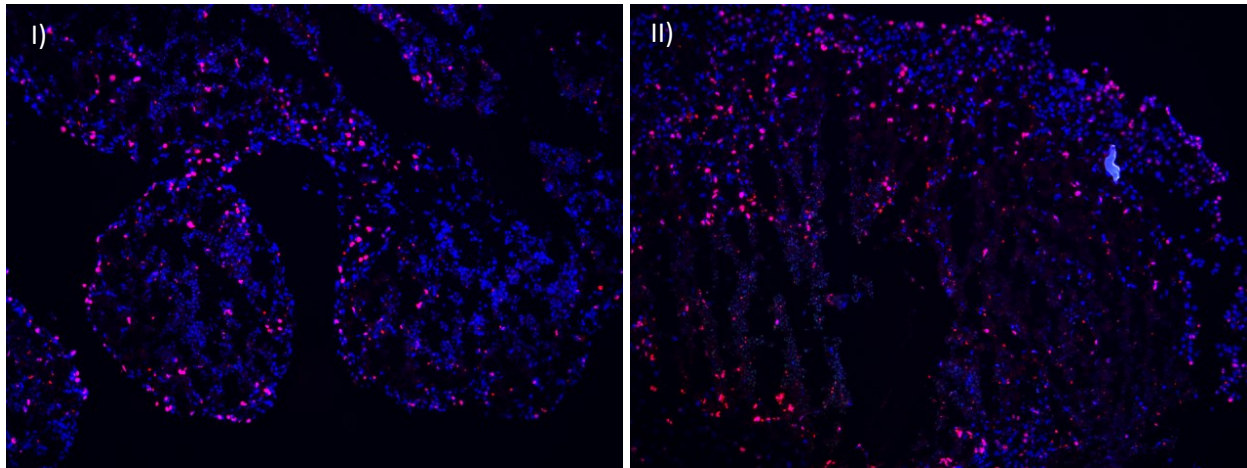


Fig. 29 TUNEL / Ki67 staining of liver equivalents cultured at direct exposure to fluid flow for 15 days in the MOC. I) Liver equivalents of three-tissue cultures, as well as II) single-tissue cultures showed a homogenous distribution of proliferating cells (red), whereas no apoptotic cells (green) could be observed. Nuclear stain (blue). Scale bar 100 μm .

Summarising, three-tissue co-cultures were successfully performed in a combined media circuit for 15 days. Liver equivalents remained viable and in a proliferative state and endothelial cells were confluent covering the channels of the MOC during the whole cultivation period. The metabolic activities again hinted at a glucose limitation in multi-tissue cultures, with the skin tissue having slightly increased glucose consumption rates during the first days of culture compared to liver and endothelial cell cultures. Still, glucose consumption to lactate production resulted in a ratio of 1:1 calculated as mmol/L. The albumin production in multi-tissue cultures decreased as was also detected by mRNA expression.

In the following, the co-cultivation of liver equivalents with neurospheres in the MOC was tested.

4.7 Liver and neurosphere co-culture in the MOC

Table 14 culture conditions of liver and neurosphere co-cultures inside the MOC

Nr.	Organs	Substance tested	Culture setup	Pump setup	Medium	Feeding regimen	Time [days]
6	Liver & Neurons	None	Exposed to flow	1.5 Hz 0.6 bar	HepaRG	12 h for 5 days, than 24 h (45%)	14

Co-cultivating human liver equivalents and neurospheres in the MOC was performed with the help of the master student Anja Ramme. Detailed analysis of neuronal aggregate behaviour in the MOC analysed by immunohistochemistry and qRT-PCR can be found in her master's thesis, entitled „Establishment of chip-based human neuronal tissue cultures for substance testing“.⁹⁵

Neurospheres were obtained from the group of Catarina Brito of the Animal Cell Technology Unit (iBET, Portugal). The spheres consisted of differentiated Ntera-2 cells that had been produced and differentiated in a stirred tank bioreactor. For more details on the production and characteristics of neuronal aggregates please refer to Serra et al.⁹⁶. Neurospheres with a medium diameter of 150 to 200 µm were shipped over-night to Berlin in 50 ml falcons containing special hibernating culture medium at 4°C. Aggregates were cultured in ultra-low attachment 6-well plates in DMEM 5% FCS, 1% Penicillin/Streptomycin after arrival. Following, the neurospheres were stepwise adjusted to HepaRG medium until the start of experiment 3 days after arrival of the cells. Clogging and fusion of the neuronal aggregates during the media adaptation hampered the distribution of neurospheres evenly over the MOCs used. 80 Neurospheres per circuit were needed to yield the miniaturisation rate of $1/_{100000}$. Still, a near homogenous distribution over all cultures was achieved.

Cultures were performed in HepaRG medium with a 45% exchange rate every 12 hours for the first 5 days of culture and every 24 hours thereafter. Again, respective single-tissue cultures were performed in parallel for comparison.

Analysis of metabolic activities revealed that co-cultures of liver and neuronal aggregates had slightly increased glucose consumption rates compared to respective single-tissue cultures during the first 5 days, when feeding rate was every 12 h. At steady state, feeding rate was reduced to every 24 h. Here, glucose consumptions of co-cultures and single-tissue cultures were comparable at around 500 µg per day and circuit (Fig. 30). The amount of lactate produced was highest in liver-neuronal aggregate co-culture at around 250 µg per day per MOC circuit, followed by neurosphere single culture and liver single-tissue cultures. Again, for the co-culture this resembled a ratio of 2:1 of glucose consumption vs. lactate production.

Furthermore, qRT-PCR revealed that no differences on mRNA-level could be observed between single-tissue cultures and co-cultures for all markers measured (data not shown).

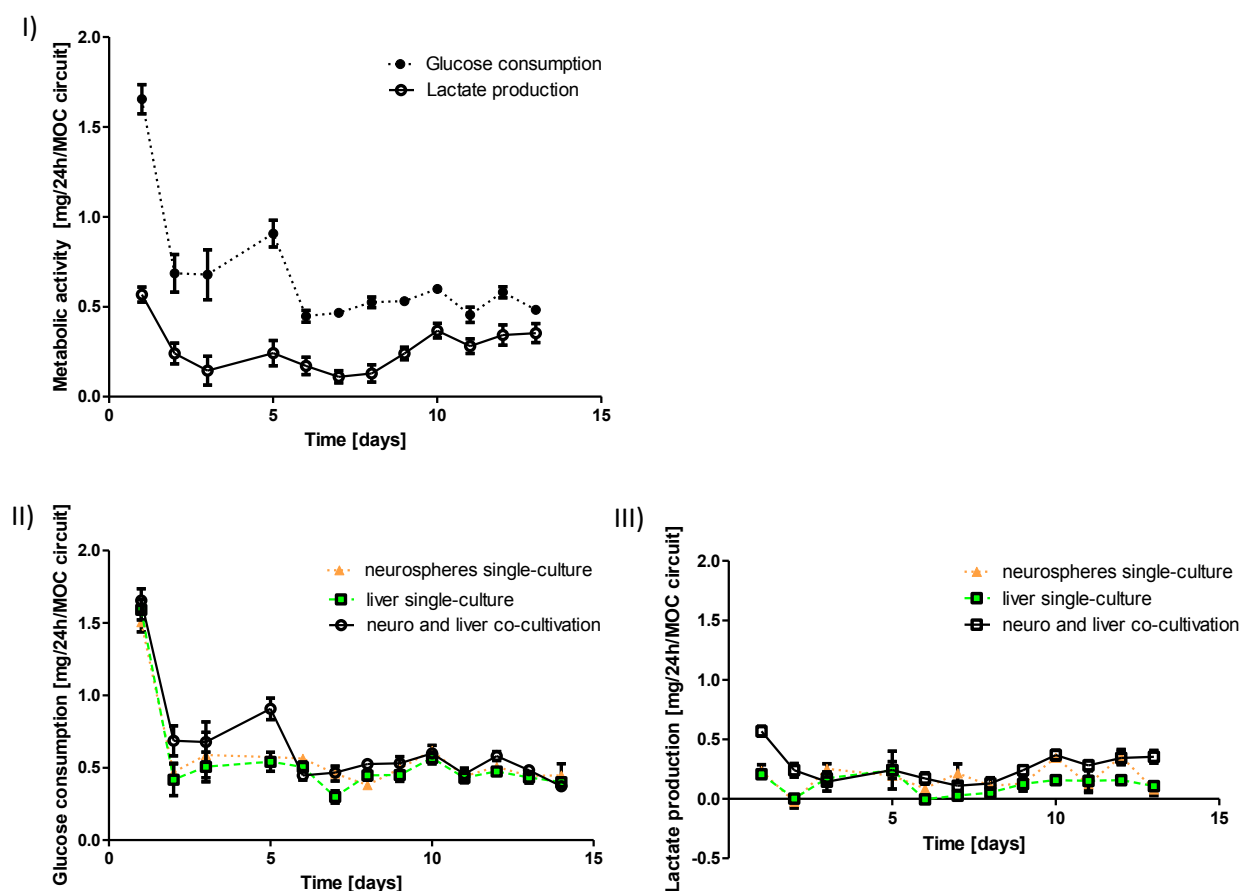


Fig. 30 15-day metabolic activity of liver-neurosphere co-culture. I) Rate of glucose consumption and lactate production (2 : 1) suggested an aerobic metabolism. Comparing II) glucose consumption and III) lactate production levels between single- and co-cultures revealed no differences. Data are means \pm SEM (n = 4).

The cultivation of liver equivalents with neurospheres in a combined media circuit was achieved over a cultivation period of 14 days. Again, a metabolic steady state was achieved from cultivation day 6 onwards.

Having cultivated liver equivalents with skin tissue, endothelial cells and neurospheres over periods relevant for sub-systemic repeated dose substance testing and having confirmed that tissues were viable and metabolically competent, first proof-of-principle substance tests were performed on liver-skin, liver-skin-endothelial and liver-neurosphere co-cultures.

4.8 Multi-tissue sensitivity to troglitazone at fluid flow

Table 15 culture conditions of liver and skin tissue co-cultures inside the MOC – toxicity testing

Nr.	Organs	Substance tested	Culture setup	Pump setup	Medium	Feeding regimen	Time [days]
7	Liver & Skin	Troglitazone, starting day 1	Exposed to flow	2 Hz 0.6 bar	HepaRG	12 h for 5 days, than 24 h (40%)	7
8	Liver & Skin & Vasculature	Troglitazone, starting day 5	liver exposed to flow, skin in culture insert (TW®)	2 Hz 0.6 bar	HepaRG 80% & HDMEC 20%	12 h for 5 days, than 24 h (50%)	15

4.5.2 MOC co-culture of liver and skin tissue at troglitazone exposure

A skin-liver MOC co-culture of both organ equivalents directly exposed to fluid flow as described above was treated with two different concentrations of troglitazone (5 μ M and 50 μ M), starting on day 1 of MOC culture. Controls were exposed to 0.25% DMSO, corresponding to the concentration needed to solve troglitazone. The differentiation inducing effects of DMSO on HepaRG cells (differentiation was routinely performed in 2% DMSO) were monitored in the control group. Troglitazone (and DMSO for control) was administered every day together with the media exchange.

Comparing to DMSO-treated controls, troglitazone had no significant effect on the metabolic activity of the co-culture (Fig. 31). Furthermore, no significant difference between DMSO treated controls and previous non-treated liver-skin co-culture experiment could be observed on metabolic activity.

Whereas, after 4 days of troglitazone exposure, LDH activity measured in the media supernatants started to increase reaching 55 U/L a significant 60% increase compared to controls after 7 days. The increased LDH concentration in the media resulted from cell lysis, supposedly being due to the exposure to the substance troglitazone.

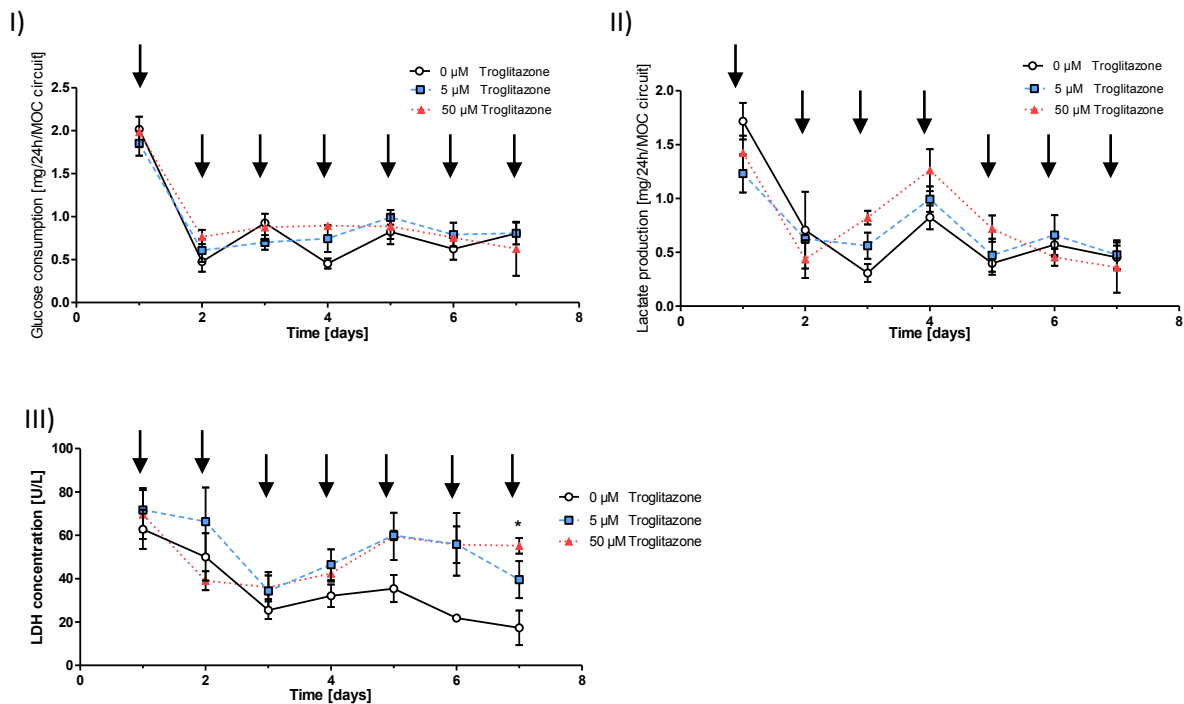


Fig. 31 7-day metabolic activity of liver-skin co-culture at troglitazone exposure. I) Rate of glucose consumption and II) lactate production did not show significant differences between treated and non-treated cultures. III) LDH activity in MOCs treated with troglitazone increased starting on day 4. Data are means \pm SEM (n = 4).

An evenly distributed over-expression of cytochrome P450 enzymes could be detected by immunohistochemistry. All MOCs exposed to 50 μ M troglitazone showed a marked increase, whereas only minute expression was detectable in the control group (Fig. 32).

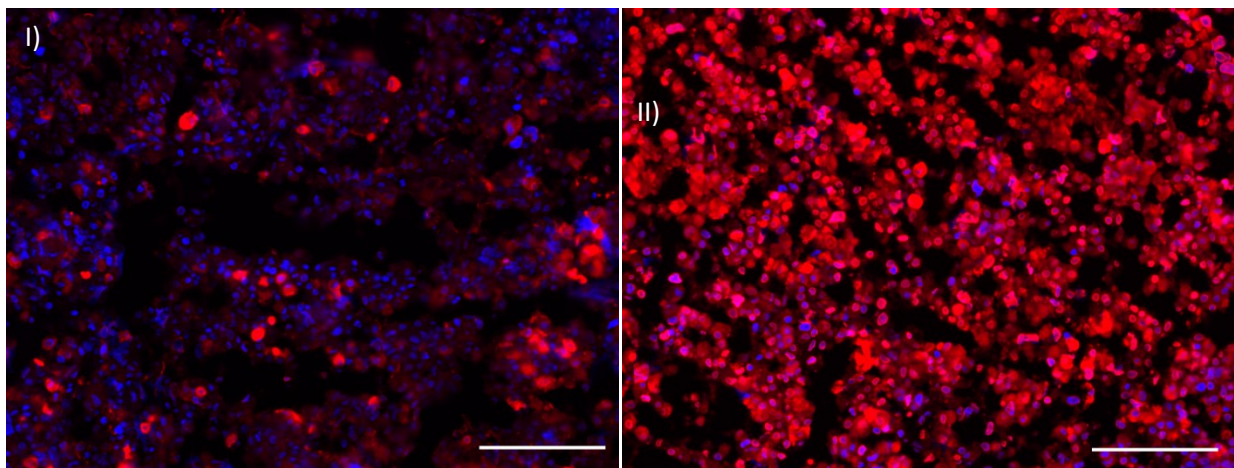


Fig. 32 Immunostaining of liver-skin co-cultures treated with troglitazone. Cytochrome P450 3A4 (red) expression in I) untreated cultures and II) cultures treated with 50 μ M troglitazone. Nuclear stain (blue). Scale bar 100 μ m.

Comparingly, qRT-PCR revealed that mRNA levels of cytochrome P450 3A4 were increased significantly in cultures exposed to 50 μ M troglitazone (Fig. 33). BSEP also increased with troglitazone treatment although not significantly. Similarly, mRNA levels for albumin and CPS-1 dropped slightly with increasing troglitazone concentrations.

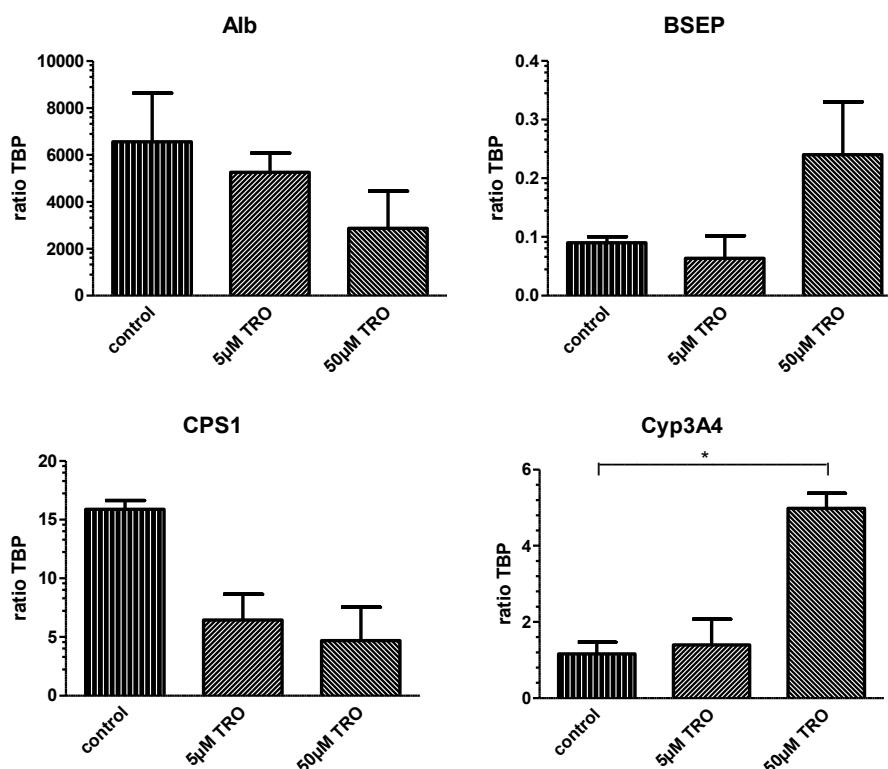


Fig. 33 Real-time qPCR of liver-skin co-cultures treated with troglitazone for 7 days. Transcription levels of albumin and CPS-1 decreased with treatment of troglitazone, whereas BSEP increased. Cytochrome P450 3A4 expression was significantly up-regulated by troglitazone. Data are normalised to TBP (n = 4). P-values smaller than or equal to 0.05 were considered significant. * indicates $p \leq 0.05$.

Having reproduced the toxic effects of troglitazone in a liver-skin two-tissue co-culture, showing the induction of troglitazone metabolising enzyme cytochrome P450 3A4, a three-tissue co-culture comprising liver, skin and endothelial cells was subjected to troglitazone treatment.

4.5.2 MOC co-culture of liver, skin and endothelial tissue at troglitazone exposure

The second experimental run evaluating troglitazone toxicity was performed in skin-liver co-cultures including endothelialised MO-chips. This experiment was performed in parallel to experiment no. 5 and, hence, experiments were performed exactly as described above. In brief,

MOCs, the channels of which were fully covered with endothelial cells after 7 to 12 days of culture, were loaded with liver equivalents as free swimming aggregates as well as human skin biopsies in Transwell® culture inserts. Skin samples were obtained from 4 patients and processed into 5 mm punch biopsies before loading them into Transwell® 96-well units. Media exchange was performed once a day during endothelialisation, every 12 hours for the first 5 days of organ co-culture and every 24 hours thereafter. Troglitazone was added at a concentration of 50 μM to the cultures together with the media exchange starting from day 5 until the end of experiment. DMSO treated controls were performed as well as respective single-tissue cultures treated with troglitazone.

The amount of troglitazone remaining in the media supernatants on day 1 to 10 after addition was analysed by Julie Zech (Institute for Bioanalytics, Technische Universität Berlin) (Fig. 34). On the first day after addition of 50 μM troglitazone only 7.5 μM could be found remaining in the media supernatants of the three-tissue co-culture. Skin single-cultures and skin cultures including endothelial cells had similarly low concentrations (10 μM). Afterwards, the amount of troglitazone in the media supernatants increased steadily with every media exchange performed reaching values of 22 μM at day 15 of culture. Conversely, cultures including liver equivalents showed a slightly higher concentration in the beginning (12 μM), which increased drastically on the second day of treatment to 23 μM and then stayed constant thereafter. Endothelial cell single-tissue cultures in the MOC showed a similar curve, only that the concentration was always about 10 μM higher. Measured concentrations were always below the added concentration of 50 μM .

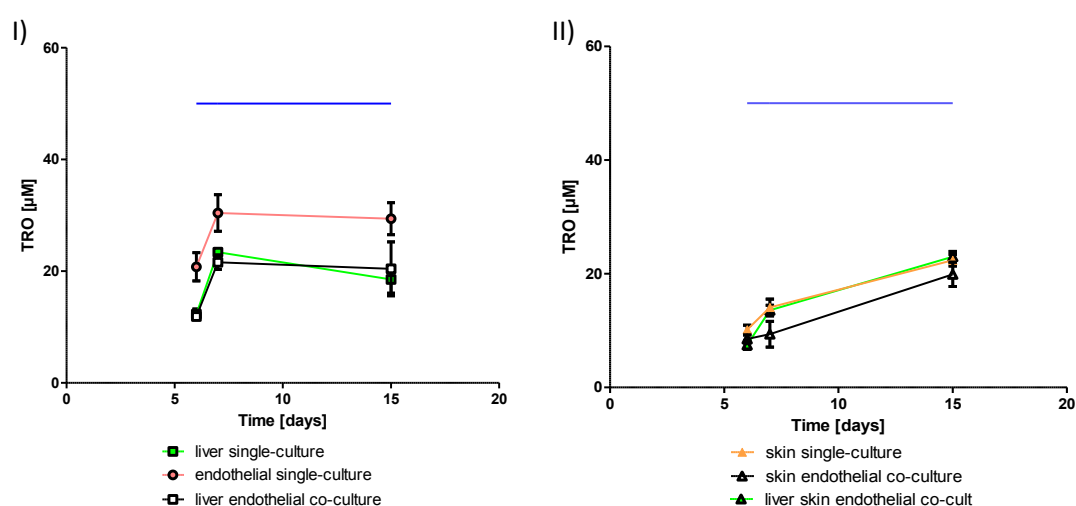


Fig. 34 Troglitazone concentrations in the media supernatants of different MOC cultures. Single-tissue and co-cultures were analysed for the amount of troglitazone present after media exchange. Blue line represents added concentration. Data are means \pm SEM (n = 4).

No effect of troglitazone treatment could be observed immunohistochemically on endothelial cells or skin biopsies as determined by my colleague Ilka Wagner (data not shown).⁹⁷ The channels of the MOC were still covered with a confluent layer of endothelial cells at the end of experiment.

Glucose consumption of the co-culture decreased during the first five days of culture, reaching a steady state thereafter. No difference could be observed between non-treated and treated cultures, as was already observed in the previous experiment (Fig. 35).

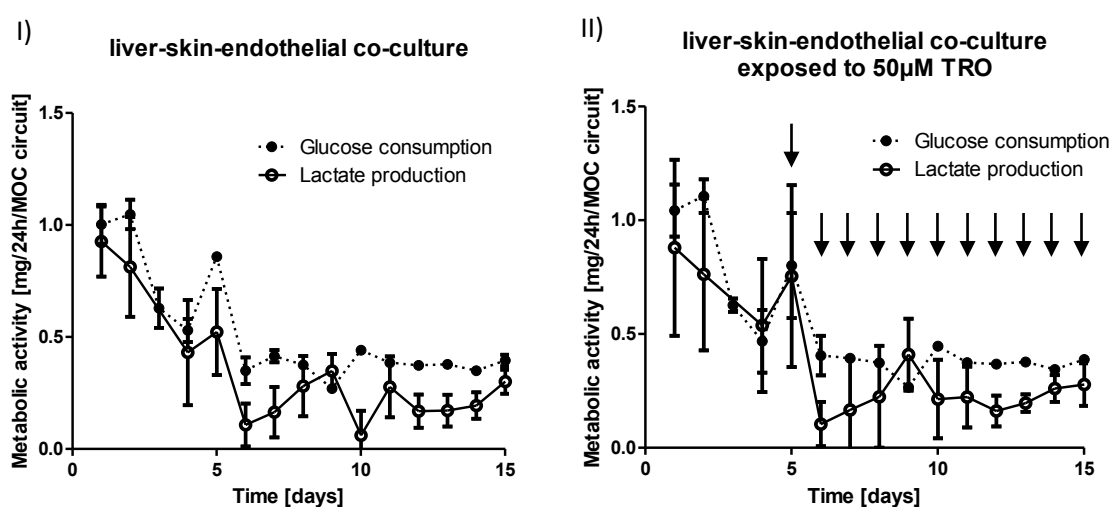


Fig. 35 15-day metabolic activity of liver-skin-endothelial cell co-culture at troglitazone exposure. Rate of glucose consumption and lactate production of I) untreated co-cultures and II) co-cultures exposed to 50 μ M troglitazone did not show any differences. Arrows indicate treatment with 50 μ M troglitazone. Data are means \pm SEM ($n = 4$).

Comparing albumin mRNA levels between three-organ cultures and respective single and two-organ cultures, a decrease in expression levels was observed (Fig. 36). Not only the treatment with troglitazone led to a reduction in albumin mRNA level, also the co-culture with additional organs reduced the expression of albumin on mRNA level, as was already observed previously. Furthermore, the treatment with troglitazone resulted in a trend of cytochrome P450 3A4 mRNA level increase for all single and co-cultures. Here, the increase was not significant, differently than in the previous experiment. Again, BSEP expression increased as well, although only for liver single-tissue cultures significantly. No differences could be found for phase II metabolising enzymes UGT-1A1 and GSTA2, for ABC transporters MDR-1 and MRP-2 as well as for tight junction protein ZO-1 (data not shown).

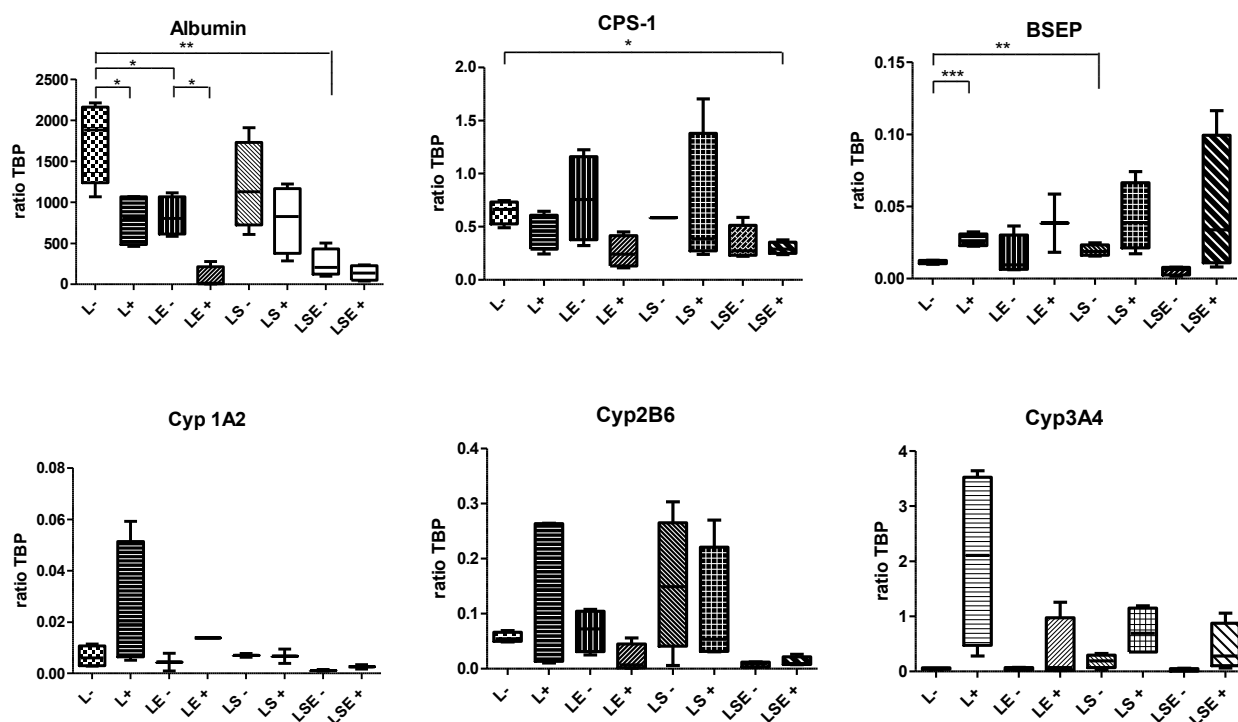


Fig. 36 Real-time qPCR of MOC liver equivalents. Transcription levels of selected marker genes were analysed in single and co-cultures, as well as in untreated samples and cultures exposed to 50 μ M troglitazone after 14 days of MOC culture presented as box plot. L -: liver single-tissue cultures untreated. L +: liver single-tissue cultures treated with 50 μ M troglitazone. LE -: liver-endothelial cell co-culture untreated. LE +: liver-endothelial cell co-culture treated with 50 μ M troglitazone. LS -: liver-skin co-culture untreated. LS +: liver-skin co-culture treated with 50 μ M troglitazone. LSE -: liver-skin-endothelial cell co-culture untreated. LSE +: liver-skin-endothelial cell co-culture treated with 50 μ M troglitazone. Data are normalised to TBP (n = 4). P-values smaller than or equal to 0.05 were considered significant. * indicates $p \leq 0.05$, ** $p \leq 0.01$ and *** $p \leq 0.001$.

Summarising, the treatment of liver-skin co-cultures with troglitazone did not alter the cellular metabolism in regard of glucose consumption and lactate production, but significant differences could be found on albumin and cytochrome P450 3A4 expression levels. The release of LDH to the culture medium hinted at an increased cell death when exposing the cells to troglitazone. Similarly, liver-skin-endothelial three-tissue cultures could reproduce main findings and, furthermore, give insights into the troglitazone concentrations remaining in the media supernatants after one day of incubation.

In the following, liver-neurosphere cultures were exposed to n-hexane and 2,5-hexanedione to evaluate their toxic potential.

4.9 Multi-tissue sensitivity to n-hexane and 2,5-hexanedione at fluid flow

Table 16 culture conditions of liver and neurosphere co-cultures inside the MOC – toxicity testing

Nr.	Organs	Substance tested	Culture setup	Pump setup	Medium	Feeding regimen	Time [days]
9	Liver & Neurons	n-hexane or 2,5-hexanedione, starting day 5	Exposed to flow	1.5 Hz 0.6 bar	HepaRG	12 h for 5 days, than 24 h (40%)	14

A liver equivalent-neurosphere co-culture as described above in experiment no. 6 was performed to evaluate the toxicity of n-hexane and 2,5-hexanedione. Therefore, cultures were performed exactly as described above, with the addition of 64 mM n-hexane or 16 mM 2,5-hexanedione or 32 mM 2,5-hexanedione starting from day 5 of culture together with the daily media exchange. Additionally, single-tissue liver and single-tissue neurosphere cultures were performed in parallel receiving the same treatment.

Media supernatants were analysed for 2,5-hexanedione concentrations by Konrad Neumann (Institute for Bioanalytics, Technische Universität Berlin) of days 1 and 5 after start of treatment for samples treated with 2,5-hexanedione and days 1, 5, 8 and 9 of samples treated with n-hexane. At the start of treatment, concentrations of 2,5-hexanedione remaining in the medium were slightly lower than the added amount, increasing slightly until reaching 85% of added concentration at day 5 of treatment (Fig. 37).

Interestingly, cultures that had been treated with n-hexane did not show any presence of 2,5-hexanedione in the medium supernatant until day 9 of treatment. From day 1 to 6 of treatment, n-hexane had been added to a medium pool before addition to the chips, whereas from day 7 of treatment onwards, n-hexane had been added directly to the MOC circuits.

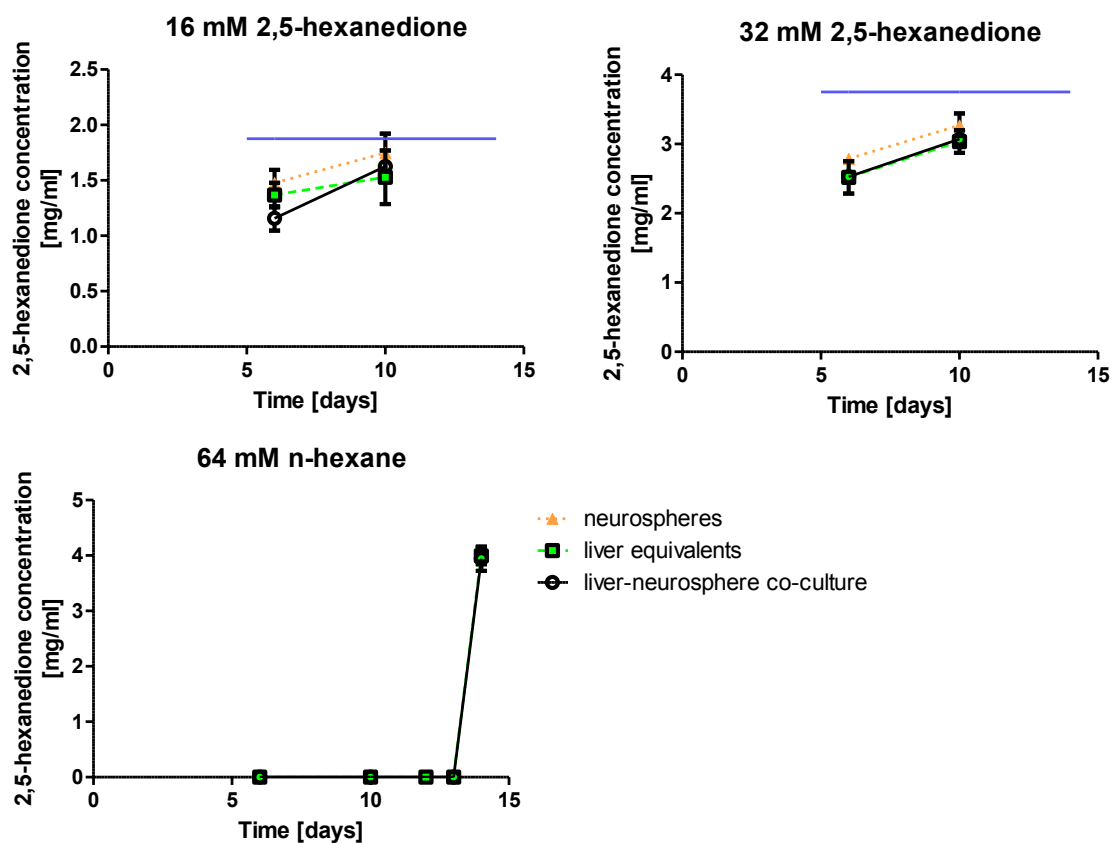


Fig. 37 Amount of substance remaining in the media supernatants. Supernatants of single-tissue and co-cultures were analysed for the amount of n-hexane and 2,5-hexanedione present after media exchange. Blue line represents added concentration. Data are means \pm SEM (n = 4).

Again, no changes between the differently treated cultures compared to non-treated controls could be found on metabolic activity. Glucose consumption as well as lactate production stayed constant over the whole cultivation time (data not shown).

Whereas the activity of LDH measured in the media supernatants increased drastically starting on day 2 of treatment for cultures treated with 32 mM 2,5-hexanedione and on day 4 of treatment for cultures treated with 16 mM 2,5-hexanedione (Fig. 38). After reaching a maximum LDH activity of 272 U/L for 32 mM and 205 U/L for 16 mM co-cultures, the activity declined slowly. Interestingly, co-cultures always showed highest activity followed by liver single-tissue cultures (198 U/L, 105 U/L) and neurosphere single-tissue cultures (95 U/L, 32 U/L). LDH activity in co-cultures treated with n-hexane increased on day 2 of treatment, on which day 2 of the strongly responding co-cultures had to be stopped due to technical reasons, and a very slight increase could be observed again for the remaining two cultures on the last day of experiment.

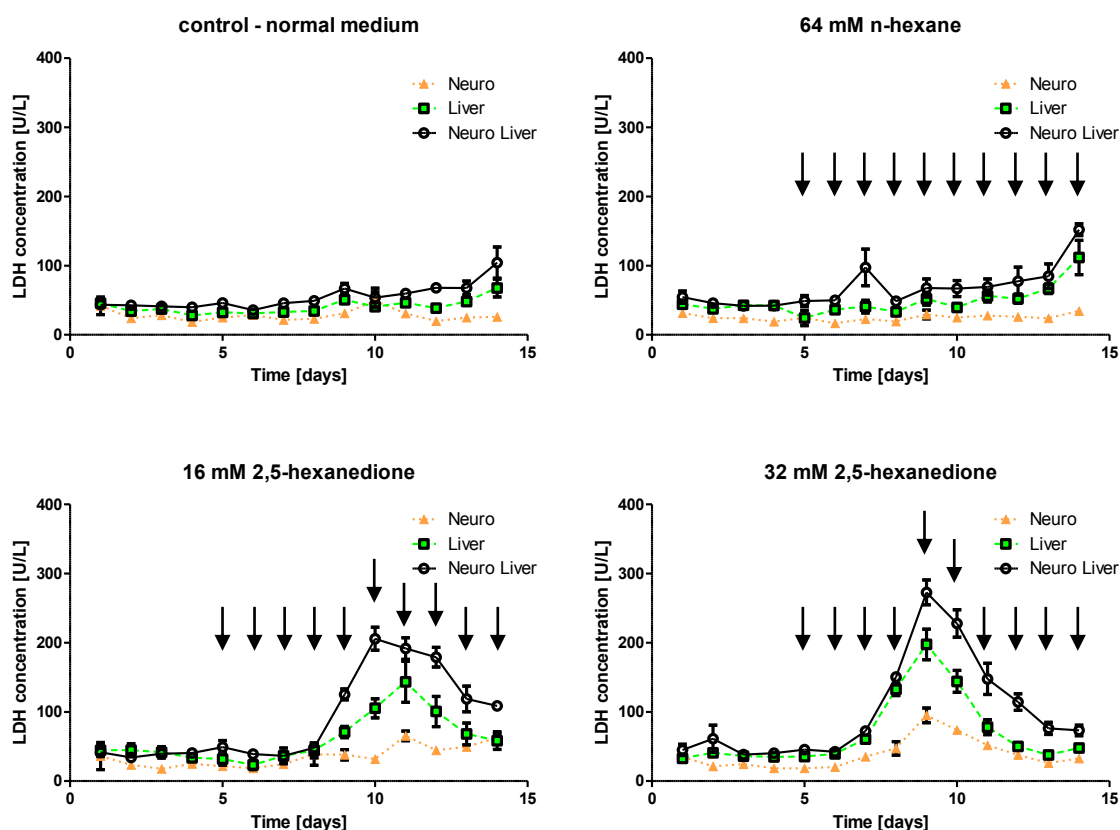


Fig. 38 14-day LDH activity of liver-neurosphere co-culture at substance exposure. Rate of LDH activity in single and co-cultures of control cultures and cultures exposed to n-hexane and 2,5-hexanedione. Data are means \pm SEM ($n = 4$).

End-point analysis by TUNEL / Ki67 staining confirmed, that there were many apoptotic cells in liver single-tissue and liver-neurosphere co-cultures treated with 32 mM 2,5-hexanedione (Fig. 39). Also in cultures treated with at 16 mM of 2,5-hexanedione, there were only very few proliferating cells and many apoptotic cells observable. Cultures treated with n-hexane showed higher numbers of proliferating cells, comparable to non-treated cultures. Strikingly, in n-hexane treated cultures there are more apoptotic cells observable in liver equivalents co-cultured with neurospheres than in those performed as single-tissue cultures.

Analysing RNA levels of cytochrome P450 iso-forms and albumin by qRT-PCR did not show significant differences between treated and non-treated cultures (data not shown).

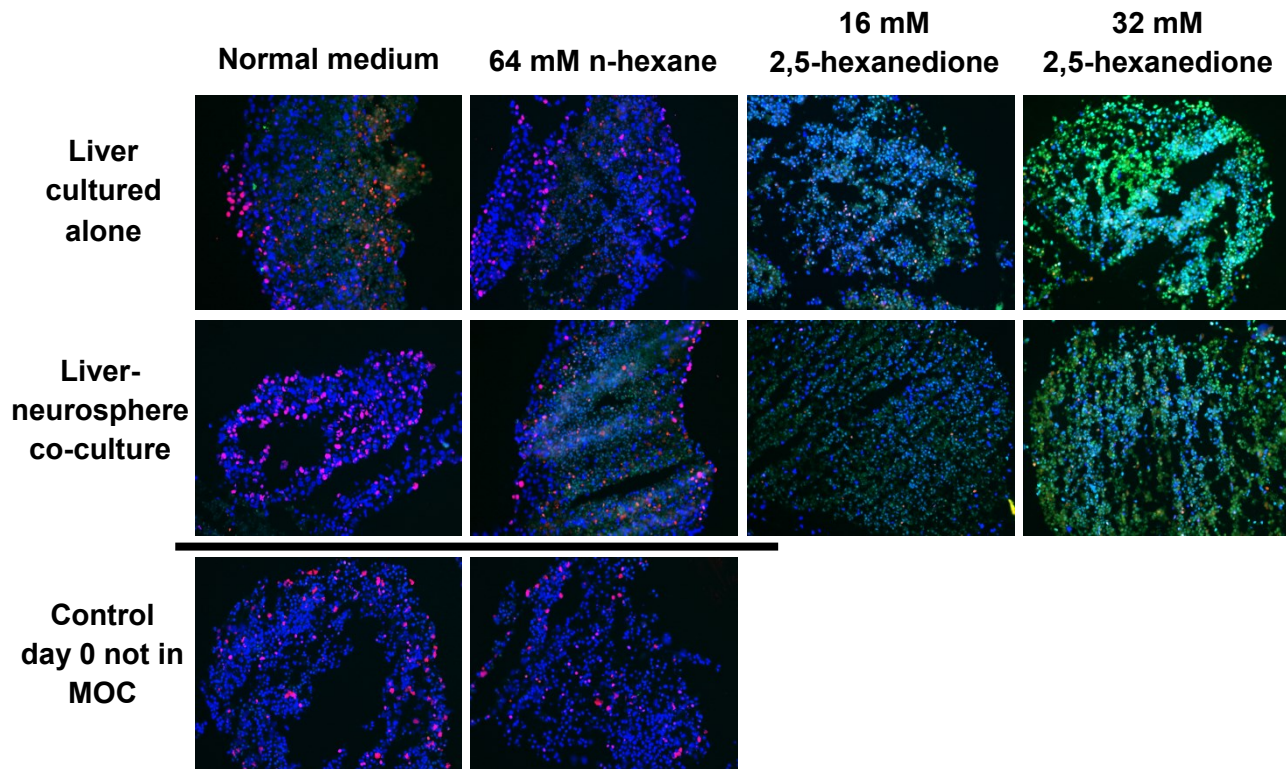


Fig. 39 TUNEL / Ki67 staining of liver equivalents co-cultured with neurospheres at direct exposure to fluid flow for 14 days in the MOC. Control liver equivalents of day 0, single-tissue cultures and co-cultures as well as cultures treated with n-hexane and 2,5-hexanedione showed distinct apoptosis (green) and proliferation (red) patterns. Nuclear stain (blue). Scale bar 100 μ m.

My colleague Anja Ramme, who did the neurosphere analysis, found out that the 2,5-hexanedione treated spheres did not have any outgrowing neurites anymore after two weeks in the MOC, in contrast to the control neurospheres or to neurospheres treated with 64 mM n-hexane, where the outgrowing neurites were still visible.⁹⁵ Furthermore, many apoptotic cells were detected by TUNEL / Ki67 staining in cells treated with 32 mM 2,5-hexanedione, whereas slightly less apoptosis was observed at the lower concentration. Again, there were no significant differences between the n-hexane and the non-treated control.

Summarising, the toxic effect of 2,5-hexanedione on neurospheres and liver equivalents could be reproduced in a dose dependent manner, whereas the toxicity of n-hexane still needs to be evaluated in further tests.

5 Discussion

The aim of this work was the generation of a 3D human liver equivalent emulating *in vivo* liver functions as closely as possible. Furthermore, the cultivation in a multi-organ-chip environment, evaluating the effects of dynamic perfusion, and the co-cultivation with other organ equivalents in a combined media circuit, studying organ-organ interactions, were envisaged. Finally, the cultures were to be exposed to toxic substances being directly toxic to the liver as well as to substances becoming toxic after being metabolised. To this end, reproducible 3D liver equivalents were produced by co-culturing well-defined HepaRG cells and primary human hepatic stellate cells (hSteC) and feasibility of cultivation in the MOC was shown in 9 different experimental setups including single-tissue culture and co-culture with skin biopsies, endothelial cells and neurospheres. Furthermore, toxicity profiles of three different substances were generated.

Are HepaRG cells an appropriate model system?

An essential part in the generation of *in vitro* liver models for metabolism studies is the adequate choice of cells. Primary cells are thought of as gold-standard for *in vitro* drug metabolism, enzyme induction and toxicity studies.⁴⁴ Especially, as liver enzymes (the cytochrome P450 family in particular) responsible for the metabolism of foreign molecules, have a wide variability in expression and catalytic activity resulting in a large phenotypical variety amongst people. Patients who develop an idiosyncratic reaction to a certain drug metabolise it in a unique way or lack certain neutralising enzymes to protect the cells from the formed reactive metabolites.²³ However, restricted access to human liver tissue and the very limited ability of adult differentiated hepatocytes to proliferate in culture, hinders widespread use of these cells.⁴⁹ Therefore, standardised industrial human *in vitro* liver toxicity studies are based on well characterised human cell lines, such as HepG2 and HepaRG even though, due to their tumorous nature, they differ from primary human hepatocytes in various aspects.^{44,52} The applicability of the HepaRG-hSteC co-culture as a system modelling liver functions will be discussed in the following.

Comparing differentiated HepaRG cells and primary human hepatocytes, it was reported that albumin synthesis and, most importantly, cytochrome P450 enzyme dependent drug metabolic capacities were stable in HepaRG cells and were comparable or even higher than in primary human hepatocytes.⁹⁸ Similarly, intrinsic clearance rates of reference drugs and enzyme induction of most cytochrome P450 enzymes were reported to be similar in HepaRG cells and primary

human hepatocytes.^{44,52,98} Darnell et al. compared HepaRG cells to fresh human hepatocytes, cryopreserved human hepatocytes and human *in vivo* data.⁹⁹ They observed that biotransformation pathways of investigated drugs were clearly different in the various cell systems. Still, all major metabolites for e.g. diclofenac were detected in HepaRG cell cultures. The expression of major cytochrome P450 iso-enzymes, various phase II enzymes and transporters could also be detected by qRT-PCR in the course of this study, some of which were significantly up-regulated after differentiation (especially cytochrome P450 enzymes). Summarising, even though HepaRG cells represent a phenotype of a single donor, thereby reducing their predictive value for the human population, the HepaRG cell line has emerged to be the gold-standard for substance testing in pharmaceutical industry due to their metabolic capacity.⁴⁴ Hence, HepaRG cells were also used in this study.

Transport function, often referred to as Phase III of drug metabolism in the liver, is critical for removal of drug metabolites. In this study, human hepatocyte transporter function of the model cell line HepaRG was demonstrated using carboxyfluorescein diacetate, a substrate of the MRP-2 transporter.⁶⁷ Carboxyfluorescein diacetate is known to be passively absorbed and metabolised by hepatocytes into fluorescein diacetate, which is actively effluxed via the MRP-2 transport protein into extended bile canalicular structures. This could be reproduced in HepaRG cells differentiated towards the hepatic lineage and was largely driven by restoration of cell polarity resulting from the formation of tightly fused cellular structures. Hence, differentiated HepaRG cells polarised, forming bile canaliculi, one of the main prerequisites for hepatocellular function.

Does the co-culture with hSteC improve cell functionality?

The use of the HepaRG cell line in combination with a change of cell culture format to 3D and, more importantly, co-cultivation with non-parenchymal liver cells was reported to improve their cellular and metabolic functions towards *in vivo*-like levels.^{5,17,41,44} Therefore, hSteC that were shown to produce liver-typical extracellular matrix proteins were co-cultivated with HepaRG cells. hSteC are the main matrix-producing cell type in the liver and play an important role in regeneration, differentiation and inflammation.^{4,14} After partial hepatectomy hSteCs participate in revascularisation of avascular islands of hepatocytes by excreting a laminin trail that endothelial cells follow to form new sinusoidal branches.²⁷ This was of particular interest, as a vascularisation of liver equivalents was envisaged for future studies. In this study, the production of laminin as well as of other extracellular matrix proteins by the cells therefore was analysed by immunohistochemistry. Cells were able to excrete laminin, collagen type I and fibronectin.

During liver fibrosis, hSteC become activated, acquiring a myofibroblast-like phenotype and start to produce more extracellular matrix. Also in *in vitro* culture, when plated on rigid substrates, these cells rapidly become activated.^{4,22} Hence, when using hSteC under standard *in vitro* culture conditions one has to keep in mind that the cells behave as they would in an injured liver.²⁵ However, when cultivating hSteC in a 3D environment, cells might revert to a non-activated state (see below).

It was reported that a co-culture of these cells with hepatocytes is beneficial for sustaining liver function. Riccalton-Banks et al. reported that a co-culture of rat hepatocytes with primary rat hepatic stellate cells on a biodegradable poly(DL-lactic acid) substratum encouraged the rapid self-organisation of 3D spheroids, which exhibited hepatocyte-specific functionality (cytochrome P450 activity and albumin secretion) after almost 2 months in static culture.²⁶ Also other groups reported that expression of albumin and cytochrome P450 iso-enzymes were better maintained under co-culture conditions using hSteC.²⁸ Maintenance of differentiated function of hepatocytes in co-culture was proposed to be mediated by direct cell-cell contacts through preferentially cell-bound signalling and transfer of lipids.^{100,101}

Summarising, a 3D co-culture of the human hepatoma cell line HepaRG and primary human hepatic stellate cells were found to be optimally suited for this project, due to their easy availability, phenotypic characteristics and supporting of each other's functions.

How do hSteC behave in prolonged liver equivalent culture?

Immunohistochemical staining of vimentin and cytokeratin 8/18 revealed that the hSteCs were distributed equally throughout the whole aggregate. In the course of this work it was shown, that hSteC co-cultivated with HepaRG cells in a 3D environment produced extracellular matrix during the first days of culture. The amount produced ceased after the first week of co-culture and no increase in extracellular matrix amount could be found thereafter. Together with the fact that hSteC could still be detected in 14 to 28 day old aggregates, it suggests, that the cells reverted to a non-activated state in the 3D environment of the liver equivalent. It was reported, that the absence of fibronectin resulted in an increased TGF- β signalling leading to excessive stellate cell activation. Hence, the production of a fibronectin bed by the hSteC, binding excess TGF- β , might result in a decreased activation of the cells.^{102,103} Already 2 days after formation, aggregates made out of HepaRG-hSteC co-cultures showed an expression of fibronectin throughout the liver equivalents being slightly higher in the core. Aggregates that had been cultivated for another 14 days in the MOC under dynamic conditions showed a homogenous distribution of fibronectin coating nearly every cell, suggesting that HepaRG cells participated producing a fibronectin bed.

Are liver equivalents prepared reproducibly?

Having specified the cell sources and co-culture conditions, a robust tissue preparation procedure had to be established. The generation of defined and reproducible liver equivalents required the application of standardised culture formats. Previous experiments had revealed that the spontaneous self-formation of aggregates in ultra-low-attachment co-cultures led to highly heterogeneous, non-reproducible spheres with a broad size distribution. Furthermore, once formed aggregates tended to fuse when cultured under ultra-low-attachment conditions, forming densely packed tissues of up to 1.5 mm diameter. Especially, this generation of huge fused aggregates was undesirable, as oxygen and nutrient limitations might occur in the core of densely packed spheres leading to massive impact on the cell's functionality. Therefore, aggregates with a radius of no more than 100 to 150 μm were envisaged. The application of Perfecta 3D® 384-Well Hanging Drop Plates resulted in the gravity assisted semi-forced formation of consistent aggregates within 2 days of hanging drop culture. Here, cells were allowed to fastly re-establish cell-cell contacts needed for cell survival and differentiation. Disk shaped aggregates of 300 to 400 μm diameter and 200 to 300 μm heights were formed. Hence, the diffusion distance to the core of one sphere was no more than 150 μm .

Do liver equivalents form bile canaliculi?

Immunohistochemical staining of newly formed aggregates for ZO-1 and MRP-2 showed that cell–cell contact supported tight junction development and polarisation. Still, staining was weak and scattered in newly formed aggregates. Only after a prolonged culture of 14 days in the MOC the bile canaliculi-like network became more apparent. MRP-2 is an important hepatobiliary transporter protein that modulates pharmacokinetics of many drugs.⁶⁷ It's expression and activity in hepatocytes under *in vitro* conditions indicates the restoration of liver-specific functions. Previous reports indicated that in conventional 2D cell culture, the expression of MRP-2 was occasionally observed as tiny unconnected dots between two adjacent hepatocytes illustrating the limited formation of bile canalicular structures under these culture conditions. Only when culturing cells in a 3D tissue-like arrangement, assisted by a perfusion-based microfluidic system, the restoration of membrane polarity was promoted, as reported.⁶⁷ The existence of a functional bile canalicular network in a 3D liver tissue equivalent was one of the main prerequisites of functional tissue homeostasis, as waste products secreted by the cells had to be removed from the tissue.

Do liver equivalents differ from well characterised terminal differentiated HepaRG cells on gene expression level?

qPCR revealed that liver equivalents had transcriptional levels comparable to differentiated monolayers of HepaRG cells for phase I and II metabolising enzymes (cytochrome P450 1A2, 2B6, GSTA-2 and UGT-1A1). Only the expression of cytochrome P450 3A4 was significantly reduced in aggregates compared to differentiated monolayers. This might be due to the omission of DMSO during the aggregation process, which is a known cytochrome P450 3A4 inducer. Still, the inducibility of this cytochrome P450 enzymes in aggregates and therefore the metabolic competence of the liver equivalents was shown using rifampicin, raising the expression to levels even significantly higher than in differentiated monolayers.

The transcriptional level of albumin varied strongly within the differentiated HepaRG monolayers. Differentiation of the cells in DMSO had been performed for one to three weeks, with the cells being differentiated longest expressing most albumin. Already on day 2 to 5 after production, liver aggregates showed similar albumin expression as the mean differentiated HepaRG monolayers, even though aggregates were not stimulated by DMSO treatment. For the production of aggregates, cells were passaged, leading to disrupted cell-cell contacts, and then forced to polarise anew by forming tight junctions with neighbouring hepatocytes. The anew differentiation of hepatocytes inside the aggregates took some time. This might be why we observed a slightly reduced albumin production capacity during the first days also in those aggregates that had been produced out of HepaRG cells that had been differentiated for longer periods. Similarly, the expression levels for BSEP, CPS-1 and GSTA-2 increased with differentiation time.

Hence, liver equivalents generated out of the well characterised HepaRG cell line did not show significant differences compared to monolayer cultures in a set of 9 important functional markers, even though aggregates were no longer treated with DMSO (a substance inducing differentiation). This omission of DMSO enabled the co-cultivation with other organs not tolerating DMSO and, furthermore, facilitated future substance tests avoiding cross reactivity. Liver equivalents were therefore applicable to further studies involving metabolism and toxicity studies.

Having established a robust tissue preparation procedure for the generation of reproducible liver aggregates showing prime liver *in vivo*-like functionality and having assessed that 3D tissue culture systems in contrast to conventional monolayer cultures more closely resembled the tissue of origin not needing chemical stimulation, the hurdles of limited nutrient and oxygen supply to these densely packed aggregates had to be overcome. The effects of dynamic perfusion on the liver equivalents generated during the course of this study were evaluated subsequently.

When cultivating liver equivalents in the MOC, what is the difference between Transwell® and exposed to fluid flow cultures?

Liver single-tissue equivalents were cultured over 14 days in the MOC, successfully keeping cells viable and metabolically active. Experiments were performed in Transwell® tissue culture inserts, as well as free floating aggregates. Here, some prime differences regarding aggregate morphology were detected by immunohistochemistry. MOC experiment 1 of liver single-tissue culture inside Transwell® units showed that cells only grew out slightly from the aggregates and that cytochrome P450 3A4 expression was higher in the cells that had spread along the membrane facing the underlying channel of the MOC circuit than in cells on the upper surface of the aggregate. In previous literature, the effect of flow in a bioreactor was reported to induce cytochrome P450 activity. Furthermore, O₂ and CO₂ supply via the cell basal pole was demonstrated to be beneficial by improving cytochrome P450 activity.⁶⁹ Hence, the cells covering the bottom membrane receiving a higher supply of nutrients from the underlying current and experiencing higher shear forces acting on their cell membranes showed a zonal increase in cytochrome P450 3A4 expression. This zonal expression confirmed the assumptions of a beneficial effect of flow on the cells.

Liver equivalents of MOC experiment 2 that were directly exposed to fluid flow also had a higher cytochrome P450 3A4 expression on the surface of the aggregate than in the core, again hinting at a better supply of oxygen and nutrients and the effects of fluid flow on the cells' behaviour. The enhanced nutrient supply might also be a reason for more proliferating cells in these areas of the liver equivalents. Preliminary experiments using fluorescence quenching (Presens GmbH, Regensburg, Germany) revealed no oxygen limitation in the circulating media (data not shown). However, inner cells of liver spheroids might experience reduced oxygen concentrations leading to a reduction in proliferation and metabolic activity. The increased shear stress experienced by the aggregates placed directly in the fluid flow did not hinder the cells from spreading along the glass surface of the MOC, leading to high proliferation.

Hence, to preserve aggregate shape a culture in Transwells® is favourable, even though, no negative effects could be detected by the exposure to fluid flow. Still, the daily media exchange is hampered by the insertion of Transwell® inserts. Especially, when cultivating more than one organ in a MOC circuit at least one cell culture compartment without Transwell® is needed for easy access to the media underneath. Therefore, most co-culture experiments were performed with the liver equivalents being directly exposed to the fluid flow.

Can we obtain zonation in the MOC?

The MOC presented in this study has the theoretical ability to generate controllable functional oxygen gradients, as the fluid flow inside the reactors was laminar and turbulence was not likely to occur. Hence, the mass transfer relied mainly on diffusion, as is the case in the human liver. Still, as the PDMS used for the construction was oxygen permeable, a continuous supply of oxygen to the channels is assumed. Therefore, to generate more sophisticated and controllable gradients a coating of the cell culture insert with an oxygen impermeable material and the alignment of cells along the fluid flow would be necessary.

Still, first hints of functional liver zonation inside the bioreactor obtained in Transwell® cultures, as described above, were promising. Especially, as the emulation of the different zones of the liver is of prime importance in liver tissue engineering. Modelling this zonation enables hepatocytes of their respective zone to concentrate their cellular and molecular capacities onto the specific function to which they are dedicated.¹⁰⁴ Drug-induced liver injury (DILI) events also show a considerable degree of zonal preference depending on the properties of the respective toxic or allergic agent. It has been thoroughly recognised that physiological fluid flow through the liver tissue is one essential prerequisite for the formation of stable, functionally important oxygen and nutrient gradients, which are a main driver of liver zonation.^{12,13,105} So far, only few groups reported on microfluidic bioreactor systems able to create zonal differences. The group of Bhatia et al. established a perfused parallel-plate bioreactor that imposed physiologic oxygen gradients on co-cultures of rat hepatocytes and non-parenchymal cells. A regional heterogeneity of cytochrome P450 iso-enzymes, mimicking the distribution seen in the zoned liver, was demonstrated. A subsequent perfusion of acetaminophen for 24 hours resulted in maximal cell death at the low-oxygen outlet region, similar to centrilobular necrotic patterns observed *in vivo*.¹⁰⁶ Still, this system was based on a monolayer of cells, reducing the similarity to *in vivo* hepatocytes. Furthermore, the bioreactor was perfused by an external syringe pump, increasing the total systemic volume to tissue ratio. To the best of my knowledge, only one group reported on a 3D hepatocyte culture system including an integrated micropump and being able to generate functional oxygen gradients so far, the group of Domansky and colleagues (see introduction). The integrated peristaltic micropump was able to circulate culture medium at adjustable flow rates through tissue scaffolds seeded with cells. Due to the oxygen consumption of the cells physiologically relevant gradients evolved in the tissue, even though the gradients were steeper than those *in vivo*, as the culture medium did not contain haemoglobin serving as an oxygen depot.⁷⁴ The physiological relevance to the *in vivo* situation of this system remains unmatched. Still, the integration of secondary organs is not envisaged by the group and, hence, systemic measurements are not possible.

Do liver equivalents in the MOC receive sufficient oxygen and nutrient supply?

Analysis of the metabolic activity of cells cultured in the MOC, as well as of LDH activity and albumin production rates were performed daily to assess the viability and functionality of the tissue. The metabolic activity of all MOC cultures was measured as glucose consumption and lactate production rate per day and MOC circuit. Elevated lactate secretion is reported as a signal of cellular stress.³⁵ In addition, it is a sign of wasteful mainly anaerobic metabolism, as further processing of glycolytic pyruvate through the tricarboxylic acid cycle (TCA cycle) instead of secretion as lactate, would yield more ATP per molecule of glucose. Still, under normal cell culture conditions a lactate production rate of 2 mM / 24 h was reported for HepaRG cells and ,therefore, everything exceeding this value was regarded as being related to cellular stress (see introduction).³⁵ Similarly, in the human body, lactate concentrations in the blood are normally in the range of 1 to 2 mM under resting conditions, but can rise ten-fold during exercise. Here, lactate metabolism is a tightly controlled and evolutionary optimised process of production (mainly in muscle cells) and consumption (mainly by periportal hepatocytes, synthesising glycogen). In the MOC at steady state, lactate concentrations were always in the range of 2 to 3 mM with the exception of the liver-skin co-culture where the skin was directly exposed to the fluid flow (which will be discussed later). Hence, lactate concentrations in the media indicated that cells did not experience excess stress being due to hypoxia or augmented shear force. Furthermore, concentrations were close to physiological although primary hepatocytes under *in vivo* conditions rather take up lactate than produce it.

Furthermore, looking at the ratios of glucose consumption and lactate production in MOC cultures, a 2 : 1 ratio or higher could be found frequently. For example, liver single-tissue cultures directly exposed to the fluid flow had a glucose consumption rate of 530 µg per day and circuit and a lactate production rate of 230 µg per day and circuit (≈2.5 mM), making a ratio of nearly 2 : 1. This was a further indicator of aerobic metabolism of the cells, as only part of the glucose consumed was converted to lactate and the lactate production rates did not exceed the values reported for well oxygenated monolayer cultures. Furthermore, it was confirmed that no oxygen limitation could be detected within the medium of the chip by a preliminary experiment using fluorescence quenching and an optical fibre-assisted read-out system. As the ratio of glucose consumption and lactate production remained low and unchanged over the whole cultivation time in all MOCs, an efficient energy metabolism at steady state was indicated for liver single-tissue cultures. A future means to more accurately predict oxygen consumption and availability might be the system of Colibri Photonics. Here sensors in the nm- and µm-range, made out of polymer-based dyes, can be inserted directly into the media or tissue and analysed online by a specialised fluorescence microscope. These sensors offer high resolution and are currently tested in our laboratory.

During MOC cultures, only part of the medium was replaced every day, hence, glucose concentrations in the medium decreased from 2 g/L, which was the glucose concentration in the primary media, to a calculated mean of 1.53 g/L present in the MOC after medium exchange. As about 35% of the amount of glucose present in the media was used up by the liver equivalents every day in single-tissue cultures, sufficient feeding rates were assumed. Under physiological conditions, the glucose concentration in the blood normally does not exceed 1 to 1.3 g/L and, therefore, the MOC culture conditions in regard to glucose availability were considered as close to physiological. In human hepatocytes *in vivo* the glucose metabolism is a complex and strictly regulated process. In *in vitro* culture, culture environment and media composition severely alter the glucose metabolism of the cells. Both consumption and release were described for *in vitro* hepatocyte cultures.⁹⁸ The liver micro-tissues generated in this study did not show measurable signs of glucose release in any of the experimental settings. However, it could not be excluded that active glucose release processes in the culture might be hidden by the immediate consumption by neighbouring hSteCs. Summarising, an adequate supply of energetic substances, in regard to glucose and oxygen, to the cells was assumed.

Were albumin production rates affected by culture in the MOC?

Looking at the albumin production of liver equivalents directly exposed to the fluid flow, it could be shown that the albumin synthesis rates were significantly increased in dynamically perfused chip cultures compared to statically cultured liver equivalents. Values obtained on day 7 of culture were comparable in dynamic and static cultures, whereas at day 14 a twenty-fold increase was observed in MOC circuits. The reduction in albumin production over time for statically cultured HepaRG aggregates was comparable to values reported in literature.⁹⁸ Whereas, the increased albumin production in MOC cultures over time might be due to a significantly improved supply of nutrients and oxygen to the aggregates, stimulating their metabolic activity and keeping the cells in a metabolically competent state. This significant increase in albumin production capacity could also be found on mRNA level. Aggregates cultivated for 14 days in the MOC (as cultures being directly exposed to the fluid flow) showed a significant up-regulation of albumin production on transcriptional level compared to statically cultured aggregates ($p = 0.0025$). Similarly, Baudoin et al. observed in their microfluidic chip system, comprising HepG2/C3A cells under dynamic perfusion, that cell metabolism and albumin synthesis were higher than in static controls, also attributing it to the improved nutrient supply.⁶⁹

Did the dynamic perfusion in the MOC alter the expression of functional markers?

qRT-PCR analysis of aggregates cultured for 14 days in the MOC showed a significant increase not only in albumin transcriptional level but also in phase II metabolising enzyme UGT-1A1 mRNA levels compared to aggregates cultured for 2 to 4 days under static conditions. This might be due to the re-established polarisation of the cells 14 days after the aggregation procedure as well as being an indicator of the beneficial effect of dynamic culture in the MOC. No significant differences could be detected on mRNA level for other phase I and II metabolising enzymes cytochrome P450 1A2, 3A4 and GSTA, as well as for ABC transporters. Hence, after 14 days of culture the densely packed aggregates in the MOC reached a differentiation state similar to monolayer cells that had been treated for one to three weeks with DMSO (a known inducer of differentiation). As aggregates in the MOC were not altered chemically, they might be even more prone to further induction with substances like rifampicin. During following studies an induction of cytochrome P450 3A4 in MOC culture by troglitazone was shown (described below).

Having established a liver single-tissue MOC culture, keeping the cells viable and metabolically active over prolonged culture periods of up to 14 days, co-cultivations of skin, endothelial cell and neuronal tissue were envisaged.

Were liver-skin co-cultures in the MOC possible at physiologically relevant ratios?

Co-cultures of liver equivalents with skin biopsies were performed in order to adapt the multi-organ-chip to current standard substance testing procedures involving topical medication. Therefore, co-cultures were performed again as being exposed to the fluid flow or inserted into Transwell® units. The latter allowed the skin to be at air-liquid interface, avoiding medium superfusion and, hence, facilitating later dermal substance exposure. This might ultimately lead to reduced shear stress and different nutrient supply characteristics between Transwell® and directly exposed to fluid flow cultures, which was examined in the following.

Skin-biopsies of 4 to 5 mm diameter consisted of approximately five million cells representing $1/100000$ of the human skin area. As the skin surface area varies strongly with a person's size, both 4 and 5 mm biopsies represented the desired size ratio. During the course of this research, larger 5 mm biopsies were inserted into Transwell® holders. Here, to assure an air-liquid-interface culture a tight fitting was needed to prevent media from the underlying circuit to flush over the skin surface. Smaller 4 mm biopsies were used for the cultures being directly exposed to the current. For these experiments it was important to retrieve a high number of biopsies out of a single skin sample increasing the number of possible repetitions. As the numbers of prepuce

samples were limited for these tests, smaller biopsies were taken. Unlike commercially available skin models that consist mainly of fibroblasts and keratinocytes, the prepuce contains a variety of different cell types – like adult stem cells that are capable of regenerating the epidermis and are present in their specific quiescent promoting niches. Furthermore, the tissue biopsies were saturated with blood borne substances like albumin. This heterogeneity of the original tissue may lead to donor-specific variations, which might explain the high variances for certain data points.

The combined tissue volume of both liver and skin culture in the system was 26 µl per circuit for the co-cultures. The total medium volume in the MOC was 600 µl per circuit without the Transwell® and 400 µl per circuit using the Transwell® insert in each compartment. This corresponded to a total systemic media-to-tissue ratio of 23 : 1 or 15 : 1, respectively. In humans, regarding a 73 kg man, the total extracellular fluid volume is 14.6 l, whereof the intercapillary fluid volume is 5.1 l. Therefore, the physiological extracellular fluid to tissue ratio would be 1 : 4. In the MOC, the excess amount of media was due to the media demand of the tissue. Cell culture medium for example is known to have a reduced oxygen storage capacity compared to blood. Furthermore, a reduction in medium volume was not feasible as it would have led to limitations in media supernatant analysis capacities. Still, in contrast to microfluidic devices described in literature, our MOC system provided a low systemic media-to-tissue ratio with the flexibility to combine different standard tissue cultures.

Did liver-skin co-cultures receive sufficient oxygen and nutrient supply?

In the 28 day Transwell® liver-skin co-culture system, the glucose consumption and lactate production rates at steady state were comparable to those of liver single-tissue cultures, even though now about 5 times the number of cells were present. This might be due to a limiting amount of glucose present in the medium, hindering cells from increased uptake. Furthermore, the increased glucose consumption rate during the first 7 days of culture, which was due to the increased feeding rate of every 12 h, decreased when the feeding rate was reduced to every 24 h. Taken together, this might hint at a glucose limitation during this later phase.

Interestingly, the co-culture that had been directly exposed to the fluid flow showed strong increase (+50%) of lactate release levels. This might be due to the poorer oxygen supply to the submerged skin tissue leading to cellular stress and anaerobic metabolism. Especially for the skin, these culture conditions are highly un-physiological. Immunohistochemical analysis of skin biopsies by my colleague Ilka Wagner showed, that biopsies cultivated as submerged cultures indeed had a totally destructed epidermis compared to Transwell® cultures.⁹⁷ This is due to

maceration of the epidermis, which is soaked in media, and finally leads to a destruction of the barrier function of the skin.

The constant LDH activity of 20 U/L of the liver skin co-culture directly exposed to the flow measured in the media supernatants indicates an artificial but stable tissue turnover in the system. *In vivo* an LDH value of < 250 U/L in blood is recognized as normal due to the high cell turnover rate, whereas under *in vitro* culture conditions lower values are expected, depending on the cell type used.³ Cell death within the MOC at steady state happened primarily in the skin culture compartment, as data from MOC skin single-tissue cultures suggest⁹⁷ and as was already suggested by lactate release data (see above). Apart from the un-physiological culture conditions for the skin, being submerged culture rather than an air-liquid interface culture, a further possible explanation might be the reaction of the tissue to the wounding by punching the skin.

TUNEL / Ki67 staining revealed that liver equivalents had proliferative cells throughout the whole aggregate. As only very few apoptotic cells were found in the core of liver equivalents, one can summarise that, even though glucose might be limiting, viable aggregates could be maintained in a liver-skin co-culture.

Was the albumin production affected by the liver-skin co-culture?

Having assessed the supply of nutrients to the MOC co-cultures, their metabolic activities in terms of albumin synthesis were analysed. In all co-cultures the amount of albumin measured in the supernatants was unexpected high during the first 2 to 4 days. Looking at single-tissue cultures it became obvious, that most of the albumin was washed out of the skin biopsies, probably being released from the inner lumen of the damaged micro-vessels of the skin and the extra-capillary depots. Nearly 50% of the extra-vascular albumin in humans is stored in the skin.¹⁰⁷ Here, albumin is absorbed by the network of collagen, proteoglycans and hyaluronans. Therefore, skin biopsies in submerged culture can act as an albumin depot.

Single-tissue liver cultures showed a constant albumin production, whereas the liver-skin co-culture did not show any signs of albumin release after the albumin had been washed out of the skin. Here, it could be suggested that the albumin produced by the liver is degraded by skin fibroblasts and as the crosstalk between liver and skin within the co-culture steadies over time, the albumin concentration stays close to zero. However, this assumption was refuted by experiment no. 5 (liver-skin-endothelial cell co-culture) where the albumin mRNA level was checked for all single-tissue cultures as well as for the co-cultures. Here, albumin mRNA levels of liver equivalents significantly decreased with the number of organs co-cultured. This might be

due to the glucose limitation experienced by liver aggregates in co-culture, as described above. The cells might reduce their metabolic activity as glucose becomes limiting.

The decreased release of albumin found in co-cultures cultivated under static conditions compared to MOC cultures (experiment 3) might be due to the decreased wash-out effect from the skin, when no underlying current was applied. Interestingly, this difference could also be found when comparing MOC Transwell® cultures (experiment no. 3) to the MOC cultures being directly exposed to the flow (experiment no. 4). In Transwell® skin biopsies, the albumin was washed out of the tissue much slower, decreasing strongly during the first 4 days but still showing albumin wash-out after 10 to 16 days of co-culture, whereas in directly exposed cultures no more release was detected after day 4. This again is an indirect indicator that the supply of substances to and from the cultures is increased when cultured in the MOC and even more so when put directly in the current of the media flow.

Can liver-skin co-cultures be performed over periods long enough for OECD relevant repeated dose toxicity testing?

OECD guidelines for dermal sub-systemic repeated dose toxicity testing of chemicals and cosmetics in animals require 21 to 28 days of exposure (OECD guideline no. 410, “Repeated Dose Dermal Toxicity: 21/28-day Study”) and, therefore, the stable performance of Transwell® co-cultures in the MOC over 28 days was especially important. TUNEL / Ki67 staining of dynamically and statically cultured liver equivalents and skin biopsies in Transwell® units after 28 days of culture showed that apoptosis was relatively low in both liver and skin tissues cultured in the MOC, whereas statically co-cultured tissues showed a strong increase in apoptotic cells especially in the core of the organ equivalents. This increase in viability in MOC cultures was a result of the improved nutrient supply to the tissues under dynamic culture conditions. The positive expression of cytochrome P450 3A4 and 7A1 revealed that liver aggregates maintained a metabolically competent phenotype over the whole cultivation period. Whereas, statically cultured liver equivalents showed a staining of equal intensity as dynamically cultured cells, expression was more defined in MOC cultures. Similarly, collagen I expression was much more intense in MOC cultures compared to static cultures, especially at the outside of the aggregate. This might be due to the shear stress experienced by cells cultured under dynamic conditions. The sheath of collagen I at the outside of the aggregate might protect the cells from excess shear stress.

Summarising, cell viability proved that the MOC system is able to cultivate a combination of two tissues for up to 28 days. To the best of my knowledge, this combination of skin and liver tissue

in a dynamically perfused system has not been published before and represents a successful prove of principle for further studies.

Having successfully co-cultured skin and liver tissue for up to 28 days in a combined media circuit, a further improvement concerning physiological relevance was performed by including endothelial cells in the chips.

Was the metabolic activity of the co-culture altered by the addition of endothelial cells?

Experiment 5 of liver-skin co-culture in an endothelialised MOC showed that combining 80% of standard HepaRG medium with 20% of HDMEC-medium supported 15 day co-culture of all tissues. All channels of the MOC were confluent covered with endothelial cells throughout the whole cultivation period.

Comparing the metabolic activities of the endothelialised MOC co-cultures with previous experiments was not possible, due to the alterations in medium composition in favour of the endothelial cells. Hence, respective single-tissue cultures had been performed in parallel under the same conditions for comparison. The total glucose levels present in the media decreased with the number of organ equivalents in the MOC. Liver single-tissue cultures had glucose levels of 1.53 g/L present in the medium after medium exchange. In skin-liver co-cultures, mean glucose concentrations in the media decreased further to 1.39 g/L and in the endothelial cells-skin-liver three-tissue co-culture lowest values of 1.26 g/L were obtained. The co-cultures consumed more glucose, therefore decreasing the available amount in the media, which in turn had a negative effect on the increased demand of the co-culture. It is worth noting, that at steady state skin single-tissue cultures had a mean glucose consumption level of 470 µg per day and MOC circuit, single-tissue liver equivalents consumed 530 µg per day and circuit and the respective co-culture 630 µg per day and circuit. The decreased glucose consumption of co-cultures compared to the added consumptions of both single cultures indicates, that the glucose level in the skin-liver co-culture is indeed limiting. Still, no further effects of the addition of endothelial cells to the co-culture was observed, apart from further lowering the glucose concentration.

The partial media exchange might not suffice to deliver enough glucose to the cells in a two or three-tissue combined experiment. For future experiments it might be of interest to increase the glucose concentration in the medium to 4 g/L or double the medium exchange rate. Both however might bring disadvantages to the system. Increasing the glucose concentration might lead to a stimulation of metabolic activity leading to enhanced lactate production. In consequence this

might lead to a further acidification of the culture medium. Furthermore, homeostasis of the system might be disrupted by enhanced cell proliferation. Increasing the feeding rate is not possible so far, as media exchanges are performed manually. The time needed to change the medium of a large number of chips is too high to increase feeding regimens to more than every 12 hours. My colleagues are establishing a robotic system at the moment, enabling automated medium exchange and therefore a more continuous supply of glucose to the cells.

Summarising, a glucose limitation is observed for co-cultures of two or more organs, leading to a decreased albumin production capacity. Still no influences on cell viability could be detected. Endothelial cells covering all channel surfaces were successfully co-cultivated with skin and liver tissue paving the way for future endothelialisation of organ equivalents, leading to a closed biological circuit and, hence, enabling the perfusion with whole blood.

Is a co-culture of liver equivalents with neurospheres possible?

Having successfully co-cultivated liver equivalents with skin biopsies and endothelial cells, a liver-neurospheres co-culture was envisaged. During MOC culture the neurospheres attached to the bottom glass surface of the MOC, growing out and fusing to each other, forming an almost monolayer-like structure in the insert. This hampered the harvesting and analysis of the tissue. Still, my colleague Anja Ramme who performed the neurosphere analysis found out that neuronal markers β -Tubulin III and MAP2, as well as the neuronal progenitor marker Nestin was expressed by the spheres, whereas embryonic stem cell marker TRA-1-60 was negative in all samples. This confirmed that the neuronal tissues kept their differentiated status over the whole MOC co-cultivation time.⁹⁵

The metabolic analysis of the media supernatants revealed that the co-culture had a slightly increase glucose consumption rate during the first 5 days of culture. During this timeframe media was exchanged twice a day, supplying the cells with higher amounts of energetic substrate. From day 6 onwards, consumption rates dropped to the levels of single-tissue cultures, suggesting that all available glucose was taken up. Again, as only a partial media exchange of 45% per day was applied, high consumption rates resulted in decreased glucose concentrations in the medium, therefore, limiting the available amount and decreasing further consumption rates. Again, the co-culture did not consume as much glucose, as the two single-tissue cultures together. Taken together, this again hints at a glucose limitation for the co-culture.

Summarising, liver equivalents were successfully co-cultivated with neurospheres over a period of 14 days in a combined medium circuit. Cells were viable keeping their differentiated status and

metabolic capacity unchanged compared to single-tissue cultures. In the following, substance testing on the established single and co-cultures were performed.

Can the toxicity of troglitazone be modelled in a liver-skin MOC culture system?

Finally, substances that were reported to lead to tissue damage were tested on the multi-organ-chip co-cultures. Troglitazone was the first substance chosen to explore whether the MOC system is suitable for repeated dose substance testing. Its dose dependent toxicity on HepaRG cells *in vitro* has been described previously.^{35,108} After 14 days of repeated exposure to a monolayer of HepaRG cells, Limonciel et al. observed a toxicity of troglitazone at a concentration of 50 μM .³⁵ During clinical trials troglitazone was administered to patients at a concentration of up to 600 mg per day.¹⁰⁹ Reducing the 600 mg down to $1/100000$ (corresponding to the miniaturisation rate of our human-on-a-chip) would give a maximum of 6 μg per day corresponding to about 10 μM in the chip. Hence, the minimal dosage of 5 μM per day and circuit was tested as well as the reported 50 μM per day and circuit.

During our first toxicity test MOC experiment, liver and skin co-cultures that had been directly exposed to the fluid flow were repeatedly treated with these two different doses of troglitazone for a total of 7 days, starting on day 1 of culture. Troglitazone was administered during the first 7 unsettled days of co-culture, because a higher sensitivity to a toxic agent at this stage was hypothesised. Nevertheless, it had no significant effect on the metabolic activity of liver and skin co-cultures. No significant differences could be found on glucose consumption or lactate production levels, contradicting findings described by Limonciel et al.³⁵ Whereas, LDH activity measured in the supernatants increased significantly in cultures treated with 5 μM and 50 μM troglitazone from day 4 of culture onwards. An increase of 60% compared to controls was measured on day 7. This is a clear indicator for increased cell death in the treated cultures. Furthermore, an increase in cytochrome P450 3A4 was detected on protein as well as on mRNA level. This enzyme was reported to play a major role in the metabolism of troglitazone *in vivo* and *in vitro* in primary human hepatocyte culture.¹⁰⁸ Rogue et al. also reported an increase in BSEP (also known as ABCB11) for PPAR agonists muralitazar and tesaglitazar, but not for troglitazone. Still, qRT-PCR results suggest that the three dimensional configuration of the cells and the dynamic perfusion might have altered the cells in a way that an increased excretory activity of the cells by treatment with troglitazone can be found. The decrease in albumin production might be due to a shift in metabolic activity towards the increased biotransformation activities. Summarising, the first experiment revealed a sensitivity of the MOC co-cultures of liver and skin equivalents to a liver toxic substance at protein and mRNA levels as well as on direct cell viability

measures. MOC co-cultures showed first indication of toxicity already at 5 μM , a concentration relating to *in vivo*-like dosage and being ten-fold lower than previously reported values.

In a second experimental run (liver-skin-endothelial cell co-culture, experiment no. 8), long-term analyses extending toward the steady state phase of culture were performed, concentrating on only one dosage of troglitazone (50 μM). Troglitazone was added to the co-cultures starting on day 5, after MOC cultures had reached their metabolic steady state. Furthermore, compared to the previous test an improvement in culture conditions was performed. Skin biopsies were placed in Transwell® holders at air-liquid interface as was shown to be beneficial for these tissues, whereas liver equivalents were cultured directly in the fluid flow of the MOC. Additionally, endothelial cells were added to the two-tissue cultures to reach a higher complexity of co-culture. This endothelialisation of the MOC circuits was stable over the whole culture period.

Analysing the troglitazone concentrations in the media supernatant revealed that most of the substance was taken up by the tissues on the first day of treatment. It had been reported previously, that troglitazone distributes extensively to various body tissues. The highest concentrations were reported to be in the liver, gastrointestinal tract and fat.¹⁰⁹ Especially, the uptake in skin biopsies containing small amounts of fatty tissue underneath were observed in this study. All cultures containing skin biopsies showed a marked decrease in troglitazone concentration in the supernatants after the first day of treatment. The concentration in the MOC after media exchange than increased gradually, suggesting a constant take-up of substance by the tissues. Cultures containing liver equivalents also showed a reduction of troglitazone concentration in the supernatants in the beginning of treatment, even though it was less prominent than in co-cultures containing skin biopsies. This might be due to the size difference between the respective organs. Skin biopsies had a mean volume of 24 μl , whereas liver equivalents had a volume of only 1 to 2 μl . The troglitazone concentration in liver single-tissue and liver-endothelial co-culture than increased to a mean of 25 μM at steady state, which equals half the amount of added substance. The depletion of half the amount of troglitazone from the medium per day matched the reported *in vivo* troglitazone elimination half-life of 8 to 24 hours.¹⁰⁹ Still, endothelial cell single-cultures showed a similar profile, only that the concentration was always 10 μM higher than liver single-cultures. The fact that the concentration added to the medium (50 μM) was not reached in any of the cultures (not even in chips only comprising endothelial cells) might indicate, that some of the troglitazone diffused into the PDMS bulk of the chip. This phenomenon had been described earlier for other substances. Especially, small-molecule drugs are absorbed readily by the porous nature of PDMS, depleting them from the medium.¹¹⁰ However, the 10 μM difference between endothelial single-culture and liver single and co-culture might be the concentration degraded by the hepatocytes every day.

Again, no differences could be found on glucose consumption or lactate production levels comparing treated and non-treated cultures. Similarly, qPCR revealed expression patterns similar to former experiments, confirming observed trends. mRNA levels for cytochrome P450 3A4 were again increased in all single and co-cultures treated with troglitazone and, similarly to former experiments, mRNA levels for BSEP showed a slight trend of being increased in all treated cultures compared to control. RNA levels for albumin decreased with the number of organs co-cultured as already described earlier, which might be due to glucose limitation. As already observed before, a decrease in albumin mRNA levels in treated cultures compared to control can be observed, indicating a shift in metabolic activity.

Summarising, troglitazone concentrations in the media depended on the type of organ cultures relating to the *in vivo* substance distribution. Furthermore, the induction of genes having relevance to the *in vivo* troglitazone metabolism could be reproduced at concentrations being lower than under standard cell culture conditions. A drawback of the current system might be the glucose limitation in the co-culture, which leads to an altered metabolism for example in regard to albumin production and the possible uptake of substances by the PDMS, leading to an underestimation of the toxic effects.

Do n-hexane and 2,5-hexanedione show their toxic effect on liver-neurosphere MOC co-cultures?

In vivo n-hexane is degraded to the metabolite 2,5-hexanedione, which was reported to cause neurotoxicity linked with chronic n-hexane exposure. Whereas, short term exposures to 2,5-hexanedione showed no effect in a monolayer of neural cells, it was reported to be highly toxic in prolonged cultures of up to 24h.⁹² Especially, the neural cell line NTera-2 was reported to be vulnerable to this substance. An IC₅₀ of 32 mM was reported for a 24 h treatment of NTera-2 monolayers with 2,5-hexanedione.⁹² Therefore, a co-culture of neurospheres, produced from differentiated NTera-2 cells, and liver equivalents was subjected to a daily treatment of 64 mM n-hexane, 16 mM 2,5-hexanedione or 32 mM 2,5-hexanedione after cultures had reached their steady state on day 5 of co-culture.

Analysing the media supernatant for 2,5-hexanedione remaining in the media, showed that there were no differences in single-tissue liver or neurosphere cultures compared to co-cultures. After the first day of treatment 70% of added concentration was present in the supernatants, which increased to 85% on day 5 of treatment. This reduced concentration during the first days of treatment might be due to the absorption of small amounts of substance in the tissues or also in the PDMS of the chip, even though it was much less prominent than in the previous troglitazone

study. Still, this might lead to an artificial lowering of the substance concentration in the medium and an underestimation of its toxic effects especially during the first days of treatment. The addition of n-hexane to the co-cultures had been performed by mixing n-hexane with the medium before addition to the chips during the first 6 days of treatment, whereas from day 7 onwards, n-hexane had been added directly to the MOC circuits. Due to the poor solubility of n-hexane in water, it might be that co-cultures did not reproducibly receive sufficient amounts to lead to toxicity. After day 7 however, n-hexane was applied directly and a subsequent increase of 2,5-hexanedione concentration in the medium in liver single-tissue cultures as well as in liver-neurosphere co-cultures on day 9 of treatment were observed. Still, these experiments need to be repeated to verify if liver aggregates were indeed able to metabolise n-hexane to 2,5-hexanedione in amounts sufficient to lead to neurotoxicity.

No changes between the differently treated cultures could be found on metabolic activity. Whereas, LDH activity increased drastically starting on day 4 in cultures treated with lower concentrations and already on day 2 of treatment in cultures exposed to 32 mM 2,5-hexanedione. A maximum LDH activity of 272 U/L for 32 mM and 205 U/L for 16 mM co-cultures was obtained that declined slowly afterwards. Especially, in the cultures treated with 32 mM 2,5-hexanedione the LDH activity declined drastically after reaching its peak on day 4 of substance exposure. This indicated, that all cells had died, which was confirmed by immunohistochemistry at the end of culture. Many apoptotic cells were detected in liver single-tissue and liver-neurosphere co-cultures treated with 32 mM 2,5-hexanedione. Interestingly, the sum of single-tissue LDH activities equalled the LDH activity of the co-culture until day 4 of treatment in the 32 mM cultures, when the maximum of LDH activity was reached. Afterwards, the LDH activities in co-culture were higher than the sum of single-tissue activities. This was also true during the whole exposure period in the 16 mM treated cultures, where co-cultures had a mean 57% higher LDH activity than the added up single-tissue cultures. Hence, a crosstalk between the two organ cultures induced a higher susceptibility of the cells to the substance. This might be due to the glucose limitation as well as due to secreted factors from the cells. One might guess that as 32 mM was reported to be the IC_{50} for 24 h treatment, all cells were affected irrespective of possible cell-cell crosstalk and only afterwards a sensitisation due to co-culture became evident. My colleague Anja Ramme, who did the neurosphere analysis, found out that the 2,5-hexanedione treated spheres did not have any outgrowing neurites anymore after two weeks in the MOC, in contrast to the control neurospheres or to neurospheres treated with 64 mM n-hexane, where the outgrowing neurites were still visible.⁹⁵

Summarising, the dose-dependent toxicity of 2,5-hexanedione in a liver-neurosphere co-culture could be modelled. Analysing the toxicity of n-hexane failed due to improper substance administration.

6 Conclusion

During the course of this work, an *in vitro* model system for substance testing, emulating *in vivo* organ functions, was generated. Co-cultivating various organ equivalents inside the multi-organ-chip (MOC) under *in vivo*-like conditions allowed for the analysis of organ interactions at steady state as well as at substance exposure.

Liver equivalents produced from HepaRG cells and primary hSteC, being a $1/100\,000$ of the biomass of a human liver, showed the production of liver-typical extracellular matrix components and the expression of key metabolising enzymes, not needing chemical stimulation, making them a model suitable for substance testing.

Subsequent liver single-tissue cultures in the MOC enhanced the expression of markers for cell polarisation, indicating the generation of bile canaliculi-like structures. Furthermore, the production of albumin in MOC cultures increased significantly compared to static controls. First indicators for functional liver zonation on cytochrome P450 3A4 level were obtained in Transwell® assisted cultures.

The long-term stability of these cultures was proven by 28 day co-cultures with skin reaching a metabolic steady state after about one week of co-culture. These two-organ cultures were shown to be glucose limited, still, viability of the cells was maintained and strongly increased compared to static cultures. The stable consumption of glucose and production of lactate indicated the establishment of an artificial coexistence between the tissues, even though albumin production was decreased due to the glucose limitation.

Furthermore, liver-skin co-culture in an endothelialised MOC, demonstrated the ability of the system to maintain three-organ cultures in a combined media circuit. Endothelial cells were kept viable over up to 21 being 14 days co-cultivated with liver and skin tissue.

Similarly, liver and neurospheres co-cultures were performed in a combined medium and showed metabolic stability over culture periods of up to 14 days.

Exposing MOC co-cultures to 3 pharmaceutical substances at regimens relevant to respective guidelines currently used for subsystemic substance testing in animals, successfully revealed a dose-dependent response of the multi-tissue cultures, showing similarities to *in vivo* observations.

Concluding, this system holds an ample perspective for future substance tests and experiments including various additional cells or organs.

7 Perspectives

The presented system successfully allowed for long-term analysis of pharmaceuticals and their impact not only on liver tissue but also on additional organs, still some improvements are conceivable.

7.1 Improvements of the liver equivalent

A better supply of nutrients to all cells and coming along with that means to control and vary stable zonation of the liver tissue are envisaged. As already described earlier, technical means facilitating the precise patterning of cells in cords along the medium flow could allow for a controlled adjustment of oxygen gradients.⁷⁵ Various approaches aiming for this goal had been pursued during the course of this research and are still ongoing. The use of technical channels, as well as biodegradable scaffolds, where cells attach to fibres forming a 3D structured network of cell cords, are still under evaluation. Furthermore, the re-cellularisation of de-cellularised rat liver grafts with human hepatocytes has been established with the help of my colleague Tobias Hasenberg using the protocols of Prof. Dr. Walles. First results of liver cell organisation and proliferation inside the grafts are promising and a joint project with the Institute of Applied Biochemistry under the supervision of Prof. Dr. Kurreck is evaluating the possibility to use these systems as disease models. Still, the applicability of these grafts to the MOC need to be assessed.

The formation of extended bile canalicular structures having connections to waste reservoirs is a further next goal for improving the liver equivalent. Microstructuring the cell compartments of liver tissue might be a way to achieve this, as reported previously.⁶⁷ Furthermore, the co-culture with other non-parenchymal cells was shown to improve hepatocyte polarity and hence stabilise the formation of bile canalicular structures.¹¹¹

Similarly, it was reported that hepatocytes co-cultured with liver sinusoidal endothelial cells were stable over prolonged periods of time. Sinusoidal endothelial cells, known to lose their differentiated phenotype *in vitro*, maintained the expression of functional marker SE-1 throughout the culture.¹¹² This might open up the opportunity for future vascularisation of the tissue, leading to a higher physiological similarity.

7.2 Endothelialisation

A first step in the direction of a fully endothelialised MOC has been performed already by my colleague Katharina Schimek, who established protocols for the successful coating of all the channels with endothelial cells. Still, a vascularisation of the tissue equivalents and a connection of these to the vascularised channels, forming a closed circuit, need to be established. There are several ways pursued by our research group to fulfil this task.

First, the possibility of printing hepatocytes and endothelial cells in a defined manner in hydrogels is currently assessed by my colleague Lutz Kloeke. This would allow the use of not only multiple cell types but also defined extracellular matrix components leading to highly *in vivo*-like structures. The self-formation of vascular structures in hydrogels is currently pursued by my colleague Tobias Hasenberg, who is combining endothelial cells and fibroblasts in a fibrin gel including collagen I. Later, organ equivalents might be added to the hydrogels leading to a connection of vascular structures with the tissues. Lastly, technical channels guiding endothelial cells towards the organs are provided by laser ablation, replica moulding and 2-photon-assisted structuring of support materials. Producing these channels in biodegradable materials might result in a physiological relevant remodelling of vessel structures.

Further improvements include the addition of secondary organs as well as improvements in analysis routines.

7.3 Systemic improvements

In addition to the skin, endothelial cell and neurosphere co-cultures reported here, the combination of, for example, commercial Transwell® barrier models of intestine with submersed liver micro-tissue cultures is currently under evaluation in a joint project with my colleague Annika Jaenicke. This might support further investigations into systemic organ interactions for substance exposure. Orally applied compounds need to pass the intestinal barrier before reaching blood circulation and liver metabolism. The availability of drugs might be more accurately mimicked by a two organ system. Furthermore, it might be of interest to study skin permeability of cosmetics with a representative number of perfused human epidermal skin equivalents in respective arrangements. Substances could be applied onto the skin, for example, in the form of creams, and penetration could be measured. Effect of the (cosmetic) substances on the liver, its metabolites and their further effect on the skin might be observable.

In near future, a 10 organ multi-layer chip will be produced in our laboratory, integrating not only liver and skin tissues, but also bone marrow equivalents, intestinal models and kidney tissue in a common blood vasculature. Here, a microfluidic device consisting of entrance ports for nutrition, bile excretion, urine and faeces removal are situated in a layer above the blood micro-circulation. Actuators providing mechanical cues for heartbeat, peristaltic intestinal movement, lung air-flow, bone compression, arteriolar constriction, and urine and bile removal are going to be integrated.

Furthermore, exact in-process monitoring of oxygen consumption of the individual tissues will be the next improvement to the MOC platform. This is necessary in order to characterise the energy balance of different tissues in various designs over extended culture periods.

These improvements of the liver equivalent, addition of endothelialisation and further organ co-cultures will finally lead to a system more closely mimicking the *in vivo* situation and leading to more predictable and relevant *in vitro* substance testing data.

8 References

1. Zakim, Boyer, T. D., Manns, M. P. & Sanyal, A. J. *Hepatolog: A Textbook of Liver Disease*. (Saunders Elsevier, 2012).
2. Sear, J. Anatomy and physiology of the liver. *Baillieres. Clin. Anaesthesiol.* **6**, 697–727 (1992).
3. E. Kuntz, H.-D. K. *Hepatology: Textbook and Atlas*. (Springer Medizin Verlag Heidelberg, 2008).
4. Nahmias, Y., Berthiaume, F. & Yarmush, M. L. Integration of Technologies for Hepatic Tissue Engineering. 309–329 (2006). doi:10.1007/10
5. Yarmush, M. L. *et al.* Hepatic tissue engineering. Development of critical technologies. *Ann. N. Y. Acad. Sci.* **665**, 238–52 (1992).
6. Hoehme, S. *et al.* Prediction and validation of cell alignment along microvessels as order principle to restore tissue architecture in liver regeneration. *Proc. Natl. Acad. Sci. U. S. A.* **107**, 10371–6 (2010).
7. Puhl, G., Schaser, K. D., Vollmar, B., Menger, M. D. & Settmacher, U. Noninvasive in vivo analysis of the human hepatic microcirculation using orthogonal polarizaton spectral imaging. *Transplantation* **75**, 756–61 (2003).
8. Dancygier, H. *Klinische Hepatologie Grundlagen, Diagnostik und Therapie hepatobiliärer Erkrankungen*. (Springer-Verlag Berlin Heidelberg New York, 2003).
9. Martinez-Hernandez, A. & Amenta, P. S. The hepatic extracellular matrix. *Virchows Arch. A Pathol Anat* 1–11 (1993).
10. Martinez-Hernandez, A. & Amenta, P. S. The extracellular matrix in hepatic regeneration. *FASEB J.* **9**, 1401–1410 (1995).
11. Powers, M. J. *et al.* A Microfabricated Array Bioreactor for Perfused 3D Liver Culture. *Biotechnol. Bioeng.* **78**, 257–269 (2002).
12. Davidson, A. J., Ellis, M. J. & Chaudhuri, J. B. A theoretical approach to zonation in a bioartificial liver. *Biotechnol. Bioeng.* **109**, 234–43 (2012).
13. Jungermann, K. & Katz, N. Functional hepatocellular heterogeneity. *Hepatology* **2**, 385–95 (1982).
14. Jungermann, K. Zonation of metabolism and gene expression in liver. *Histochem. Cell Biol.* **103**, 81–91 (1995).
15. Balis, U. J. *et al.* Oxygen consumption characteristics of porcine hepatocytes. *Metab. Eng.* **1**, 49–62 (1999).

16. Foy BD, Rotem A, Toner M, Tomphins RG, Y. M. A device to measure the oxygen uptake rate of attached cells: importance in bioartificial organ design. *Cell Transplant.* **3**, 515–27 (1994).
17. Dash, A. *et al.* Liver tissue engineering in the evaluation of drug safety. *Expert Opin. Drug Metab. Toxicol.* **5**, 1159–74 (2009).
18. Kidambi, S. *et al.* Oxygen-mediated enhancement of primary hepatocyte metabolism, functional polarization, gene expression, and drug clearance. *Proc. Natl. Acad. Sci. U. S. A.* **106**, 15714–9 (2009).
19. Braet, F. & Wisse, E. Structural and functional aspects of liver sinusoidal endothelial cell fenestrae: a review. *Comp. Hepatol.* **1**, 1 (2002).
20. Elvevold, K., Smedsrød, B. & Martinez, I. The liver sinusoidal endothelial cell: a cell type of controversial and confusing identity. *Am. J. Physiol. Gastrointest. Liver Physiol.* **294**, G391–400 (2008).
21. James, L. P., Mayeux, P. R. & Hinson, J. a. Acetaminophen-induced hepatotoxicity. *Drug Metab. Dispos.* **31**, 1499–506 (2003).
22. Malik, R., Selden, C. & Hodgson, H. The role of non-parenchymal cells in liver growth. **13**, 425–431 (2002).
23. Bleibel, W., Kim, S., D'Silva, K. & Lemmer, E. R. Drug-induced liver injury: review article. *Dig. Dis. Sci.* **52**, 2463–71 (2007).
24. Brouwer, a *et al.* Isolation and culture of Kupffer cells from human liver. Ultrastructure, endocytosis and prostaglandin synthesis. *J. Hepatol.* **6**, 36–49 (1988).
25. Ramadori, G. The stellate cell (Ito-cell, fat-storing cell, lipocyte, perisinusoidal cell) of the liver. **61**, 147–158 (1991).
26. Riccalton-Banks, L., Liew, C., Bhandari, R., Fry, J. & Shakesheff, K. Long-term culture of functional liver tissue: three-dimensional coculture of primary hepatocytes and stellate cells. *Tissue Eng.* **9**, 401–10 (2003).
27. Lee, J. S., Semela, D., Iredale, J. & Shah, V. H. Sinusoidal remodeling and angiogenesis: a new function for the liver-specific pericyte? *Hepatology* **45**, 817–25 (2007).
28. Abu-Absi, S. F., Hansen, L. K. & Hu, W.-S. Three-dimensional co-culture of hepatocytes and stellate cells. *Cytotechnology* **45**, 125–40 (2004).
29. Friedman, S. L. Hepatic Stellate Cells : Protean, Multifunctional, and Enigmatic Cells of the Liver. *Physiol. Rev.* **88**, 125–172 (2008).
30. Busher, J. T. Serum Albumin and Globulin. *Clin. Merhods Hist. Phys. Lab. Exam.* 497-499 (1990).
31. Seliskar, M. & Rozman, D. Mammalian cytochromes P450--importance of tissue specificity. *Biochim. Biophys. Acta* **1770**, 458–66 (2007).

32. Bock, K. W. Functions and transcriptional regulation of adult human hepatic UDP-glucuronosyl-transferases (UGTs): mechanisms responsible for interindividual variation of UGT levels. *Biochem. Pharmacol.* **80**, 771–7 (2010).
33. Martínez, A. I., Pérez-Arellano, I., Pekkala, S., Barcelona, B. & Cervera, J. Genetic, structural and biochemical basis of carbamoyl phosphate synthetase 1 deficiency. *Mol. Genet. Metab.* **101**, 311–23 (2010).
34. Kojima, T. *et al.* Regulation of the blood-biliary barrier: interaction between gap and tight junctions in hepatocytes. *Med. Electron Microsc.* **36**, 157–64 (2003).
35. Limonciel, A. *et al.* Lactate is an ideal non-invasive marker for evaluating temporal alterations in cell stress and toxicity in repeat dose testing regimes. *Toxicol. In Vitro* **25**, 1855–62 (2011).
36. Mulukutla, B. C., Khan, S., Lange, A. & Hu, W.-S. Glucose metabolism in mammalian cell culture: new insights for tweaking vintage pathways. *Trends Biotechnol.* **28**, 476–84 (2010).
37. Ozturk, S. S. & Hu, W.-S. *Cell Culture Technology for Pharmaceutical and Cell-Based Therapies*. (Taylor & Francis Group, 2006).
38. Griffith, L. G. *et al.* In vitro organogenesis of liver tissue. *Ann. N. Y. Acad. Sci.* **831**, 382–97 (1997).
39. Griffith, L. G. & Naughton, G. Tissue engineering--current challenges and expanding opportunities. *Science* **295**, 1009–14 (2002).
40. Tissue Engineering and Regeneration: Technologies and Global Markets. *A BCC Res. Healthc. Rep.* **HLC101A**, (2012).
41. Gebhardt, R. *et al.* New hepatocyte in vitro systems for drug metabolism: metabolic capacity and recommendations for application in basic research and drug development, standard operation procedures. *Drug Metab. Rev.* **35**, 145–213 (2003).
42. Price, R. J. *et al.* Use of precision-cut rat liver slices for studies of xenobiotic metabolism and toxicity: comparison of the Krumdieck and Brendel tissue slicers. *Xenobiotica* **28**, 361–371 (1998).
43. Toutain, H. J., Sarsat, J. P., Chelin, C., Hoet, D. & Leroy, D. Morphological and functional integrity of precision-cut rat liver slices in rotating organ culture and multiwell plate culture: Effects of oxygen tension. 175–190 (1998).
44. Soldatow, V. Y., LeCluyse, E. L., Griffith, L. G. & Rusyn, I. In vitro models for liver toxicity testing. *Toxicol. Res. (Camb)*. (2013).
45. Jager, R., De, Jurva, A. & Meijer, P. Drug-metabolizing activity of human and rat liver, lung, kidney and intestine slices. **32**, (2002).
46. Ekins, S. Past, present, and future applications of precision-cut liver slices for in vitro xenobiotic metabolism. *Drug Metab. Rev.* **28**, 591–623 (1996).

47. Lerche-langrand, C. & Toutain, H. J. Precision-cut liver slices: characteristics and use for in vitro. **153**, 221–253 (2000).
48. Olinga, P., Meijer, D. K., Slooff, M. J. & Groothuis, G. M. Liver slices in in vitro pharmacotoxicology with special reference to the use of human liver tissue. *Toxicol. In Vitro* **12**, 77–100 (1997).
49. Jover, R. Hepatocyte cell lines: their use, scope and limitations in drug metabolism studies. **2**, 183–212 (2006).
50. Dunn, J. C. Y., Yarmush, M. L., Koebe, H. G. & Tompkins, R. G. Hepatocyte function and extracellular matrix geometry: long-term culture in a sandwich configuration. *FASEB J.* **3**, 174–177 (1989).
51. Wu, M.-H., Huang, S.-B. & Lee, G.-B. Microfluidic cell culture systems for drug research. *Lab Chip* **10**, 939–56 (2010).
52. Guguen-Guillouzo, C. & Guillouzo, A. *General Review on In Vitro Hepatocyte Models and Their Applications*. **640**, (Humana Press, 2010).
53. Hitara, Y. S. *et al.* Function of Uptake Transporters for Taurocholate and Estradiol 17 β - D-Glucuronide in Cryopreserved Human Hepatocytes. *Drug Metab. Pharmacokin.* **18**, 33–41 (2003).
54. Hariparsad, N., Carr, B. A., Evers, R. & Chu, X. Comparison of Immortalized Fa2N-4 Cells and Human Hepatocytes as in Vitro Models for Cytochrome P450 Induction. *Drug Metabol. and Dispos.* **36**, 1046–1055 (2008).
55. Corlu, A., Griscom, L. & Leclerc, E. Trends in the development of microfluidic cell biochips for in vitro hepatotoxicity. *Toxicol. In Vitro* **21**, 535–544 (2007).
56. Cerec, V. *et al.* Transdifferentiation of hepatocyte-like cells from the human hepatoma HepaRG cell line through bipotent progenitor. *Hepatology* **45**, 957–67 (2007).
57. United Nations. Consolidated List of Products Whose Consumption and/or Sale Have Been Banned, Withdrawn, Severely Restricted or not Approved by Governments. (2005).
58. Paul, S. M. *et al.* How to improve R&D productivity: the pharmaceutical industry's grand challenge. *Nat. Rev. Drug Discov.* **9**, 203–14 (2010).
59. Burch, R. . & Russell, W. M. . *The Principles of Humane Experimental Technique*. (1959). at <http://altweb.jhsph.edu/pubs/books/humane_exp/het-toc>
60. Krewski, D., Westphal, M., Al-Zoughool, M., Croteau, M. C. & Andersen, M. E. New directions in toxicity testing. *Annu. Rev. Public Health* **32**, 161–78 (2011).
61. Collins, F. S., Gray, G. M. & Bucher, J. R. Transforming Environmental Health Protection. *Science*. **319**, 906–907 (2008).
62. Gibb, S. Toxicity testing in the 21st century: a vision and a strategy. *Reprod. Toxicol.* **25**, 136–8 (2008).

63. Basketter, D. *et al.* Optimised testing strategies for skin sensitization--the LLNA and beyond. *Regul. Toxicol. Pharmacol.* **64**, 9–16 (2012).
64. Ceridono, M. *et al.* The 3T3 neutral red uptake phototoxicity test: practical experience and implications for phototoxicity testing--the report of an ECVAM-EFPIA workshop. *Regul. Toxicol. Pharmacol.* **63**, 480–8 (2012).
65. Spielmann, H. *et al.* The International EU/COLIPA In Vitro Phototoxicity Validation Study: Results of Phase II (Blind Trial). Part 1: The 3T3 NRU Phototoxicity Test. *Toxicol. In Vitro* **12**, 305–27 (1998).
66. Spielmann, H. *et al.* A Study on UV Filter Chemicals from Annex VII of European Union Directive 76/768/EEC, in the In Vitro 3T3 NRU Phototoxicity Test. *ATLA* **26**, 679–708 (2000).
67. Goral, V. N. *et al.* Perfusion-based microfluidic device for three-dimensional dynamic primary human hepatocyte cell culture in the absence of biological or synthetic matrices or coagulants. *Lab Chip* **10**, 3380–6 (2010).
68. Prot, J.-M. *et al.* Improvement of HepG2/C3A Cell Functions in a Microfluidic Biochip. *Biotechnol. Bioeng.* **108**, 1704–15 (2011).
69. Baudoin, R., Griscom, L., Prot, J. M., Legallais, C. & Leclerc, E. Behavior of HepG2/C3A cell cultures in a microfluidic bioreactor. *Biochem. Eng. J.* **53**, 172–181 (2011).
70. Esch, M. B., Sung, J. H. & Shuler, M. L. Promises , challenges and future directions of CCAs. **148**, 64–69 (2010).
71. Huh, D., Torisawa, Y., Hamilton, G. a, Kim, H. J. & Ingber, D. E. Microengineered physiological biomimicry: organs-on-chips. *Lab Chip* **12**, 2156–64 (2012).
72. Marx, U. *et al.* “ Human-on-a-chip ” Developments: A Translational Cutting-edge Alternative to Systemic Safety Assessment and Efficiency Evaluation of Substances in Laboratory Animals and Man. *ATLA*. **40**, 235–257 (2012).
73. Materne, E.-M., Tonevitsky, A. G. & Marx, U. Chip-based liver equivalents for toxicity testing--organotypicalness versus cost-efficient high throughput. *Lab Chip* **13**, 3481–95 (2013).
74. Domansky, K. *et al.* Perfused multiwell plate for 3D liver tissue engineering. *Lab Chip* **10**, 51–8 (2010).
75. Toh, Y.-C. *et al.* A novel 3D mammalian cell perfusion-culture system in microfluidic channels. *Lab Chip* **7**, 302–9 (2007).
76. Ong, S.-M. *et al.* A gel-free 3D microfluidic cell culture system. *Biomaterials* **29**, 3237–44 (2008).
77. Goral, V. N. *et al.* Perfusion-based microfluidic device for three-dimensional dynamic primary human hepatocyte cell culture in the absence of biological or synthetic matrices or coagulants. *Lab Chip* **10**, 3380–6 (2010).

78. Zhang, C., Zhao, Z., Abdul Rahim, N. A., van Noort, D. & Yu, H. Towards a human-on-chip: culturing multiple cell types on a chip with compartmentalized microenvironments. *Lab Chip* **9**, 3185–92 (2009).
79. Imura, Y., Sato, K. & Yoshimura, E. Micro total bioassay system for ingested substances: assessment of intestinal absorption, hepatic metabolism, and bioactivity. *Anal. Chem.* **82**, 9983–8 (2010).
80. Imura, Y., Yoshimura, E. & Sato, K. Micro total bioassay system for oral drugs: evaluation of gastrointestinal degradation, intestinal absorption, hepatic metabolism, and bioactivity. *Anal. Sci.* **28**, 197–9 (2012).
81. Sin, A. *et al.* The design and fabrication of three-chamber microscale cell culture analog devices with integrated dissolved oxygen sensors. *Biotechnol. Prog.* **20**, 338–45 (2004).
82. Sung, J. H. & Shuler, M. L. A micro cell culture analog (microCCA) with 3-D hydrogel culture of multiple cell lines to assess metabolism-dependent cytotoxicity of anti-cancer drugs. *Lab Chip* **9**, 1385–94 (2009).
83. Sung, J. H. & Shuler, M. L. In vitro microscale systems for systematic drug toxicity study. *Bioprocess Biosyst. Eng.* **33**, 5–19 (2010).
84. Ziółkowska, K., Kwapiszewski, R. & Brzózka, Z. Microfluidic devices as tools for mimicking the in vivo environment. *New J. Chem.* **35**, 979 (2011).
85. Wu, M.-H., Huang, S.-B., Cui, Z., Cui, Z. & Lee, G.-B. Development of perfusion-based micro 3-D cell culture platform and its application for high throughput drug testing. *Sensors Actuators B Chem.* **129**, 231–240 (2008).
86. Schimek, K. *et al.* Integrating biological vasculature into a multi-organ-chip microsystem. *Lab Chip* **13**, 3588–98 (2013).
87. Wu, M.-H., Huang, S.-B. & Lee, G.-B. Microfluidic cell culture systems for drug research. *Lab Chip* **10**, 939–56 (2010).
88. Tilles, a W., Baskaran, H., Roy, P., Yarmush, M. L. & Toner, M. Effects of oxygenation and flow on the viability and function of rat hepatocytes cocultured in a microchannel flat-plate bioreactor. *Biotechnol. Bioeng.* **73**, 379–89 (2001).
89. Hewitt, N. J. *et al.* Correlation between troglitazone cytotoxicity and drug metabolic enzyme activities in cryopreserved human hepatocytes. *Chem. Biol. Interact.* **142**, 73–82 (2002).
90. Alvarez-Sanchez, R., Montavon, F., Hartung, T. & Pähler, A. Thiazolidinedione bioactivation: a comparison of the bioactivation potentials of troglitazone, rosiglitazone, and pioglitazone using stable isotope-labeled analogues and liquid chromatography tandem mass spectrometry. *Chem. Res. Toxicol.* **19**, 1106–16 (2006).
91. Spencer, P. S., Bischoff, M. C. & Schaumburg, H. H. On the specific molecular configuration of neurotoxic aliphatic hexacarbon compounds causing central–peripheral distal axonopathy. *Toxicol. Appl. Pharmacol.* **44**, 17–28 (1978).

92. Woehrling, E. K., Zilz, T. R. & Coleman, M. D. The toxicity of hexanedione isomers in neural and astrocytic cell lines. *Environ. Toxicol. Pharmacol.* **22**, 249–54 (2006).
93. Gripon, P. *et al.* Infection of a human hepatoma cell line by hepatitis B virus. *Proc. Natl. Acad. Sci. U. S. A.* **99**, 15655–60 (2002).
94. Ceelen, L. *et al.* Critical selection of reliable reference genes for gene expression study in the HepaRG cell line. *Biochem. Pharmacol.* **81**, 1255–61 (2011).
95. Ramme, A. Establishment of chip-based human neuronal tissue cultures for substance testing. (2013).
96. Serra, M., Brito, C., Costa, E. M., Sousa, M. F. Q. & Alves, P. M. Integrating human stem cell expansion and neuronal differentiation in bioreactors. *BMC Biotechnol.* **9**, 82 (2009).
97. Wagner, I. Multi-Organ-Chip Based Skin Models for Research and Substance Testing. (2013).
98. Lübberstedt, M. *et al.* HepaRG human hepatic cell line utility as a surrogate for primary human hepatocytes in drug metabolism assessment in vitro. *J. Pharmacol. Toxicol. Methods* **63**, 59–68 (2011).
99. Darnell, M., Ulvestad, M., Ellis, E., Weidolf, L. & Andersson, T. B. In vitro evaluation of major in vivo drug metabolic pathways using primary human hepatocytes and HepaRG cells in suspension and a dynamic three-dimensional bioreactor system. *J. Pharmacol. Exp. Ther.* **343**, 134–44 (2012).
100. Krause, P., Saghatolislam, F., Koenig, S., Unthan-Fechner, K. & Probst, I. Maintaining hepatocyte differentiation in vitro through co-culture with hepatic stellate cells. *In Vitro Cell. Dev. Biol. Anim.* **45**, 205–12 (2009).
101. Hamilton, G., Westmorel, C. & George, A. Effects of medium composition on the morphology and function of rat hepatocytes cultured as spheroids and monolayers. *Vitr. Cell Dev Biol Anim* **37**, 656–67 (2001).
102. Kawelke, N. *et al.* Fibronectin protects from excessive liver fibrosis by modulating the availability of and responsiveness of stellate cells to active TGF- β . *PLoS One* **6**, e28181 (2011).
103. Xu, G. *et al.* Gene expression and synthesis of fibronectin isoforms in rat hepatic stellate cells. Comparison with liver parenchymal cells and skin fibroblasts. *J. Pathol.* **183**, 90–98 (1997).
104. Jungermann, K. & Kietzmann, T. Zonation of parenchymal and nonparenchymal metabolism in liver. *Annu. Rev.* 179–203 (1996).
105. Gebhardt, R. Metabolic zonation of the liver: regulation and implications for liver function. *Pharmacol. Ther.* **53**, 275–354 (1992).
106. Allen, J. W., Khetani, S. R. & Bhatia, S. N. In vitro zonation and toxicity in a hepatocyte bioreactor. *Toxicol. Sci.* **84**, 110–9 (2005).

107. Peters, T. All About Albumin: Biochemistry, Genetics, and Medical Applications. *Acad. Press. San Diego* (1996).
108. Rogue, A. *et al.* Comparative gene expression profiles induced by PPAR γ and PPAR α/γ agonists in human hepatocytes. *PLoS One* **6**, e18816 (2011).
109. Loi, C. M., Young, M., Randinitis, E., Vassos, A. & Koup, J. R. Clinical pharmacokinetics of troglitazone. *Clin. Pharmacokinet.* **37**, 91–104 (1999).
110. Toepke, M. W. & Beebe, D. J. PDMS absorption of small molecules and consequences in microfluidic applications. *Lab Chip* **6**, 1484–6 (2006).
111. Bhatia, S. N., Balis, U. J., Yarmush, M. L. & Toner, M. Effect of cell-cell interactions in preservation of cellular phenotype: cocultivation of hepatocytes and nonparenchymal cells. *FASEB J.* **13**, 1883–900 (1999).
112. Domansky, K. *et al.* Perfused multiwell plate for 3D liver tissue engineering. *Lab Chip.* **10**, 51–58 (2010).

9 Acknowledgement

I would like to express my gratitude to all those helping me during the last three years and enabling this work.

First of all, I would like to thank Prof. Dr. Roland Lauster for giving me the opportunity to work in his laboratory granting me all the freedom I needed to progress and at the same time giving valuable support and encouragement. I also would like to thank Dr. Uwe Marx for letting me being part of this great project, animating me and providing many brilliant new ideas. I am very thankful for your constant good advice and support. I thank Prof. Jens Kurreck and Prof. Horst Spielmann for their friendly support, expert opinion and assessment of my thesis.

This work would not have been possible without the help of many colleagues who worked hand in hand procuring an unparalleled working atmosphere, facilitating daily work life and giving support during hard times.

Many experiments have been performed together with Ilka Wagner and I enjoyed the joint planning of experiments and many long hours of media exchanges. It was always a pleasure to work in a team with you. Furthermore, I would like to thank Anja Ramme who performed the liver-neurosphere co-culture experiments with me and always had a helping hand. Alexandra Lorenz, who outstandingly managed our laboratory, gave helpful advice and support in all our experiments. Many thanks also go to Reyk Horland for being imperturbably positive, for your good humor and creating an enjoyable working atmosphere. I would like to thank Annika Jaenicke and Tobias Hasenberg for many long joint hours establishing the de-cellularization procedure. Thanks for always being ready for discussions, bringing up new ideas and improvements. Special thanks also go to Katharina Schimek, Sven Brinker and Lutz Kloeke for establishing the chip fabrication procedure, vascularisation and giving technical support. In this context I would also like to thank Frank Sonntag and Mathias Busek for their cooperation, providing excellent solutions for chip generation, pumping systems and technical support. My students Ute Süßbier and Caroline Frädrich always were of great help during onset of experiments. Thanks for the diligent pipetting and having a helping hand. Furthermore, I would like to thank Agnes Schumacher for her immense help in the preparation of cDNA. Alexander Thomas assisted me concerning questions about the microscope and Corinna Margauer helped a lot during chip fabrication. Thanks! I also would like to thank Mark Rosowski and Christopher Drewell for their diligent reading of this work and for always being ready for discussions. I would like to thank Silke Hoffmann for taking care of all the regulatory issues and Luzia Reiners-Schramm for making everything run well in the laboratory and also in the kitchen. I also would like to thank Reinmar Undeutsch for taking care

of all IT problems. Jennifer Binder, Shirin Fatehi, Karolina Tykwinska and Marielle Königsmark always gave helpful advice also with new methods. Thanks for being friendly and supportive.

My special appreciation goes to Tilo Dehne and my family, Manfred, Renate, Christoph and Matthias Materne for their persistent confidence in me, for sharing my worries and successes and for being the best support I could dream of.

10 Publications

Parts of this work have already been published in the following peer reviewed journals:

Materne, E.-M., Tonevitsky, A. G., & Marx, U. (2013). Chip-based liver equivalents for toxicity testing—organotypicalness versus cost-efficient high throughput. *Lab on a chip*, 13(18), 3481—95.

Materne, E.-M.*, Wagner, I.*, & Marx, U. (2013). A dynamic multi-organ-chip for long-term cultivation and substance testing proven by 3D human liver and skin tissue co-culture. *Lab on a chip*, 13(18), 3538—47.

This publication was voted as Top 10% publication by the editors.

* Authors contributed equally

Parts of this work have already been presented on the following congresses:

18th European Congress on Alternatives to Animal Testing (Linz, Austria 15.09.-18.09.2013):

Oral Presentation: “A multi-organ-chip platform for long-term maintenance and substance testing of human tissue co-culture” Eva-Maria Materne, Ilka Wagner, Alexandra Lorenz, Sven Brincker, Annika Jaenicke, Caroline Frädrich, Christopher Drewell, Tobias Hasenberg, Katharina Schimek, Reyk Horland, Roland Lauster, Uwe Marx

23rd ESACT meeting “Better Cells for Better Health” (Lille, France 23.6.-26.06.2013):

Poster: “Assessment of troglitazone induced liver toxicity in a dynamically perfused two-organ Micro-Bioreactor system” Eva-Maria Materne, Caroline Frädrich, Reyk Horland, Silke Hoffmann, Sven Brincker, Alexandra Lorenz, Mathias Busek, Frank Sonntag, Udo Klotzbach, Roland Lauster, Uwe Marx, Ilka Wagner

Poster: “Dynamic culture of human liver equivalents inside a micro-bioreactor for long-term substance testing” Eva-Maria Materne, Caroline Frädrich, Ute Süßbier, Reyk Horland, Silke Hoffmann, Sven Brincker, Alexandra Lorenz, Matthias Gruchow, Frank Sonntag, Udo Klotzbach, Roland Lauster, Uwe Marx

This poster was awarded with the poster prize by the organisers of the congress.

3D Cell Culture “Advanced Model Systems, Applications & Enabling Technologies (Zurich, Switzerland 14.03.-16.03.2012):

Poster: “Perfused 3D human liver equivalents for biomedical research” Eva-Maria Materne, Tobias Hasenberg, Reyk Horland, Silke Hoffmann, Roland Lauster, Uwe Marx

Stem Cell Network Congress “6th International Meeting” (Essen, 05.04.-06.04.2011):

Poster: “Micro-scale human liver equivalents for chip based biomedical research” Eva-Maria Materne, Reyk Horland, Gerd Lindner, Niels Schilling, Mathias Gruchow, Frank Sonntag, Silke Hoffmann, Udo Klotzbach, Roland Lauster, Uwe Marx

11 Appendix

Lizenzen



Confirmation Number: 11144183
Order Date: 12/12/2013

[Print this page](#)

Customer Information

Customer: Eva-Maria Materne
Account Number: 3000618836
Organization: Eva-Maria Materne
Email: eva-maria.materne@tu-berlin.de
Phone: +49 3031427907
Payment Method: Invoice

This not an invoice

Order Details

Lab on a chip

Billing Status:
N/A

Order detail ID: 64190049
Article Title: Perfused multiwell plate for 3D liver tissue engineering
Author(s): Domansky, Karel ; et al
DOI: 10.1039/B913221J
Date: Jan 01, 2010
ISSN: 1473-0197
Publication Type: Journal
Volume: 10
Issue: 1
Start page: 51
Publisher: ROYAL SOCIETY OF CHEMISTRY
Author/Editor: Royal Society of Chemistry (Great Britain)

Permission Status: **Granted**

Permission type: Republish or display content
Type of use: reuse in a thesis/dissertation
Order License Id: 3286581455223

Type of Use	
Requestor type	academic/educational
Portion	figures/tables/images
Number of figures/tables/images	1
Distribution quantity	5
Format	print and electronic
Will you be translating?	no
Order reference number	
Title of the thesis/dissertation	Generation of chip-based liver equivalents for substance testing
Expected completion date	Jan 2014
Estimated size	100


Note: This item was invoiced separately through our **RightsLink service**. [More info](#)

\$ 0.00

Lab on a chip

Billing Status:
N/A

Order detail ID: 64190079

Permission Status:  Granted

Article Title: A micro cell culture analog (μ CCA) with 3-D hydrogel culture of multiple cell lines to assess metabolism-dependent cytotoxicity of anti-cancer drugs

Permission type: Republish or display content
Type of use: reuse in a thesis/dissertation

Order License Id: 3286581461085

Author(s): Sung, Jong Hwan ; Shuler, Michael L.
DOI: 10.1039/B901377F
Date: Jan 01, 2009
ISSN: 1473-0197
Publication Type: Journal
Volume: 9
Issue: 10
Start page: 1385
Publisher: ROYAL SOCIETY OF CHEMISTRY
Author/Editor: Royal Society of Chemistry (Great Britain)

Type of Use	
Requestor type	academic/educational
Portion	figures/tables/images
Number of figures/tables/images	1
Distribution quantity	5
Format	print and electronic
Will you be translating?	no
Order reference number	
Title of the thesis/dissertation	Generation of chip-based liver equivalents for substance testing
Expected completion date	Jan 2014
Estimated size	100


Note: This item was invoiced separately through our **RightsLink service**. [More info](#)

\$ 0.00

Lab on a chip

Billing Status:
N/A

Order detail ID: 64190086

Permission Status:  Granted

Article Title: Perfusion-based microfluidic device for three-dimensional dynamic primary human hepatocyte cell culture in the absence of biological or synthetic matrices or coagulants

Permission type: Republish or display content
Type of use: reuse in a thesis/dissertation

Order License Id: 3286581467322

Author(s): Goral, Vasiliy N. ; et al
DOI: 10.1039/C0LC00135J
Date: Jan 01, 2010
ISSN: 1473-0197
Publication Type: Journal
Volume: 10
Issue: 24
Start page: 3380
Publisher: ROYAL SOCIETY OF CHEMISTRY
Author/Editor: Royal Society of Chemistry (Great Britain)

Type of Use	
Requestor type	academic/educational
Portion	figures/tables/images
Number of figures/tables/images	1
Distribution quantity	5
Format	print and electronic
Will you be translating?	no
Order reference number	
Title of the thesis/dissertation	Generation of chip-based liver equivalents for substance testing
Expected completion date	Jan 2014
Estimated size	100

Note: This item was invoiced separately through our **RightsLink service**. [More info](#)

\$ 0.00

Eidesstattliche Erklärung

Hiermit bestätige ich, Eva-Maria Materne, geboren am 21.02.1984 in Augsburg, dass ich die vorliegende Arbeit selbstständig angefertigt habe. Einzelne Experimente wurden in Kooperation mit Ilka Wagner und Anja Ramme durchgeführt, was in den entsprechenden Abschnitten vermerkt wurde.

Ich versichere, dass ich ausschließlich die angegebenen Quellen und Hilfen in Anspruch genommen habe.

Die geltende Promotionsordnung ist mir bekannt.

Eva-Maria Materne

Berlin, 13.01.2014

Ausschluss weiterer Promotionsverfahren

Ich, Eva-Maria Materne, bestätige, dass ich weder in der Vergangenheit, noch zum jetzigen Zeitpunkt, Promotionsabsichten oder Promotionsverfahren bei einer anderen Hochschule als der Technischen Universität Berlin oder bei einer anderen Fakultät der Technischen Universität Berlin beantragt habe.

Eva-Maria Materne

Berlin, 13.01.2014